北京大学
PEKING UNIVERSITY

新型医用金属材料及其介入器械研发现状

郑玉峰

LBMD
Laboratory of Biomedical Materials and Devices

MATURE:
- Pure Metals(Au, Pt, Ta)……
- 304V&316L stainless steel
- Ti&Ti alloys
- CoCr CoCrMo alloys

NEW:
- Ti based alloys
- Fe based alloys
- Mg based alloys
- Bulk metallic glasses
- Nanocrystalline Metals……

To be Recognized as New Metallic biomaterials

Requirements

举例1——医用镍钛合金及其在介入医学工程中的应用

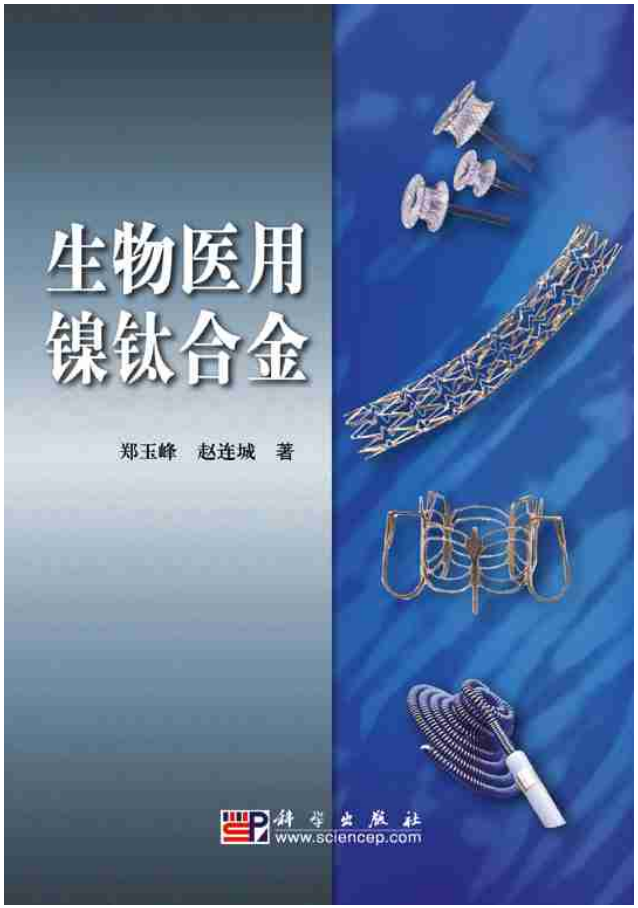

镍钛合金————意外的发现

1963年 美国海军军械研究室Buehler等偶然间发现等原子NiTi合金（当时作为阻尼材料开发研究）在室温（马氏体态）经形变（弯曲）、再经加热（与点燃的香烟火苗接触，发生马氏体→母相逆转变）后，自动恢复形状（自动弹直，对应母相的形状），命名为形状记忆。

NiTiNOL Nickel Titanium Navy Ordnance Laboratory

镍钛合金的形状记忆效应

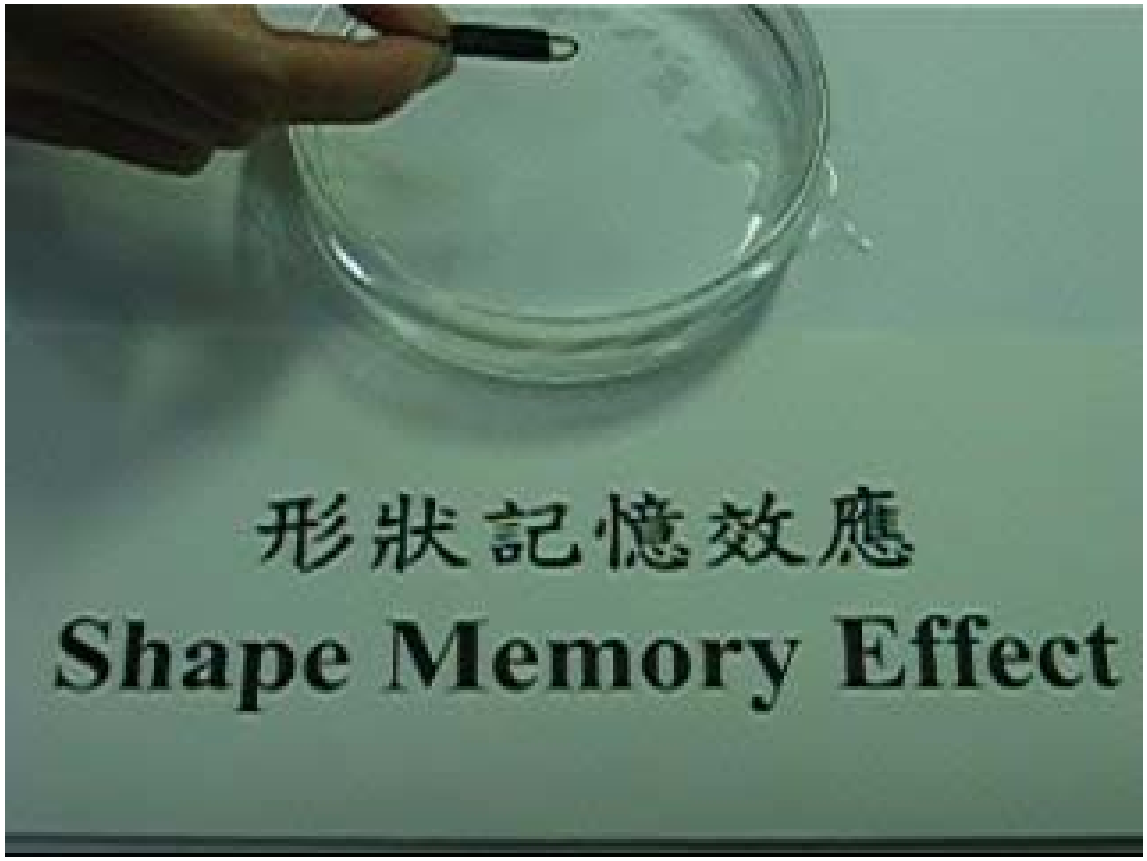

不同温度下镍钛合金对应不同的相结构

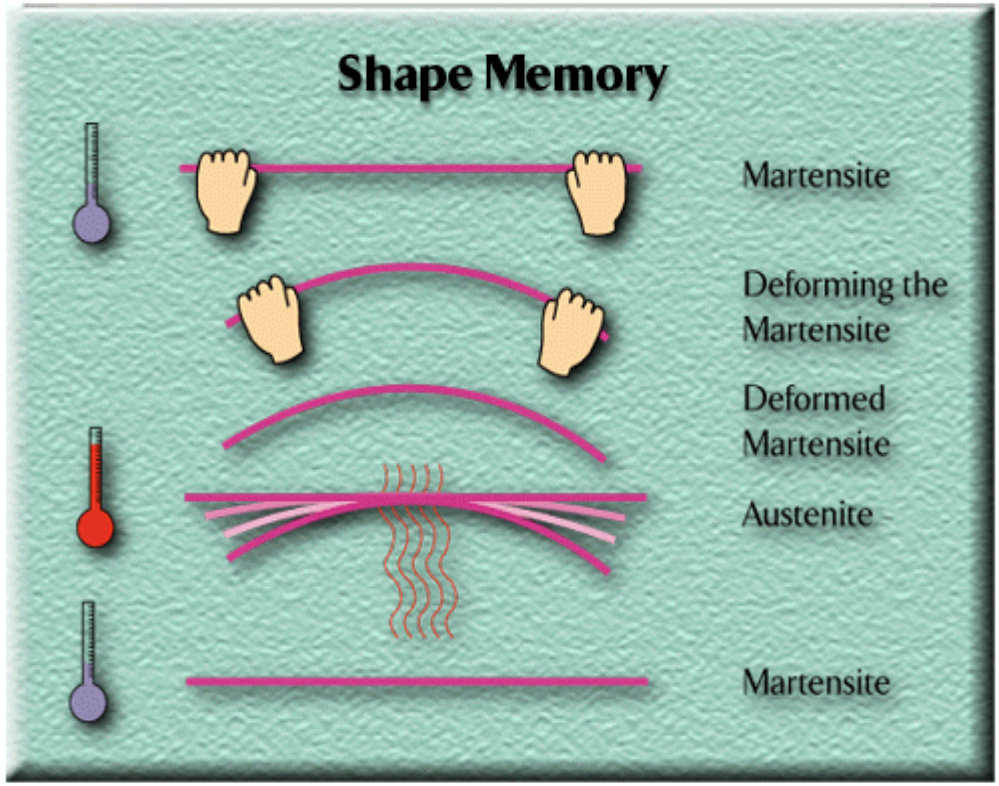

降温

- 母相 ⇒ 马氏体

类似水⇒冰

- 马氏体状态下形变

设想将冰块敲碎

升温

- 马氏体 ⇒ 母相

类似冰⇒水

此相变过程伴随形状恢复

镍钛合金其母相和马氏体晶胞是呈有序结构排列的

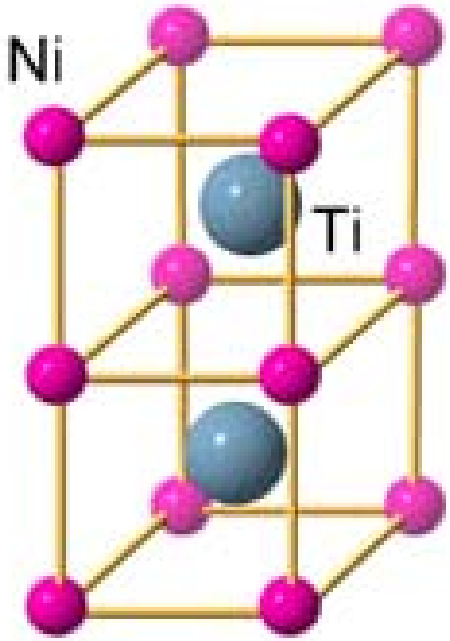

母相晶胞（体心立方结构）

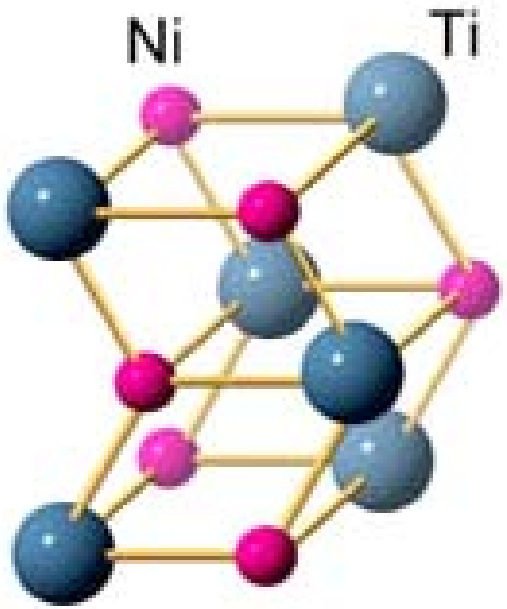

马氏体晶胞（单斜B19’结构）

注:材料学中的晶胞类似于生物学中的细胞,是构成晶体的最小结构单元

高温态　　低温态

镍钛合金的超弹性

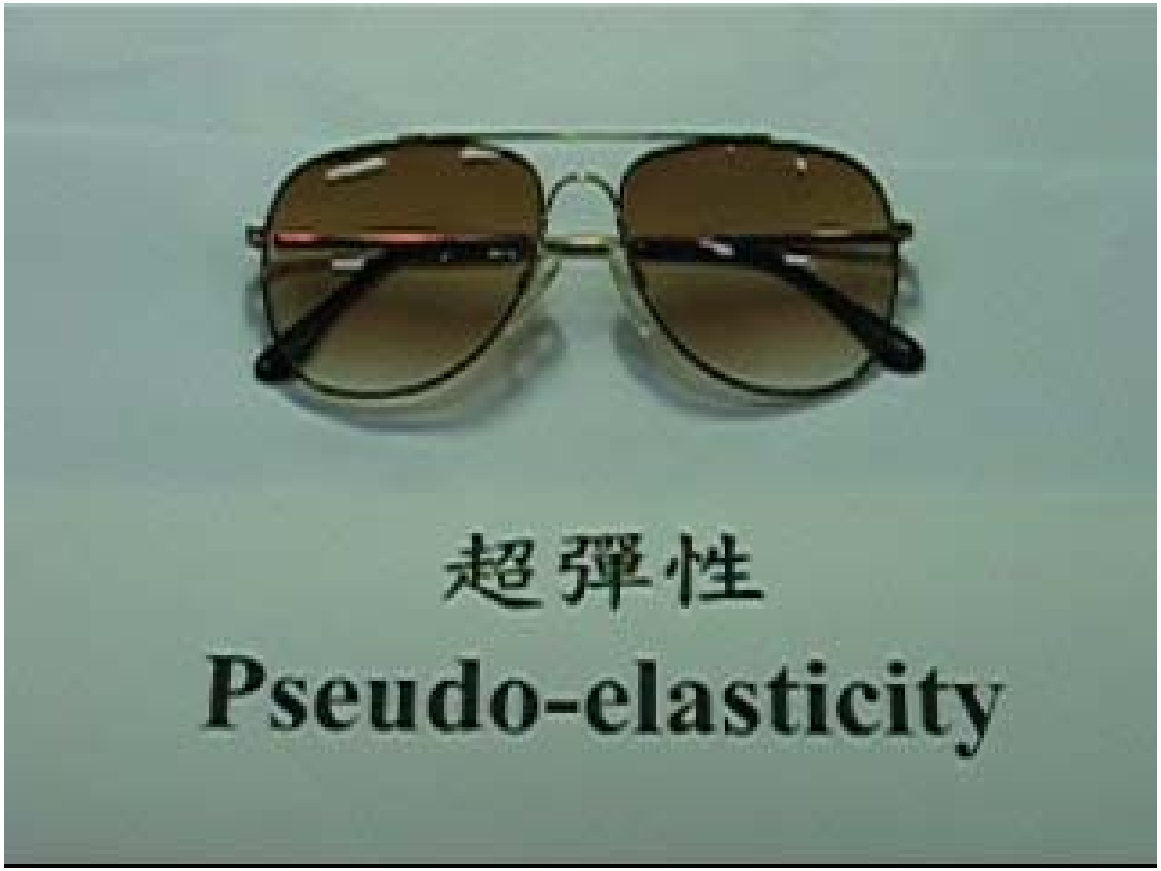

超弹性力学行为的表现

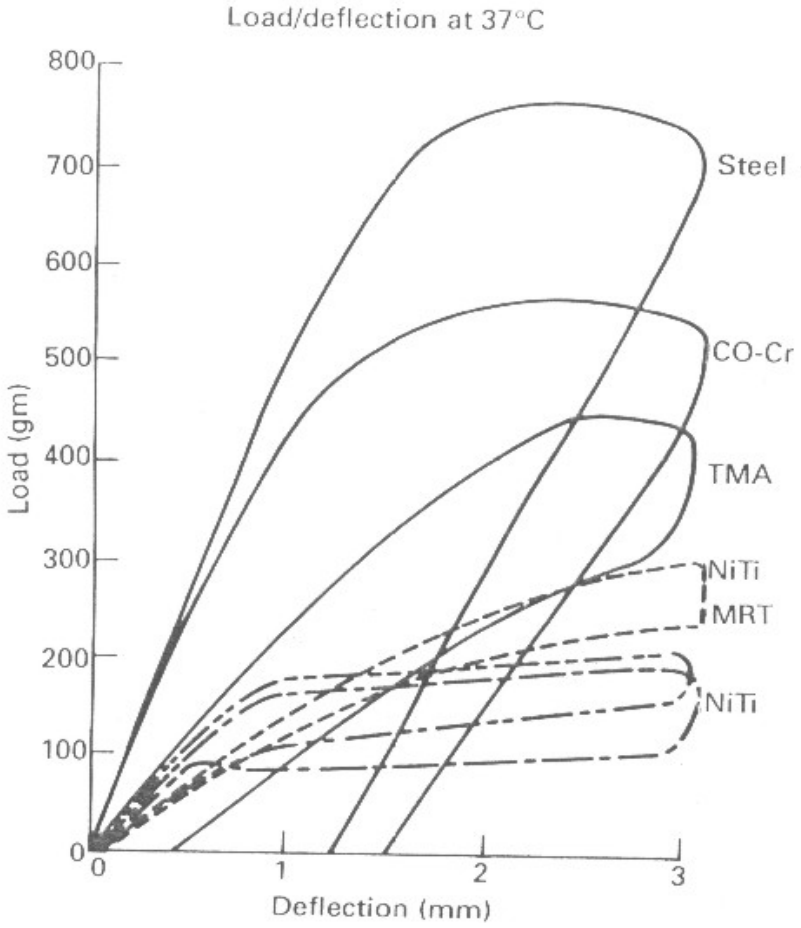
Load/deflection at 37°C
800
700
600
500
400
300
200
100
0
Load (gm)
0
1
2
3
Deflection (mm)
Steel
CO-Cr
TMA
NiTi
MRT
NiTi

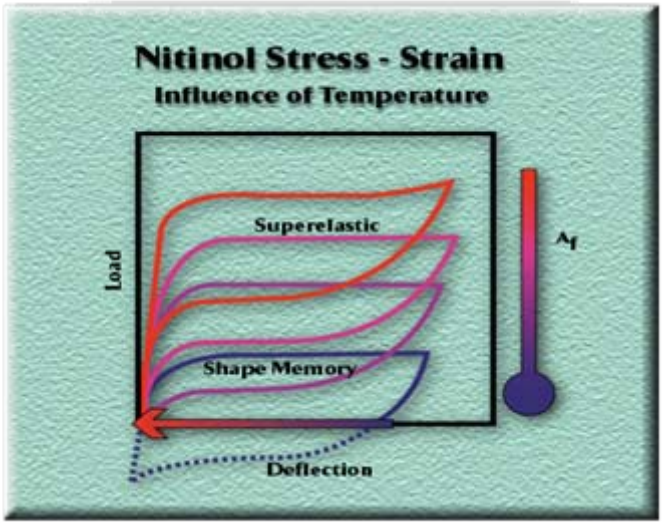
Nitinol Stress - Strain
Influence of Temperature
Superelastic
Shape Memory
Load
Deflection
Af

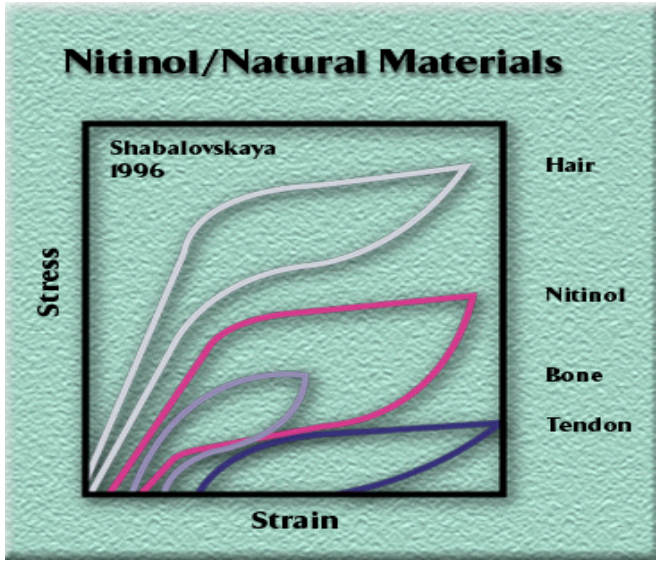
Nitinol/Natural Materials
Shabalovskaya
1996
Hair
Nitinol
Bone
Tendon
Stress
Strain

镍钛合金原材料与半成品的制造

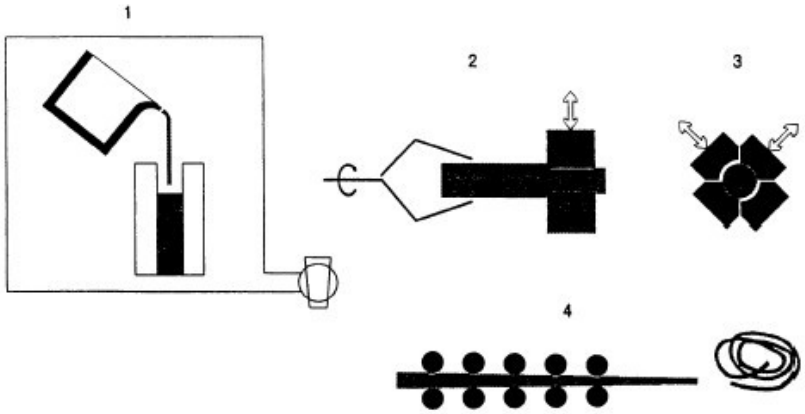

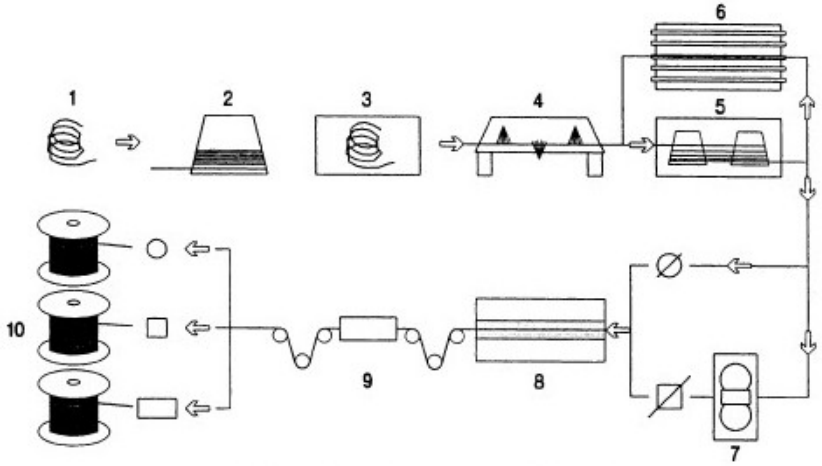

热加工

连续退火

酸洗

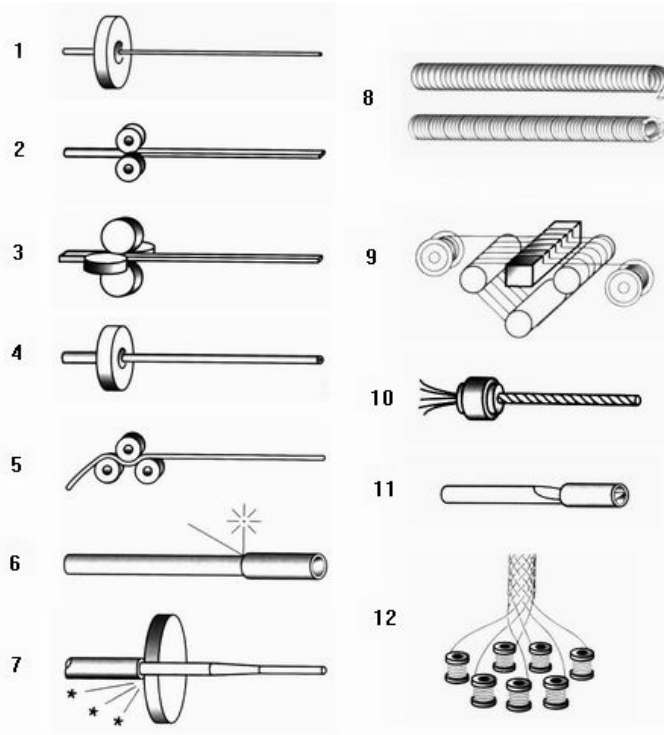
1
2
3
4
5
6
7
8
9
10
11
12

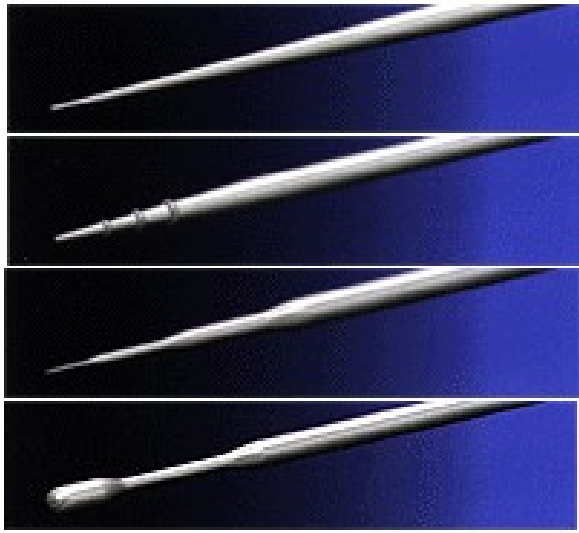

目前商业销售的各种形式镍钛合金半成品的指标对比

	丝材(wire)	板材(ribbion)	管材(tube)	薄板(sheet)	棒材(bar/rod)
通常尺寸	丝径 ≥0.017mm	厚度：0.025-1mm 宽度：0.05-12.5mm	外径：0.125-15mm 壁厚：≥0.05mm	厚度：≥0.018mm 宽度：25-500mm	冷拔：≥50mm 热轧：>100mm
合金	大成分范围供应形状记忆或超弹性合金	主要为超弹性；有限成分供应形状记忆	主要为超弹性；有限成分供应形状记忆	有限成分供应形状记忆或超弹性合金	大成分范围供应合金
表面	表面氧化、表面酸洗、表面喷丸、表面研磨、表面抛光	表面氧化、表面酸洗、表面抛光	表面氧化、表面研磨	表面氧化、表面酸洗	表面氧化、表面酸洗、表面喷丸、表面研磨
供货状态	校直态、拔制态、定型态	校直态、拔制/轧制态、定型态	校直态、拔制态、定型态	平直退火态、轧制态	校直态、拔制态
成熟程度	八十年代	八十年代	自1994	自1996	八十年代
应用实例	导丝、驱动器、手机天线、眼镜架	牙齿矫形丝	支架、鞘管	化学刻蚀或模压器械	管接头
成本	低	低—中等	高	中等—高	最低

形状记忆或超弹性热处理

盐浴炉

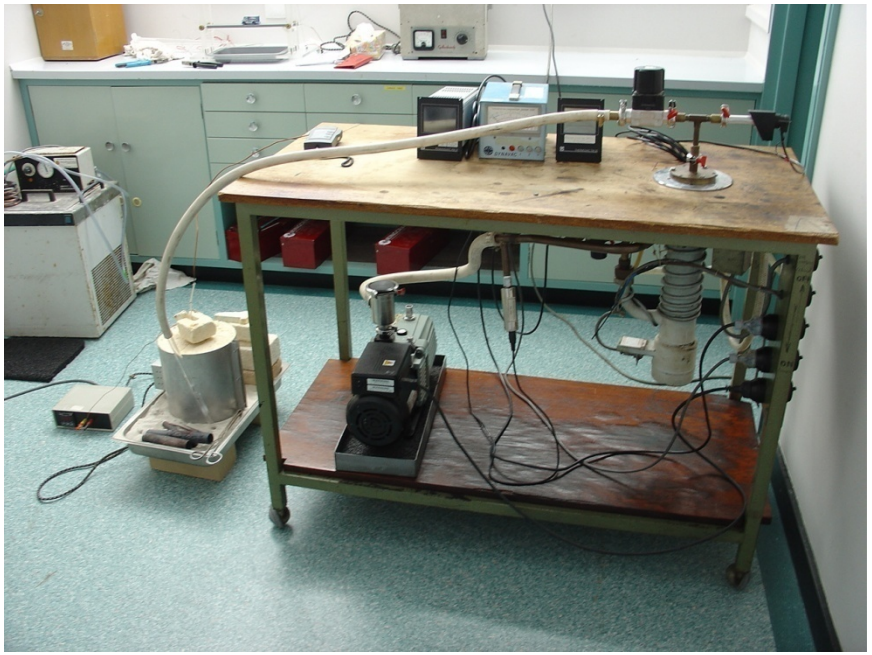

真空退火炉

动作温度(As相变温度)的设定

****

As = +95 °C　　Shape Memory Alloys

As = +70 °C

As = +60 °C

As = +55 °C

As = +45 °C

****

As = +30 °C　　Body Temperature Alloys

As = +15 °C

****

As = +5 °C　　Superelastic Alloys

As = 0 °C

As = -5 °C

As = -10 °C

As = -15 °C

****

As = -25 °C　　High Strength Superelastic Alloys

As = -50 °C

****

医用镍钛合金的光刻腐蚀

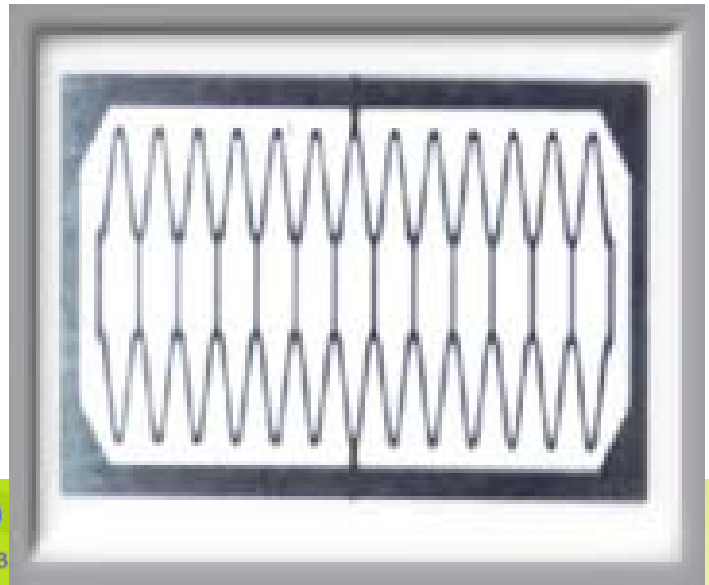

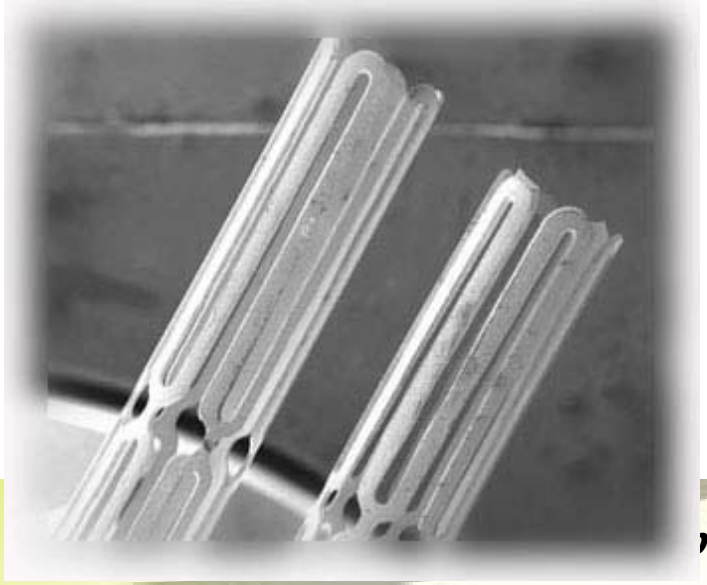

二维
平面

三维
曲面

医用镍钛合金的激光切割

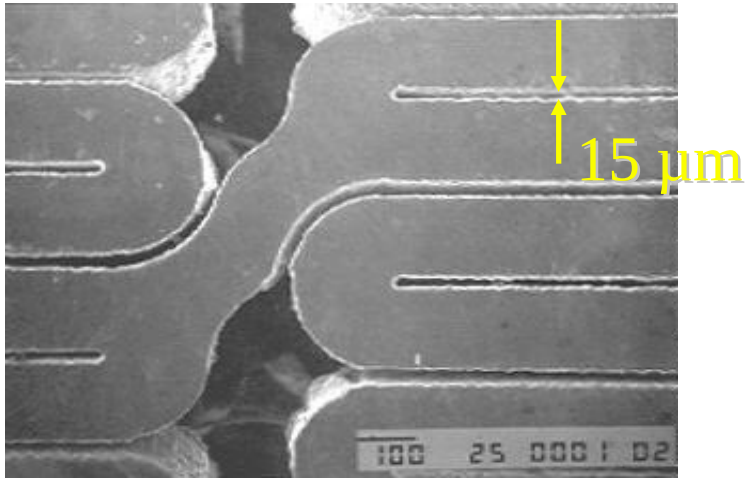

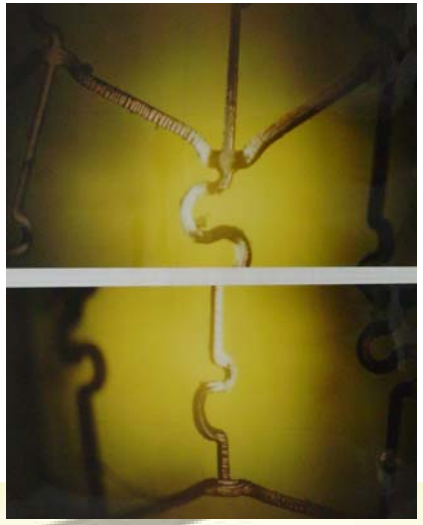

医用镍钛合金的机械抛光与电化学抛光处理

离心光饰机

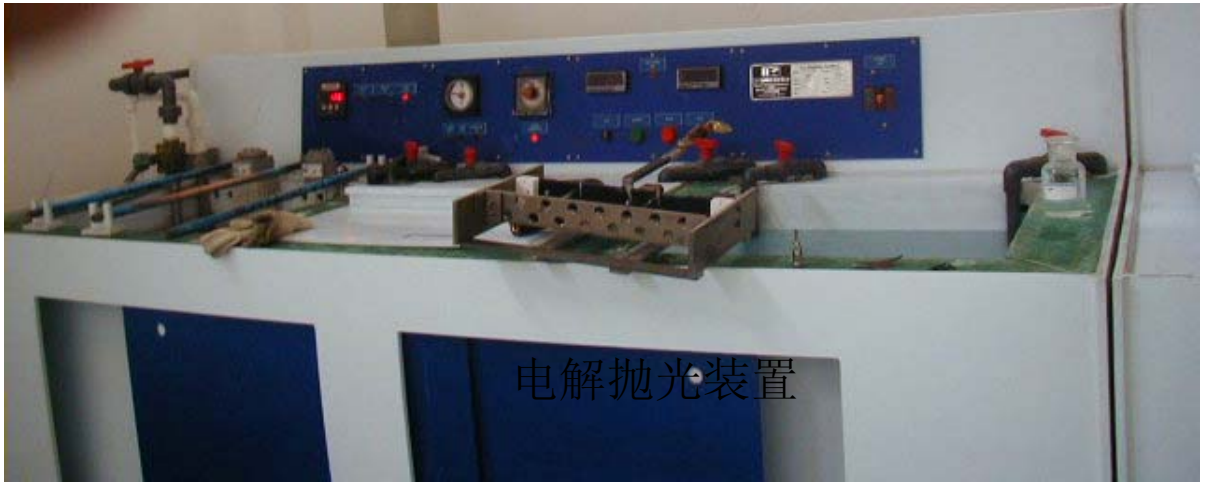

电解抛光装置

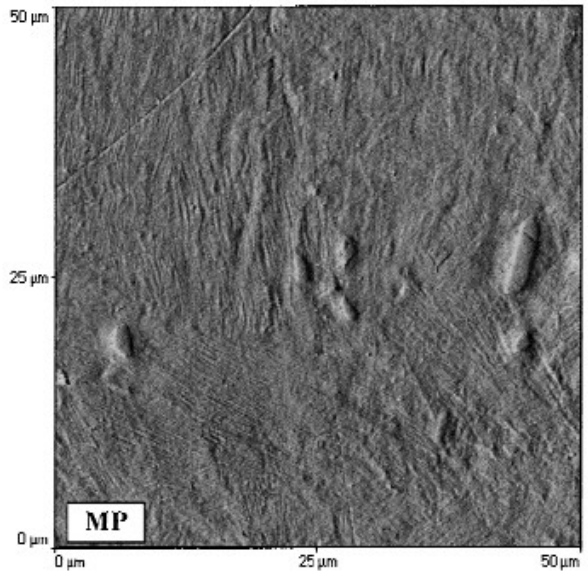

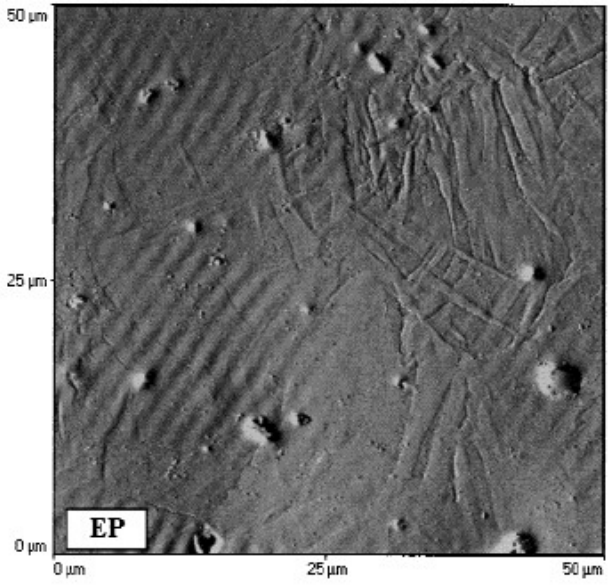

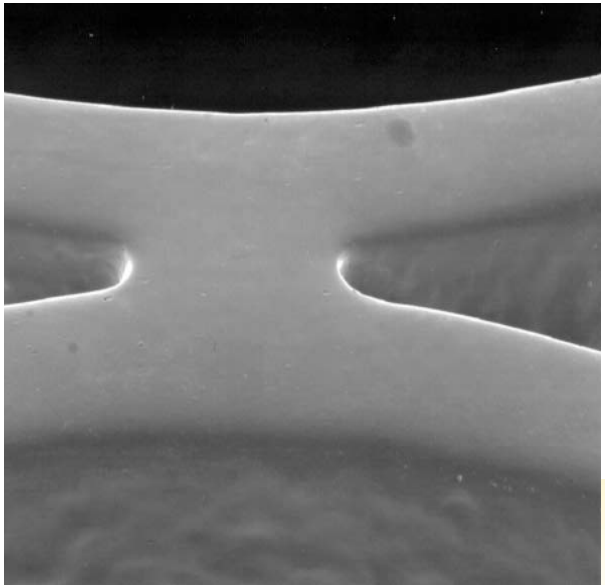

脉冲Nd:YAG激光焊接机

医用镍钛合金的激光焊接

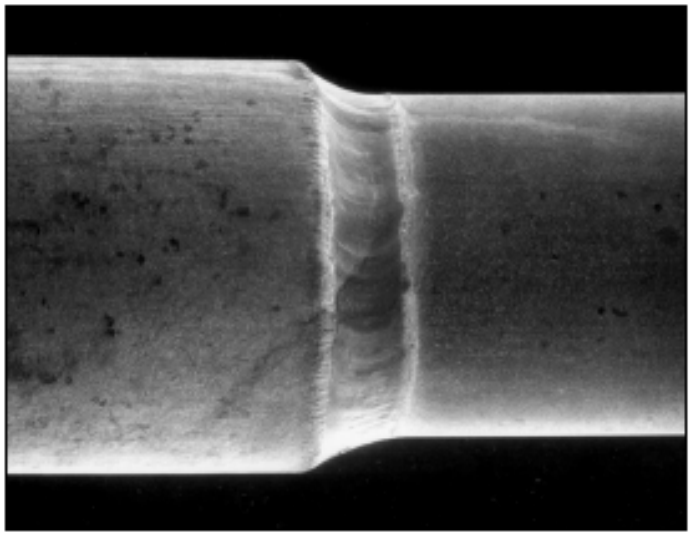

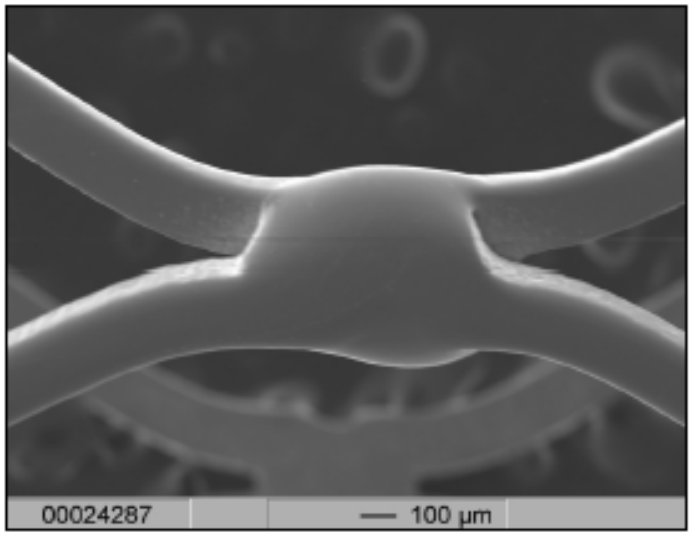

介入医学工程概述

- 介入医学包括介入放射学、介入超声学、介入腔镜学等。其中介入放射学是介入医学的主要组成部分，其基本概念由两大部分组成：①以影像诊断学和临床诊断学为基础，在医学影像设备的引导下，利用简单的器材获得病理学、细胞学、生理生化学、细菌学和影像资料的一系列诊断方法；②在医学影像设备的引导下，结合临床治疗学原理，通过导管等器材对各种病变进行治疗的一系列治疗技术。

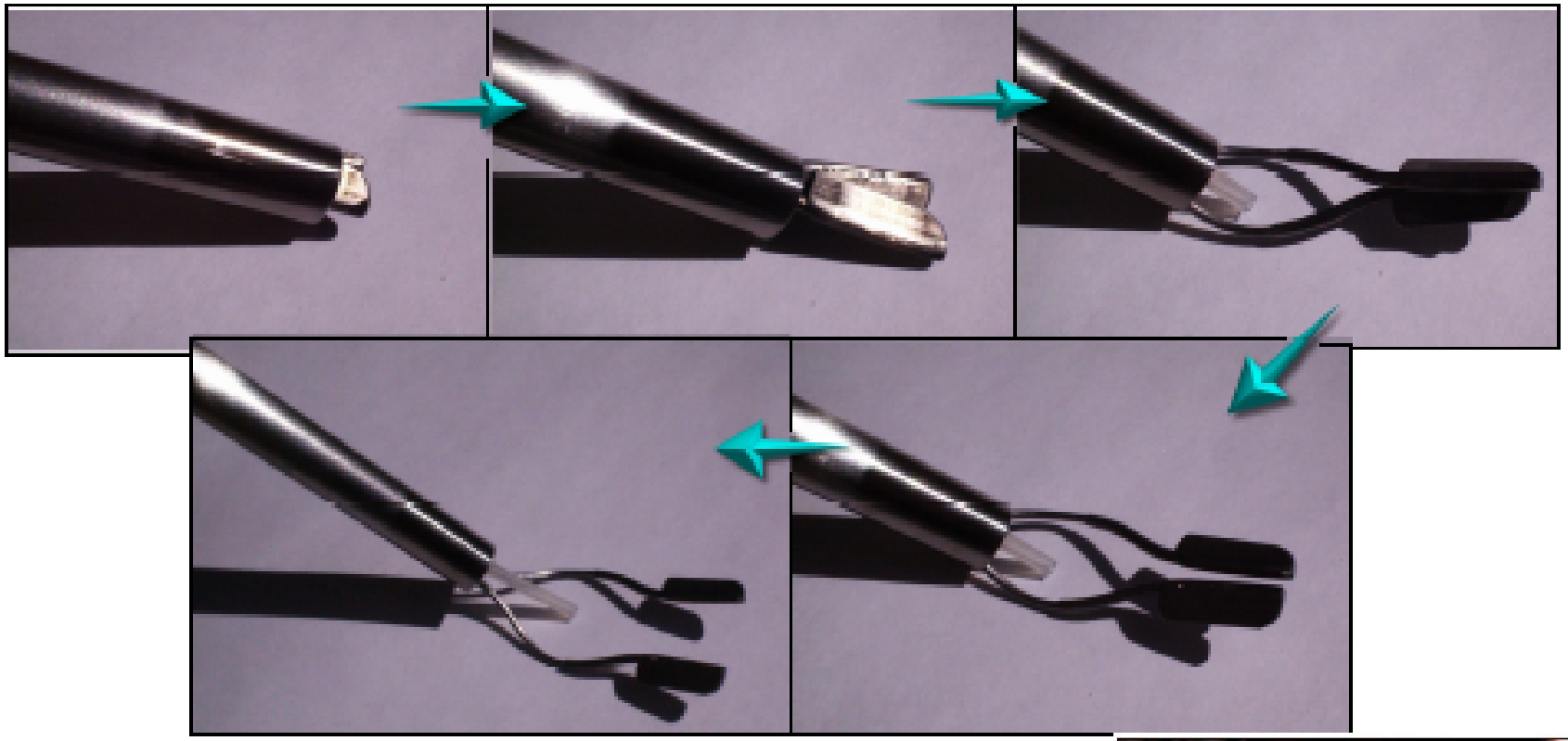

超弹性NiTi合金介入医学器械的工作应用原理多数情况下是利用外界约束器械，到体内状态去除约束，器械自行完成超弹性形状恢复的动作。

超弹性镍钛合金在增加微创治疗器械的自由度进而克服操作空间限制方面具有独特功效。

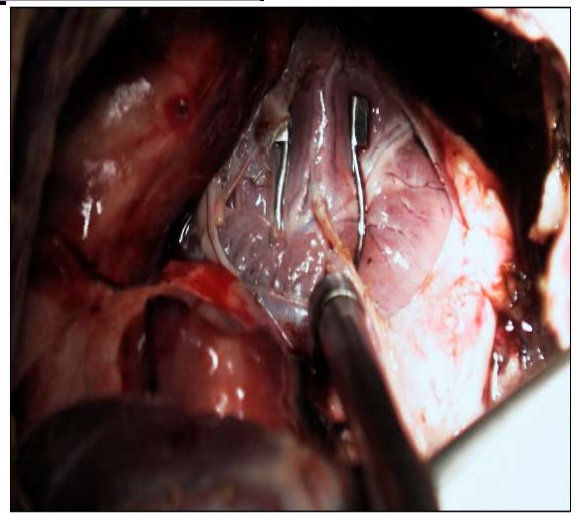

医用镍钛合金被广泛应用于介入医学的常用临床技术“通、堵、注、取、消中。

（1）再通技术

（2）栓塞技术

（3）灌注技术

（4）取出技术

（5）消融技术

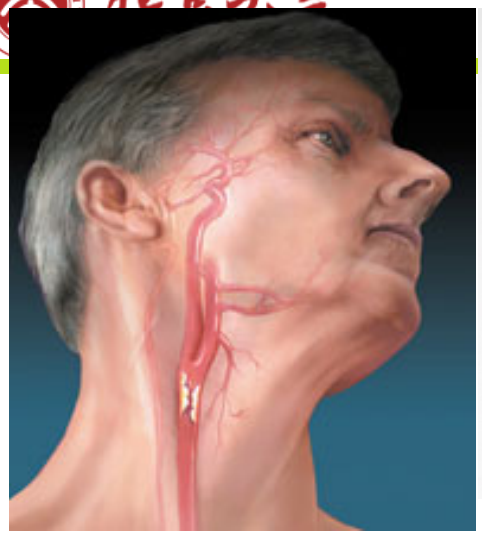

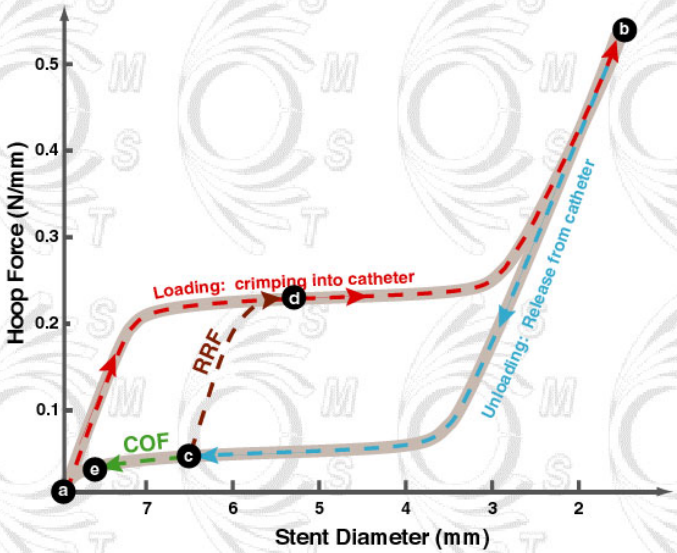
Hoop Force (N/mm)
0.5
0.4
0.3
0.2
0.1
Loading: crimping into catheter
RRF
COF
Unloading: Release from catheter
a
b
c
d
e
7
6
5
4
3
2
Stent Diameter (mm)

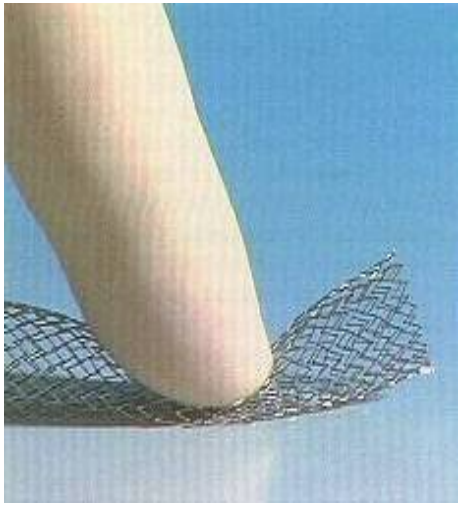

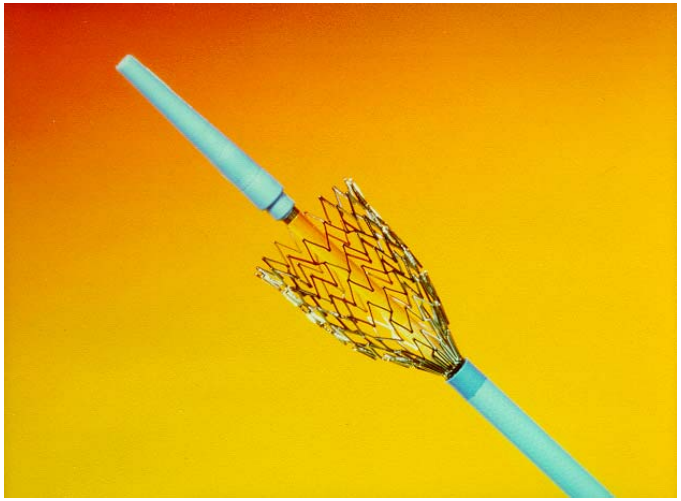

镍钛合金颈动脉支架

镍钛合金大动脉覆膜支架

- 用于大动脉（弓降以下，髂动脉以上部位）的动脉瘤和动脉夹层
- 分直管型大动脉覆膜支架；分叉型大动脉覆膜支架

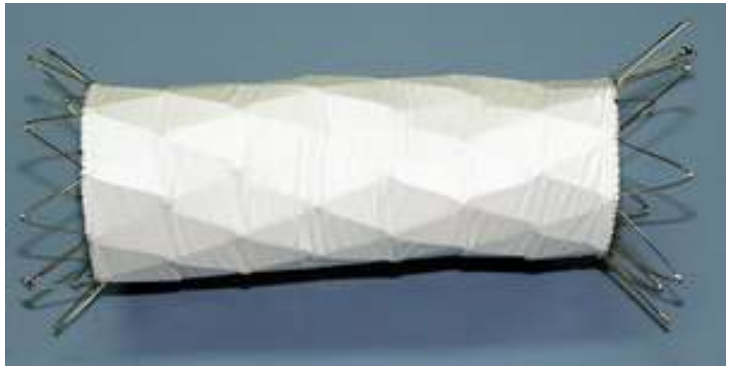

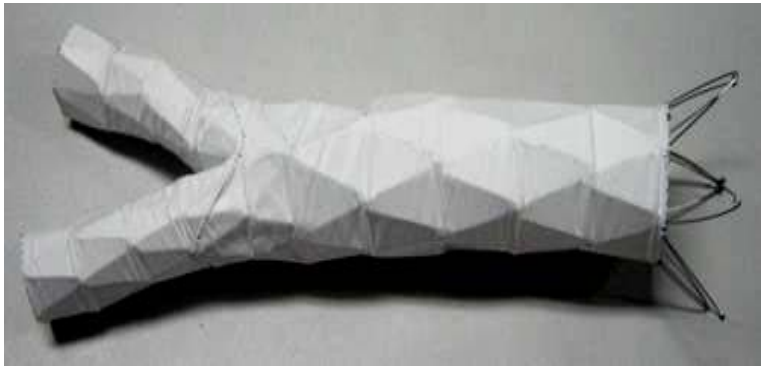

腔道内支架

- 按用途可分为食道支架、呼吸道支架、胆道支架、尿道支架、直肠支架和十二指肠支架等；
- 按形状可分为直通口、喇叭型口、球型口、T型口、Y型口和防返流型口等；
- 按结构可分为线圈式、编织型和网格状等；
- 按表面形态可分为覆生物膜型、镀金型和表面氧化处理型等。

本所主项是记忆合金的应用和医疗器械的技术开发。旨在对介入人体腔内支架的国产化作一份贡献，本所研制了食道支架、胆道支架、气管支架、腔静脉支架、肝静脉支架和尿道支架。

本所研制的“前列腺段尿道扩张用形状记忆合金支架”、“金属网状支架”和“人体腔内支架推送器”等已获国家实用新型专利权。

专利号如下:

ZL 90226379.X　ZL 92225280.7　ZL 92239771.6
ZL 96209419.6　ZL 96241122.1　ZL 96241123.X
ZL 96244863.X　ZL 96244817.6
ZL 96244862.1　ZL 97201653.8
ZL 98204142.X　ZL 99207902.0

由于本所与多家医院合作，医工结合，从而增强了本所的产品设计开发能力。

食道支架的用途及适用范围:

食道支架置入食道狭窄处以扩宽和支撑食道，解除进食困难。

食道支架适用于食道癌狭窄、食道术后吻合狭窄、食道化学灼伤狭窄、贲门失驰、放射性及霉菌性食管炎狭窄、十二指肠狭窄和肺癌压迫食道狭窄。

食道支架不宜用于食道合并多发性狭窄、合并声带麻痹患者、食管下段贲门癌侵及胃体者和严重出血倾向者。

食道支架供应规格:

食道支架置入方法:

1. 通过胃镜或x光造影响确定狭窄部位和尺寸，以选定支架型号（支架两端应长出病区2-3cm）同时在体表作上标记。

2. 对咽部及食道进行喷雾麻醉。

3. 患者取侧卧位，摘去义齿，放上牙托。先下导丝然后沿导丝下气囊导管以扩张狭窄段。扩张直径以支架推送器能顺利通过为宜。

4. 将经消毒的推送器，在x射线透视下经口腔沿导丝导入，使推送器的前端超过标定线，并记准此时推送器与门齿或牙托的相对位置。

5. 推杆固定位置不动，后撤外鞘管则释放出支架。外鞘后撤到终端即支架全部释放

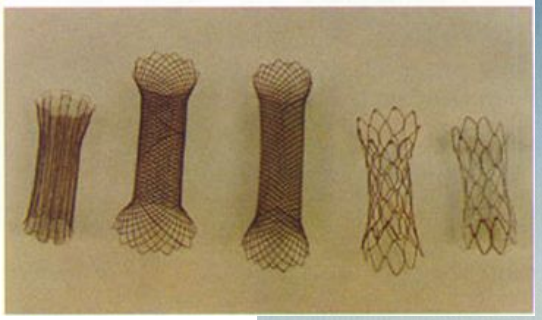

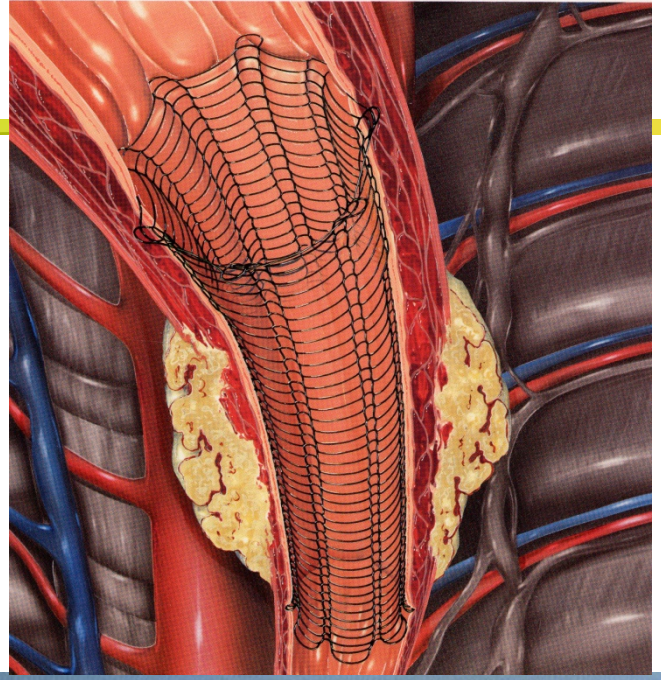

LBMD
Laboratory of Biomedical Materials and Devices

胆道支架的用途及使用范围

胆道支架置入胆管治疗阻塞性黄疸。

胆道支架实用于胆管癌、胰头癌胆总管阻塞、胆管术后狭窄、胆转移瘤引起的胆道梗阻和肝门淋巴结转移引起的胆道梗阻。

胆道支架不宜使用于十二指肠阻塞、肝功能衰竭、肾功能不全、大腹水和重度食管静脉曲张并有出血倾向者。

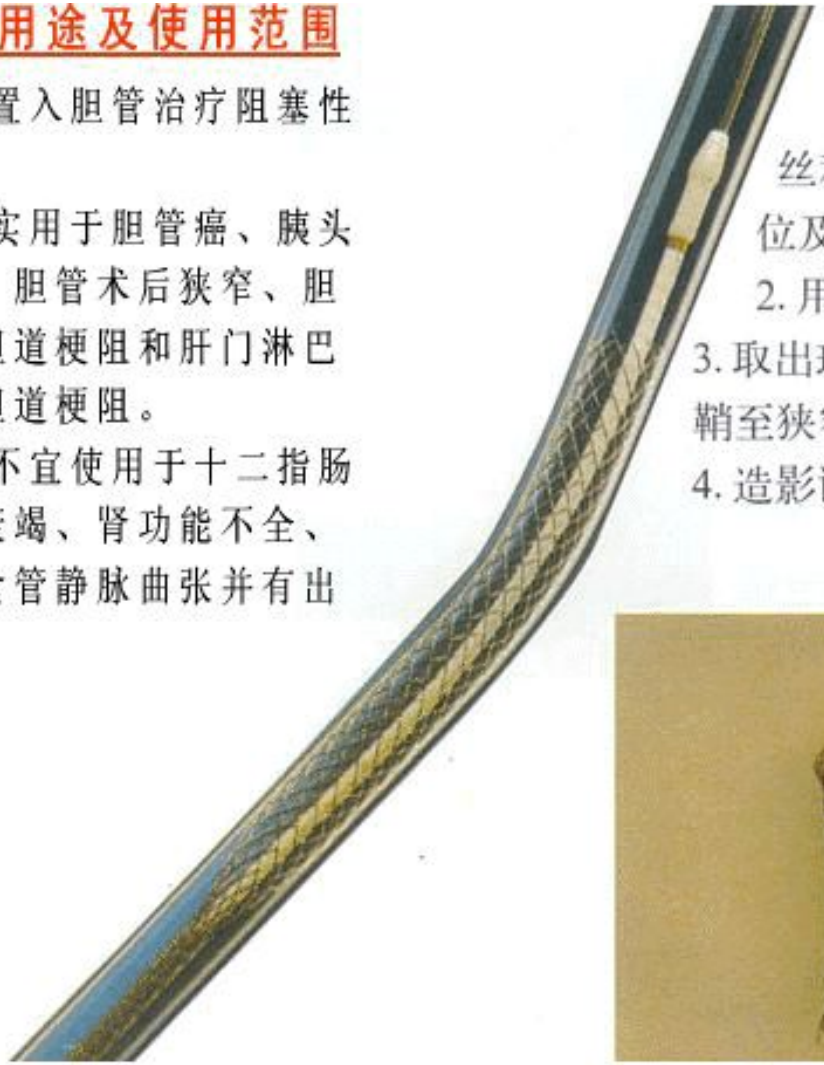

胆道支架置入方法：

1. 经皮肝穿刺胆，插入导丝和导管后造影，测定狭窄的部位及尺寸，以便选定支架型号。
2. 用球囊扩张管作胆道扩张。
3. 取出球囊扩张管，沿导丝置入支架鞘至狭窄部位后推出胆道支架。
4. 造影证实胆管通畅后技拔出导管。

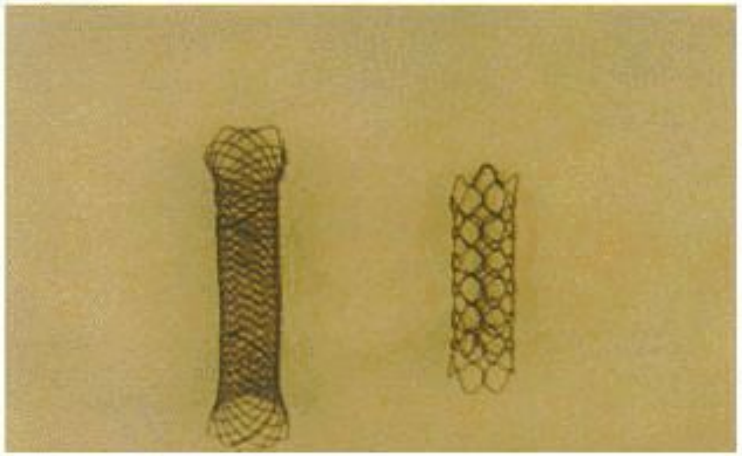

前列腺支架

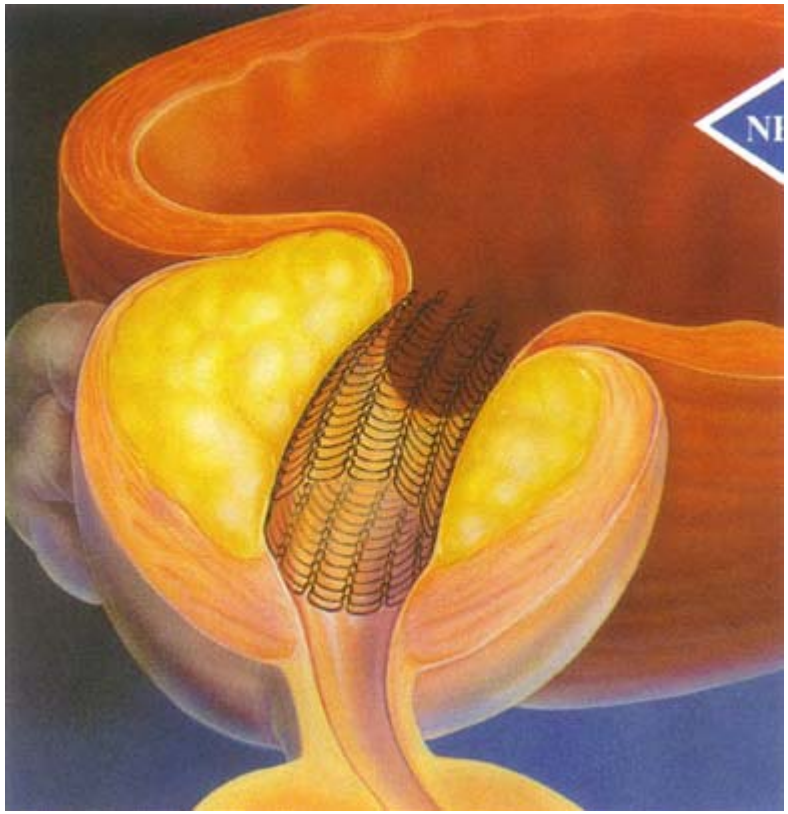

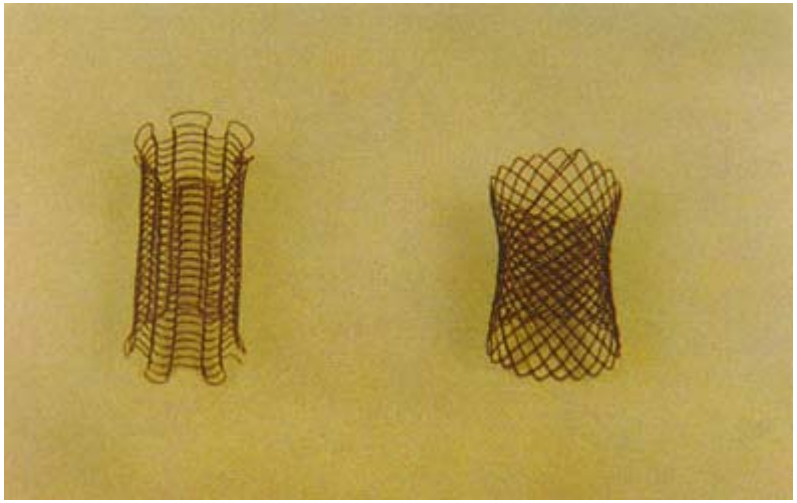

股骨头支架

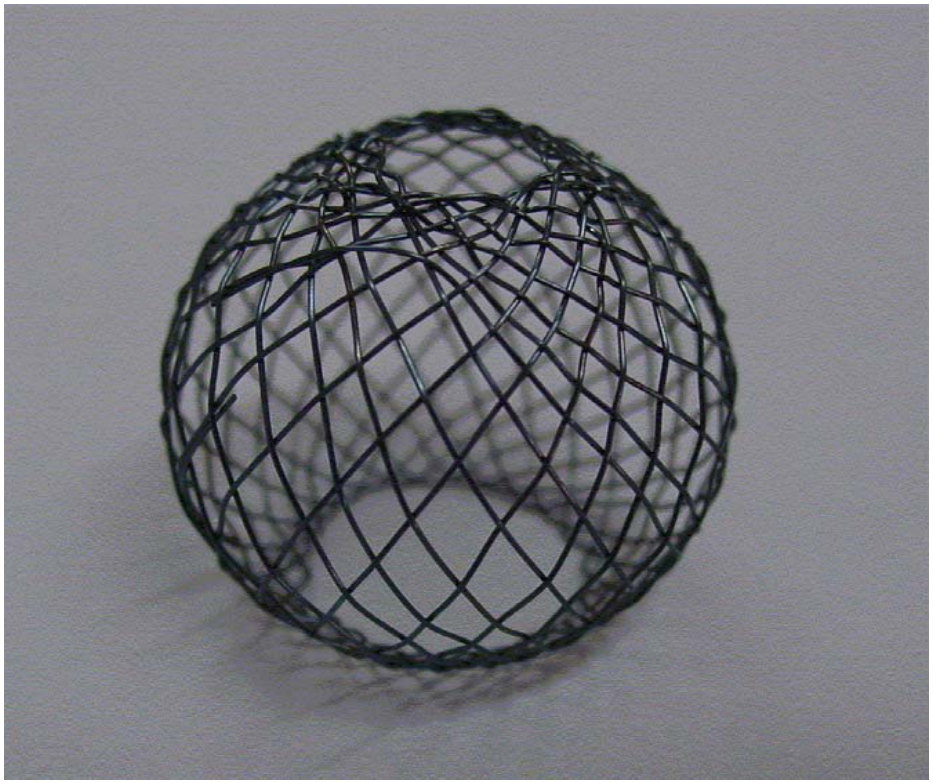

各种形状的腔道内支架

血管支架-第I代

血管支架－第II代

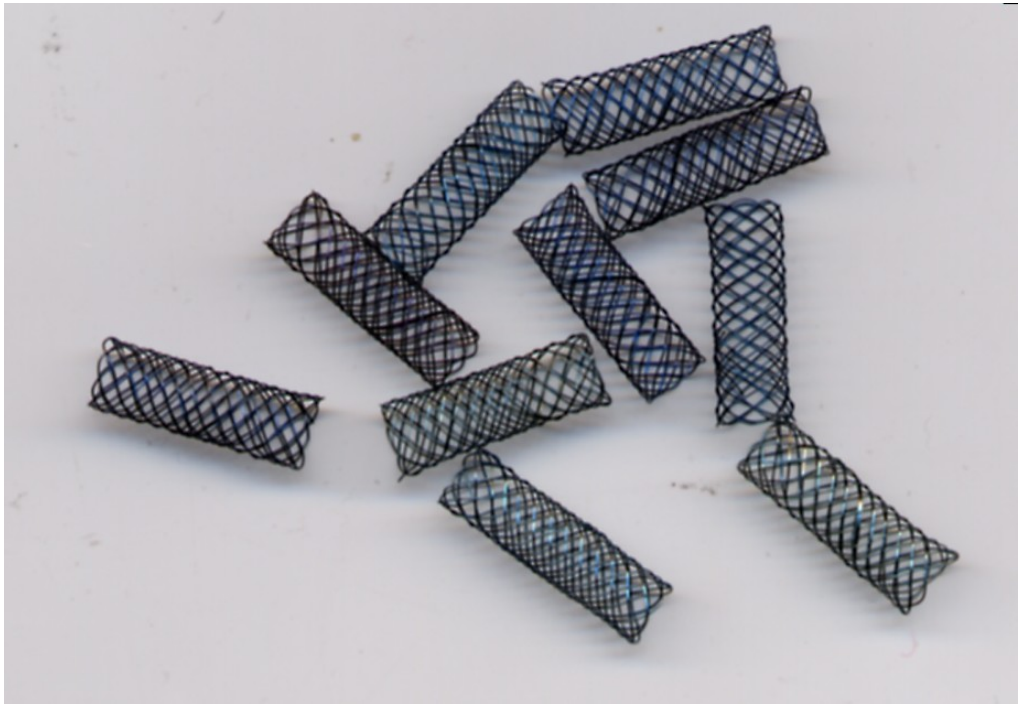

血管支架－第III代

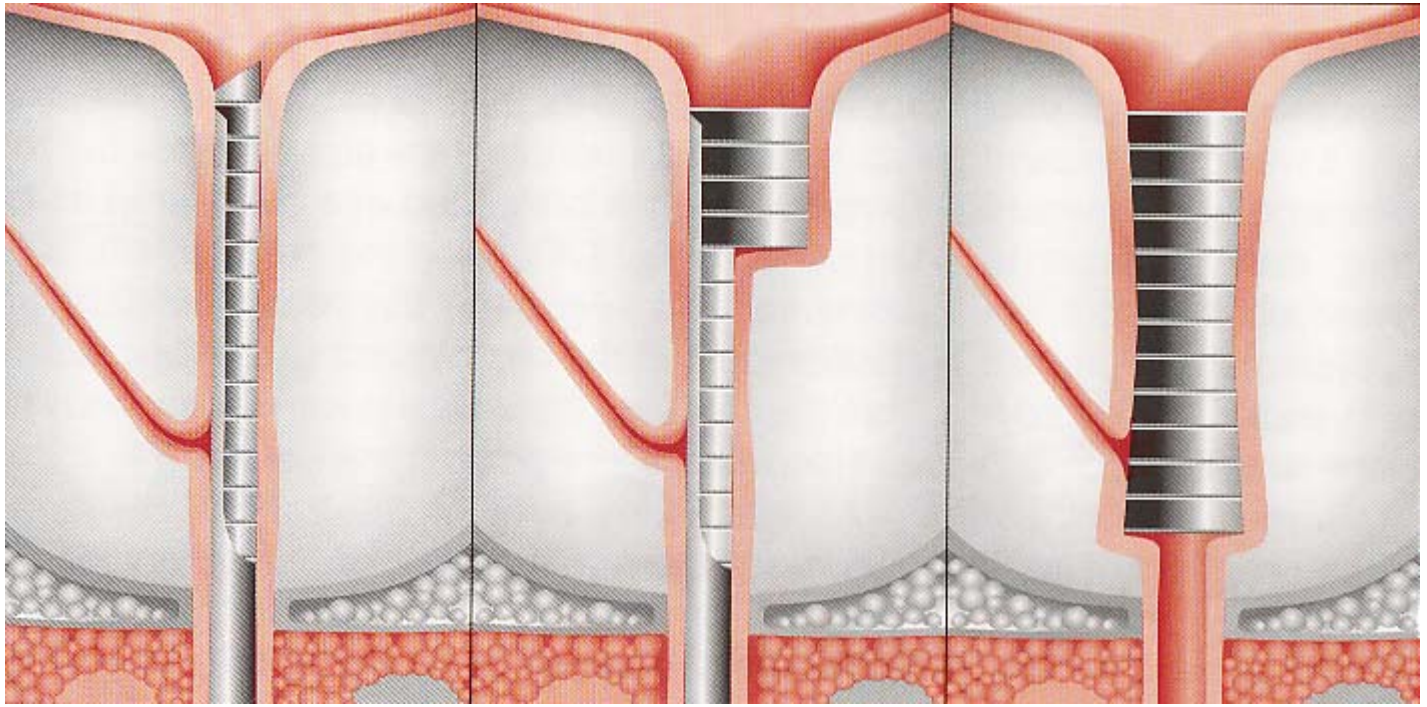

血管支架－第Ⅳ代

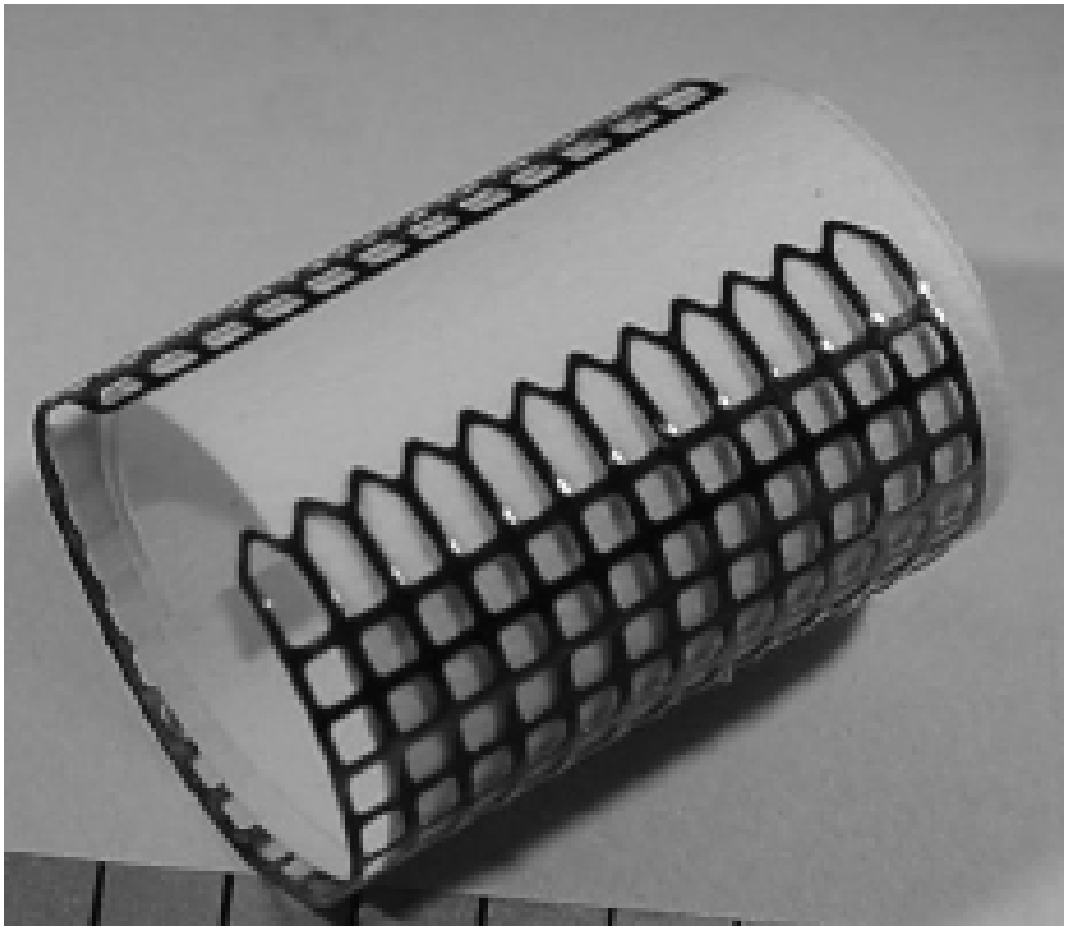

血管支架－第V代

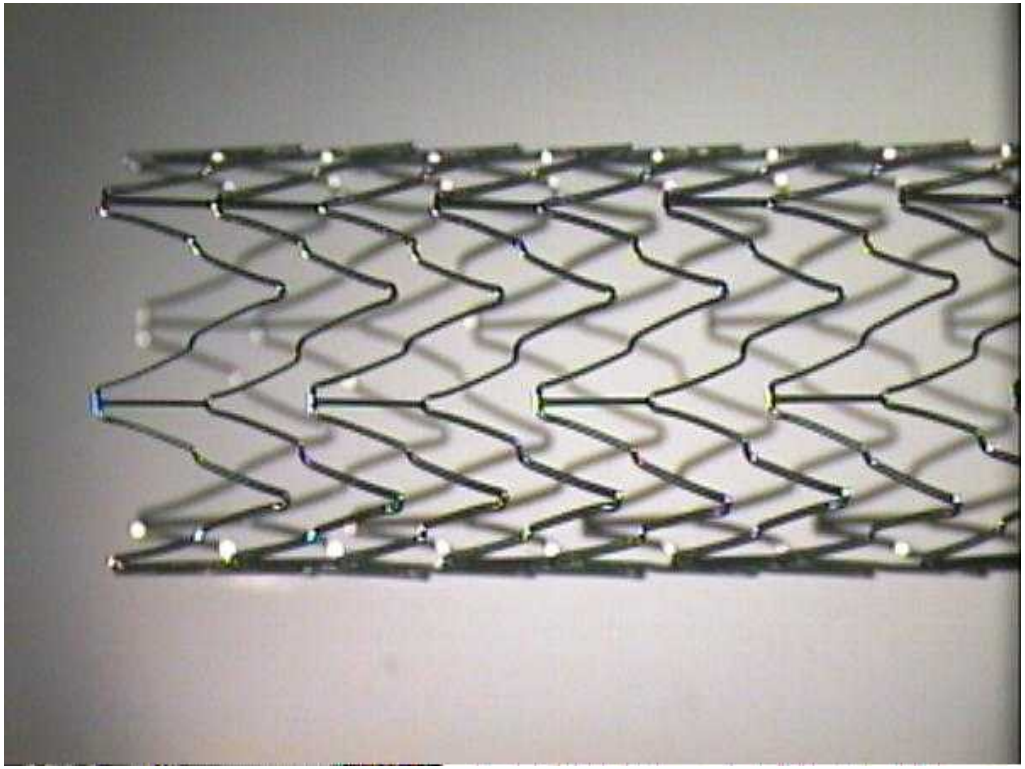

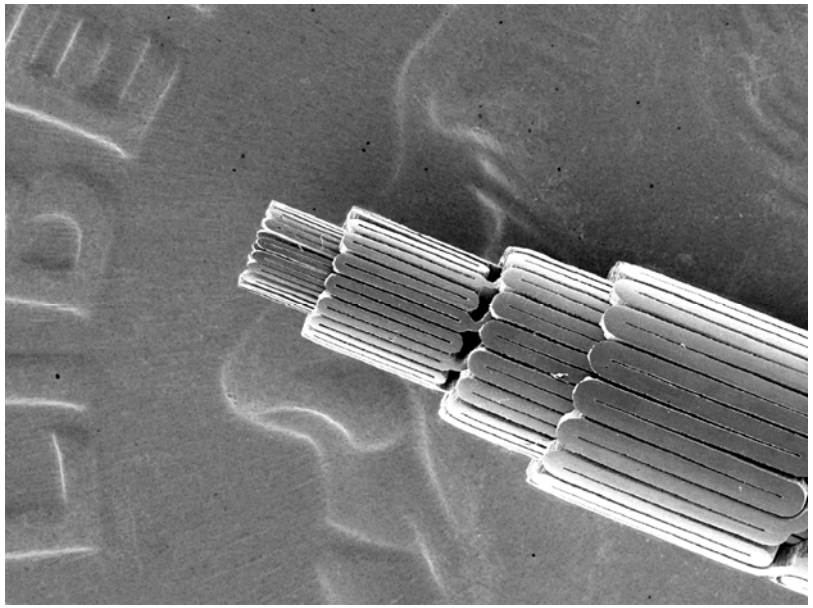

镍钛合金腹主动脉血管支架

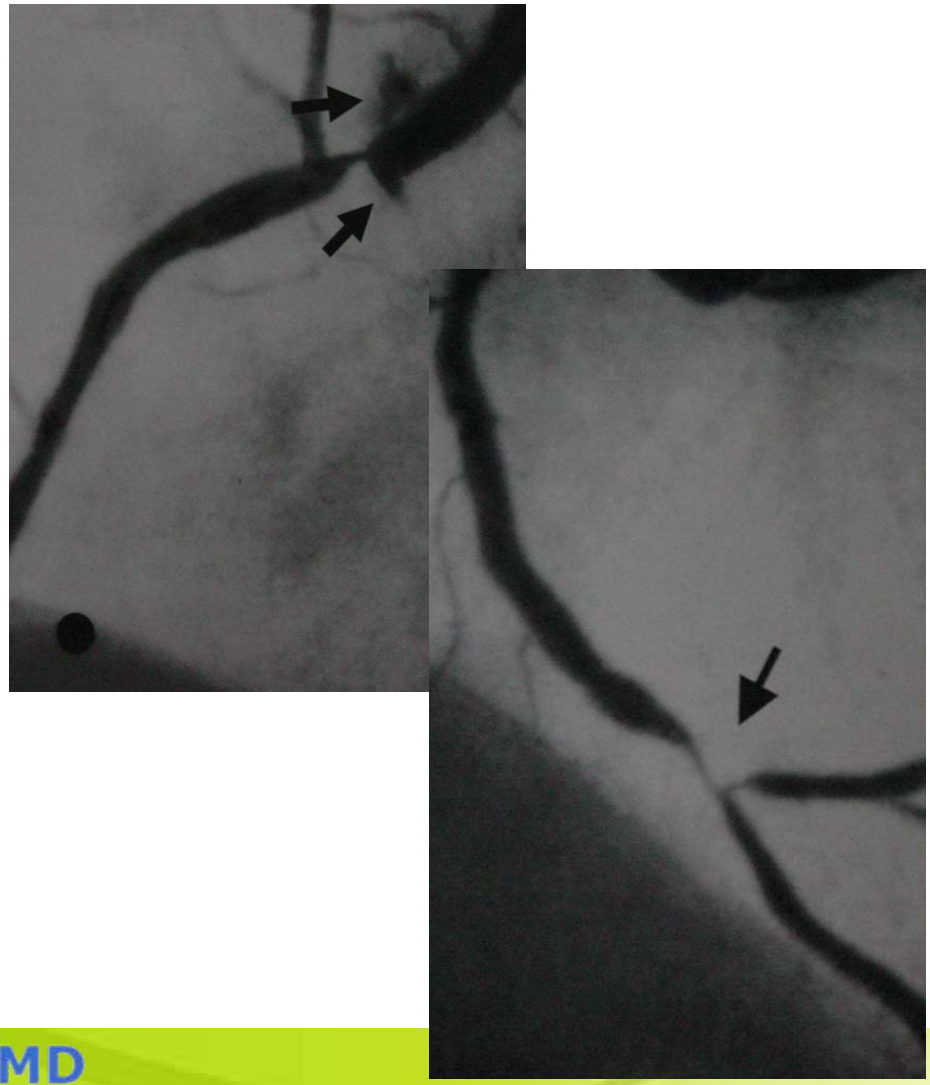

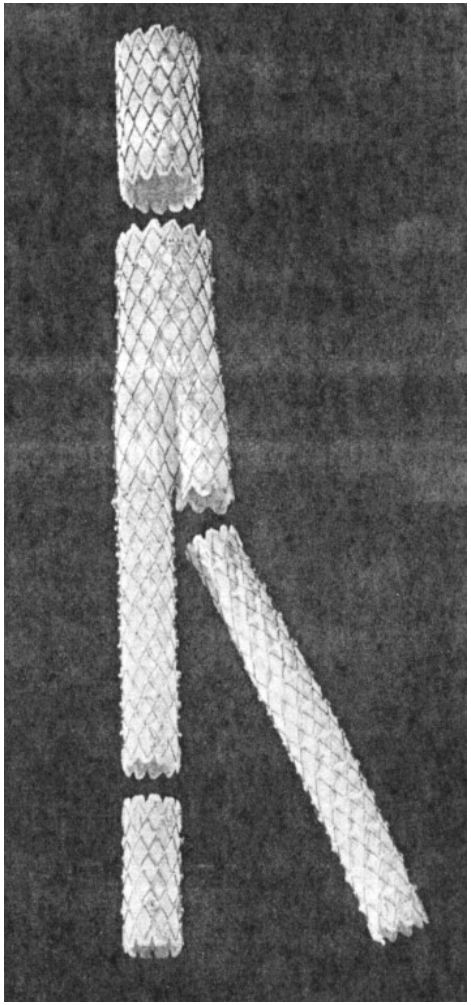

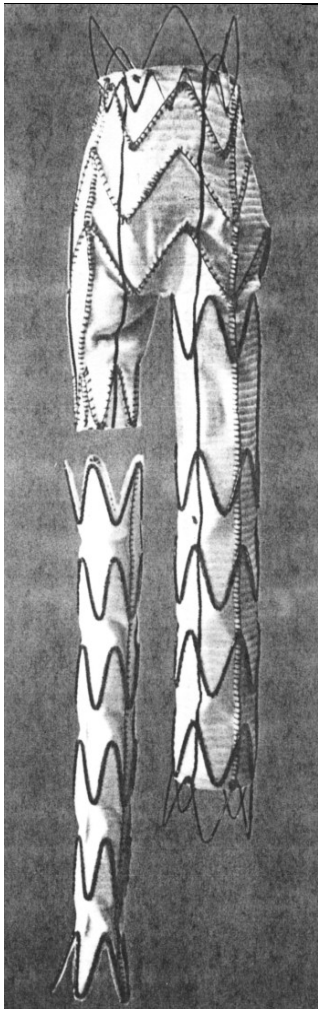

镍钛合金碎片收集装置

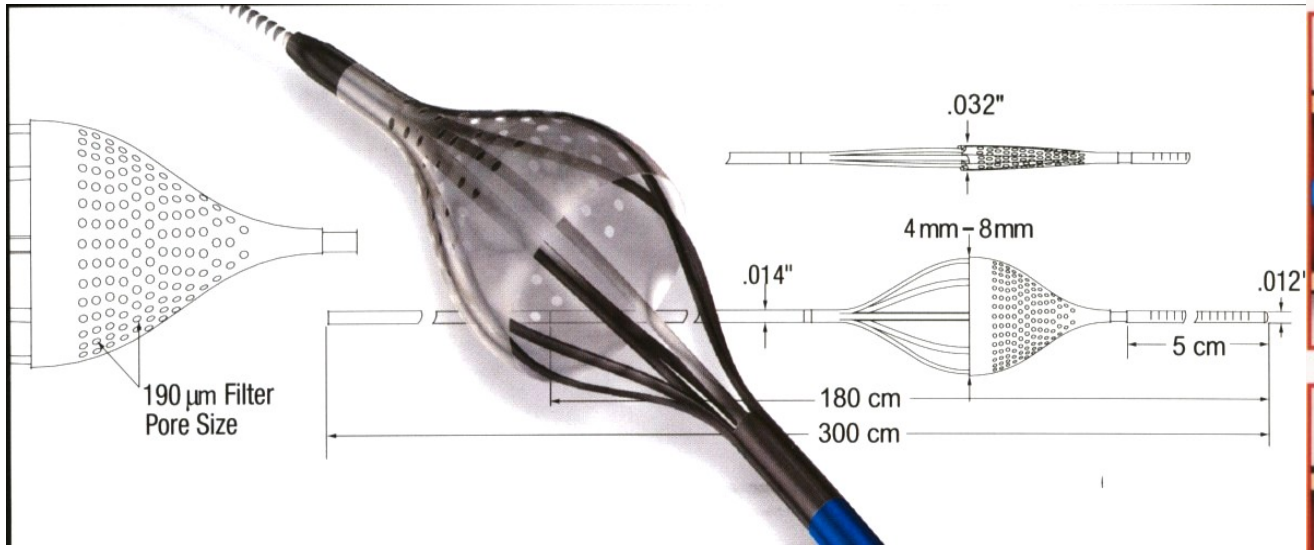

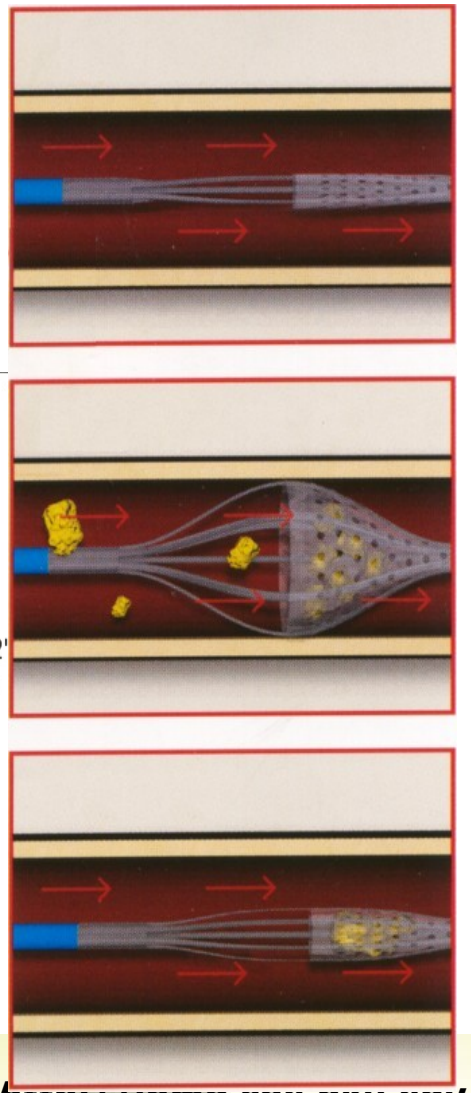

镍钛合金远端保护装置

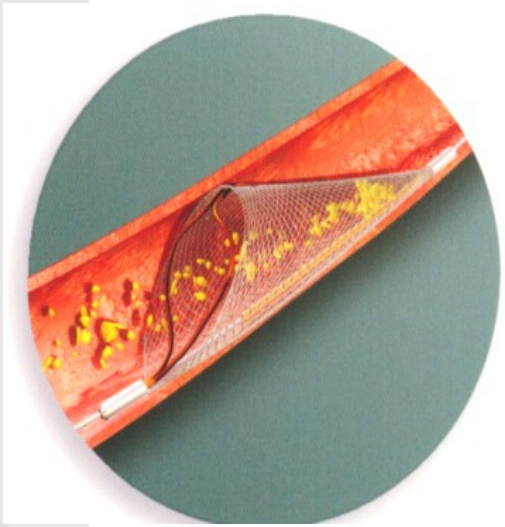

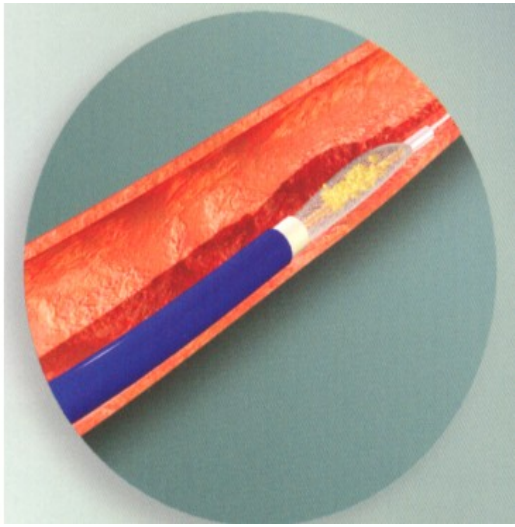

镍钛合金远端保护装置

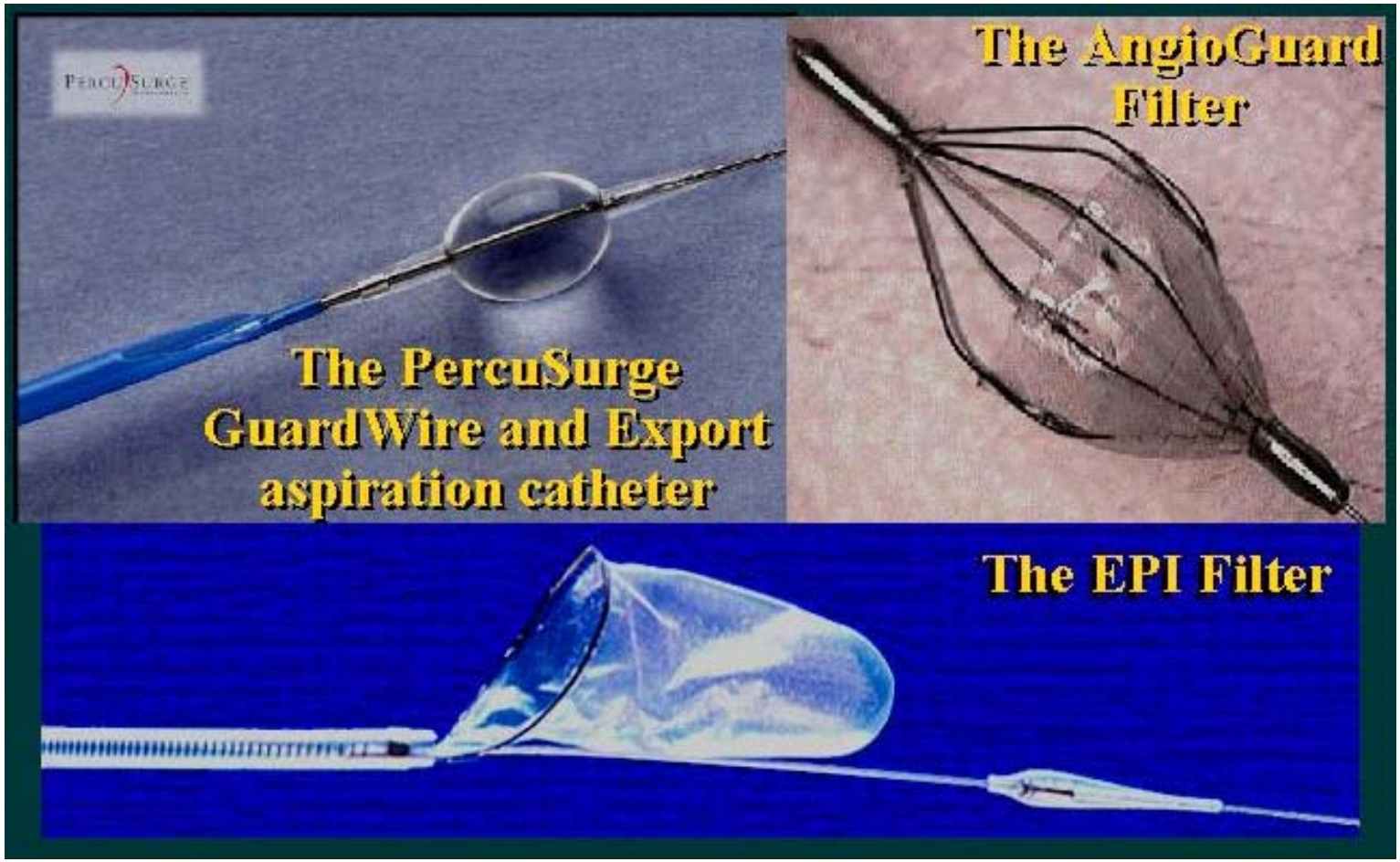
The PercuSurge GuardWire and Export aspiration catheter
The AngioGuard Filter
The EPI Filter

镍钛合金导引导丝(guidewire)

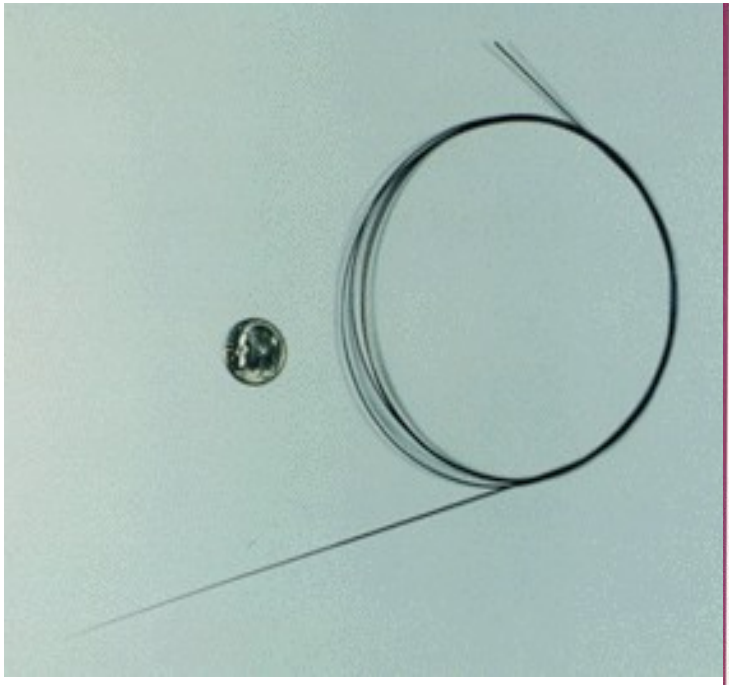

导丝也是经皮冠状动脉腔内成形术系统的重要组成之一。导丝有3个基本组成：中间操纵杆、远端弹性弹簧圈及外涂层。

镍钛合金房间隔缺损堵闭器(ASD Occluder)

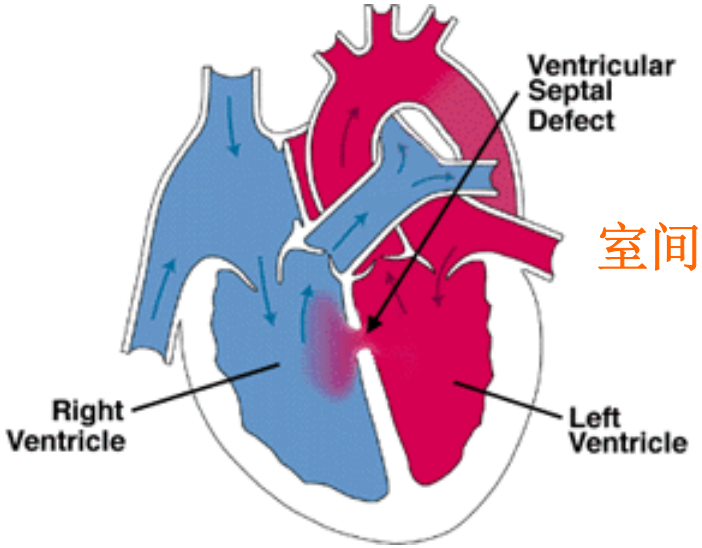

室间隔缺损

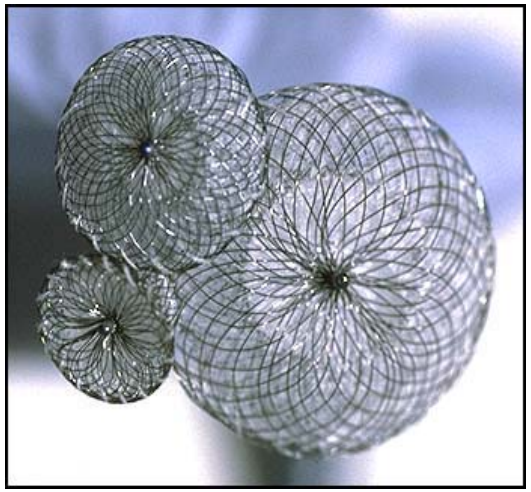

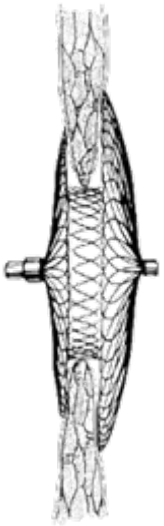

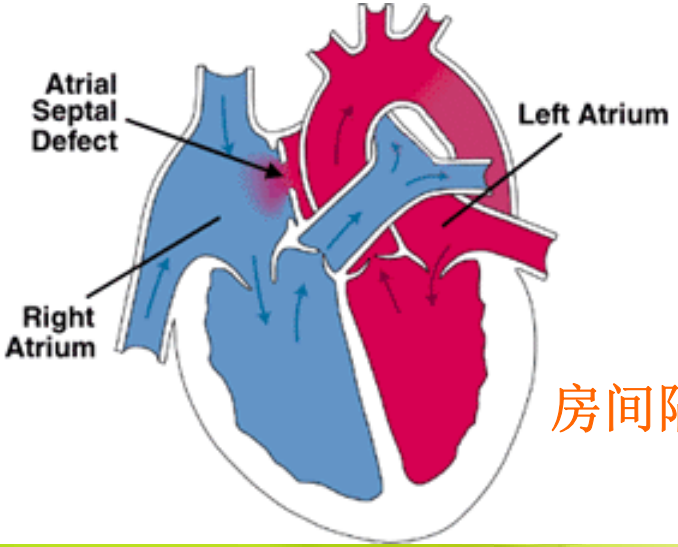

房间隔缺损

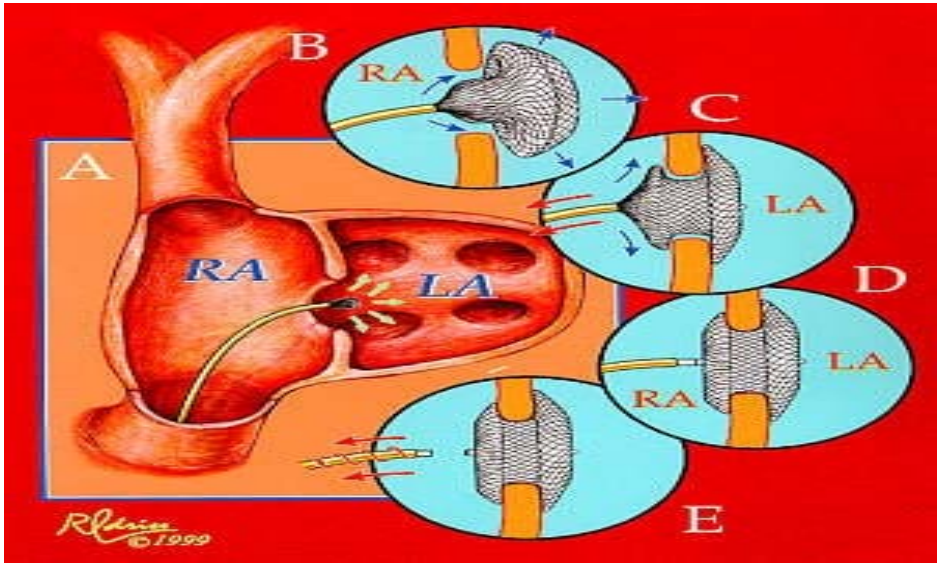

镍钛合金动脉导管未闭堵闭器(PDA Occluder)

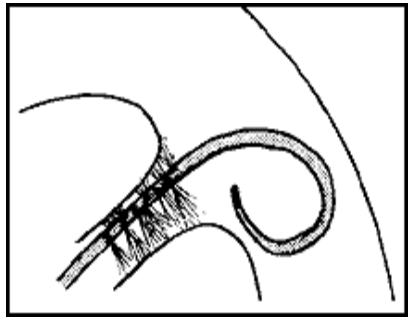
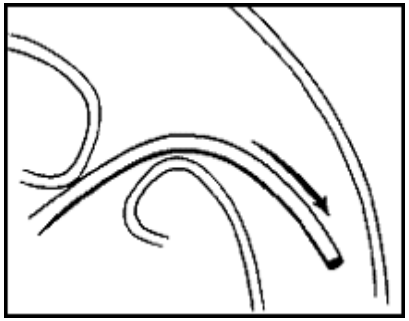
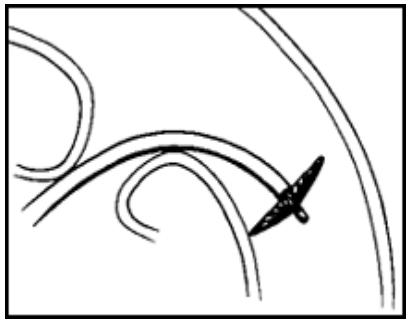
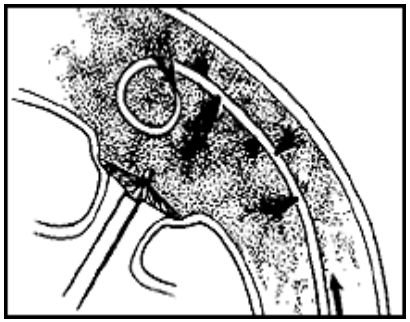
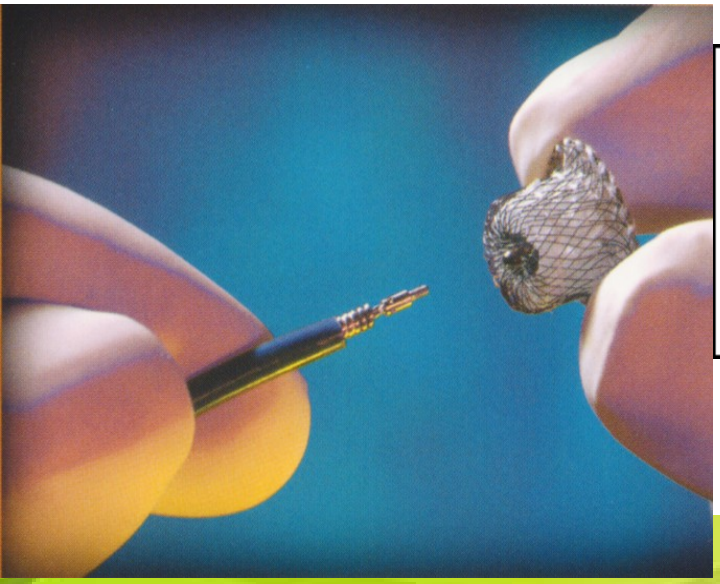
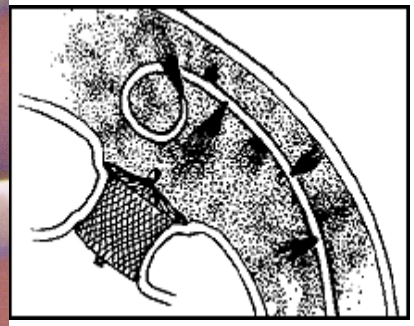
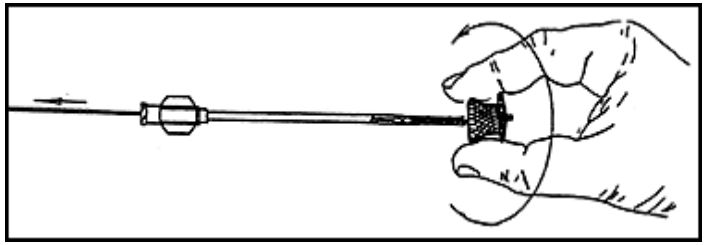

镍钛合金室间隔缺损堵闭器(VSD Occluder)

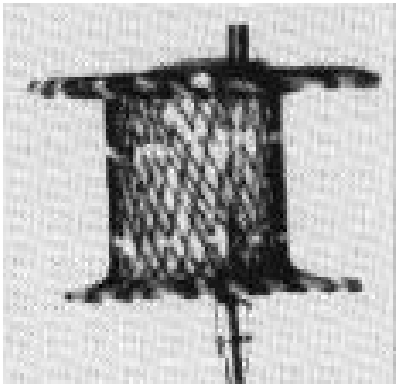

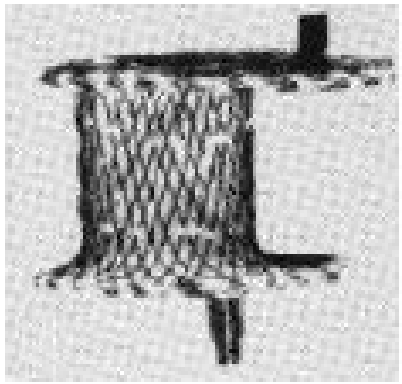

镍钛合金房间隔缺损堵闭器(ASD Occluder)

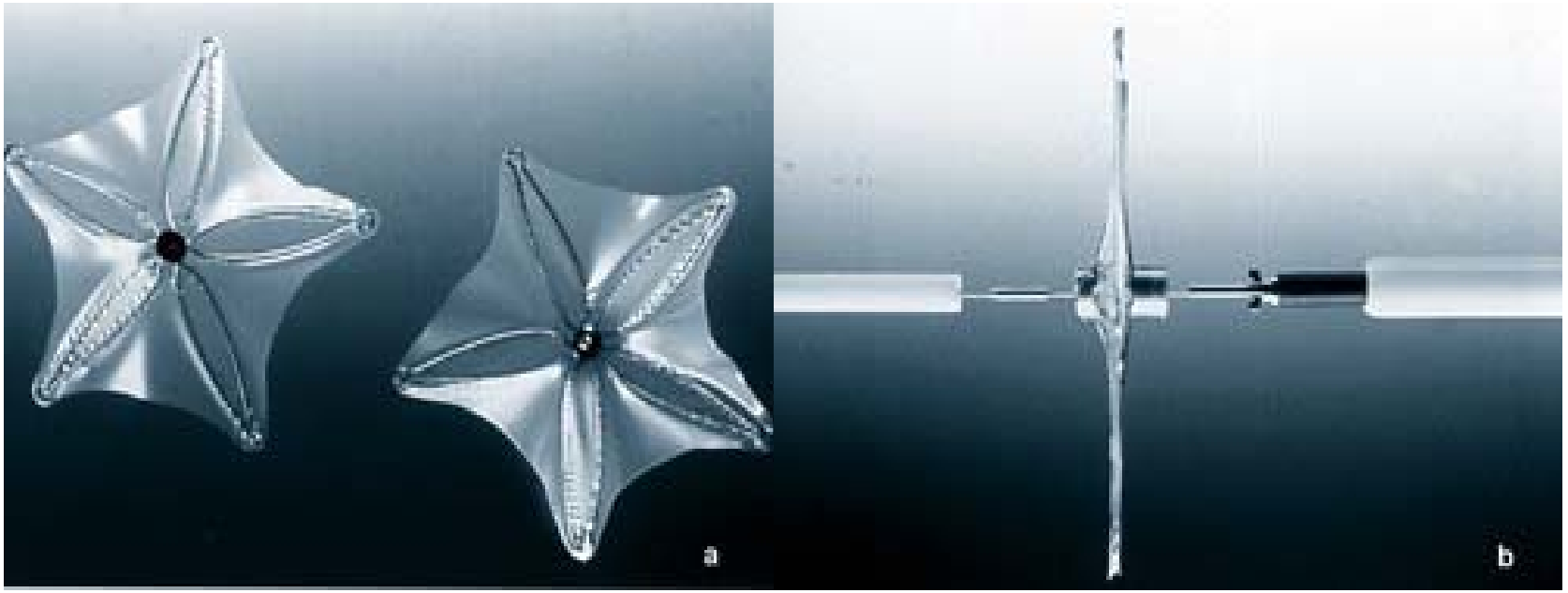

镍钛合金血栓过滤器(filter)

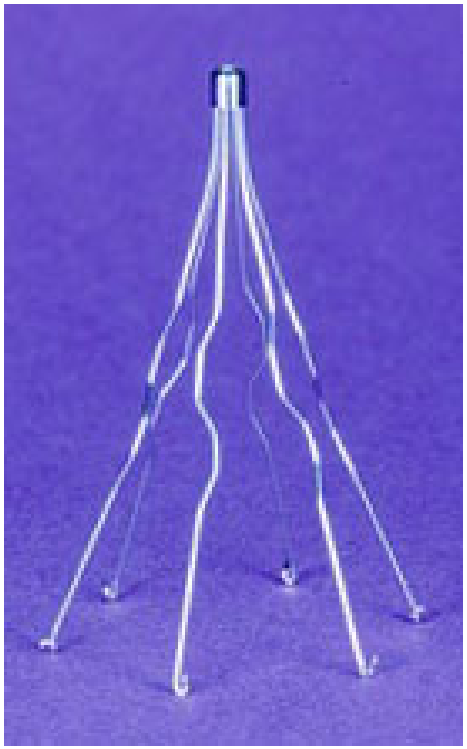

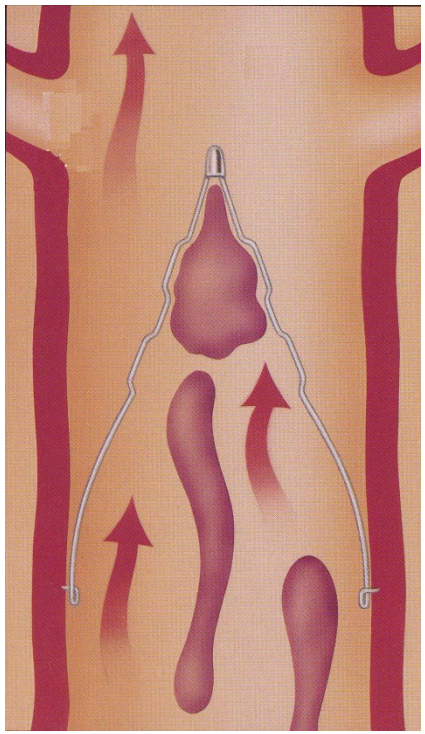

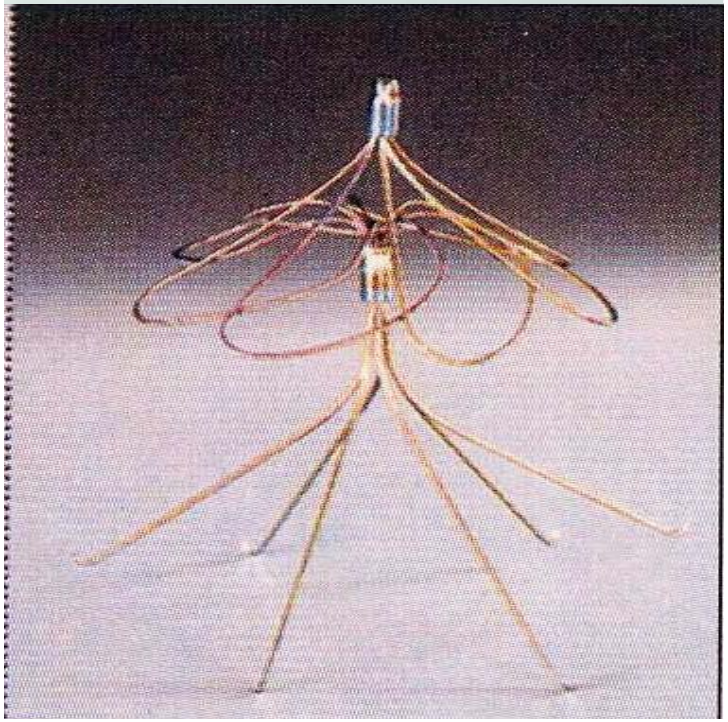

镍钛合金血栓过滤器(filter)

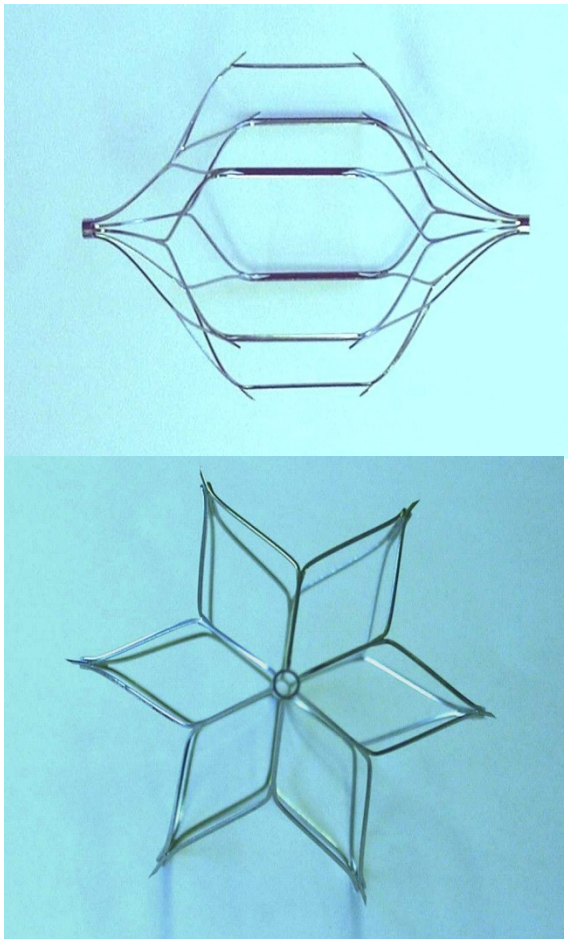

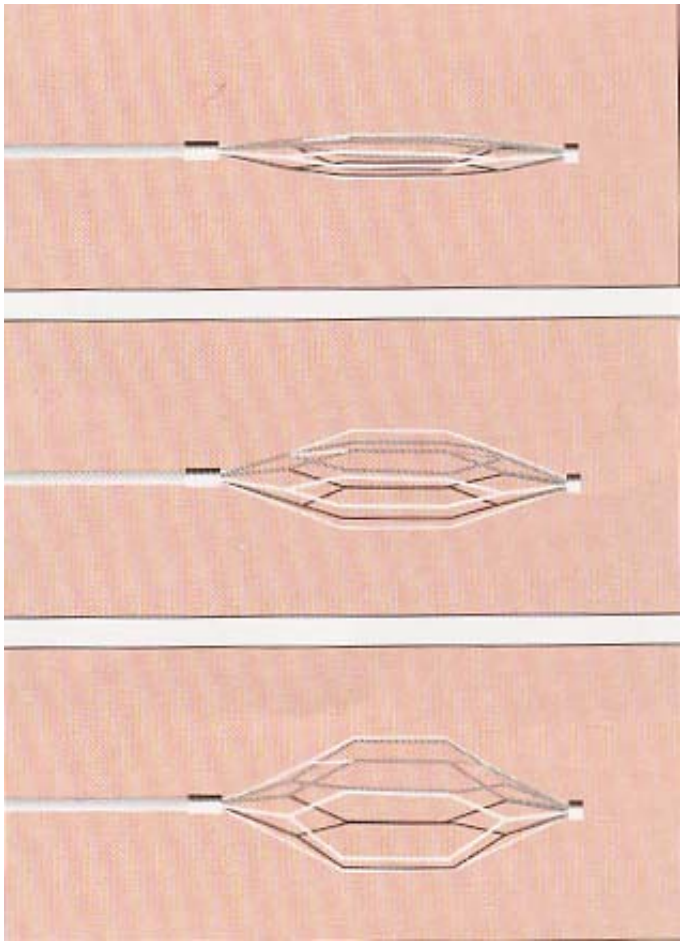

镍钛合金网篮(basket)

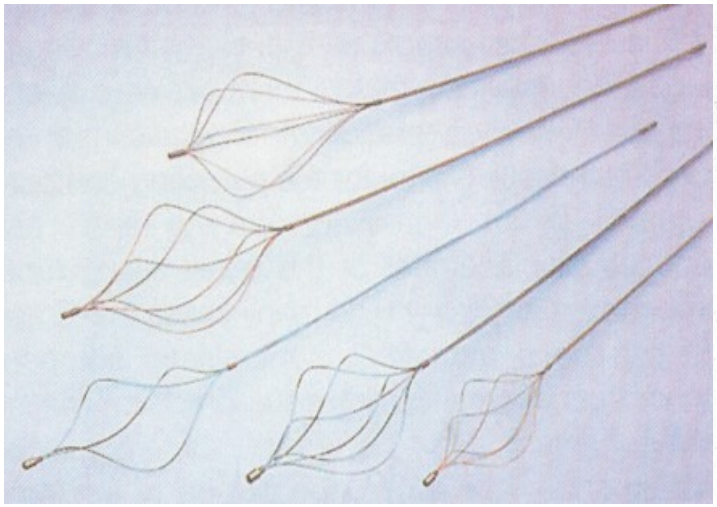

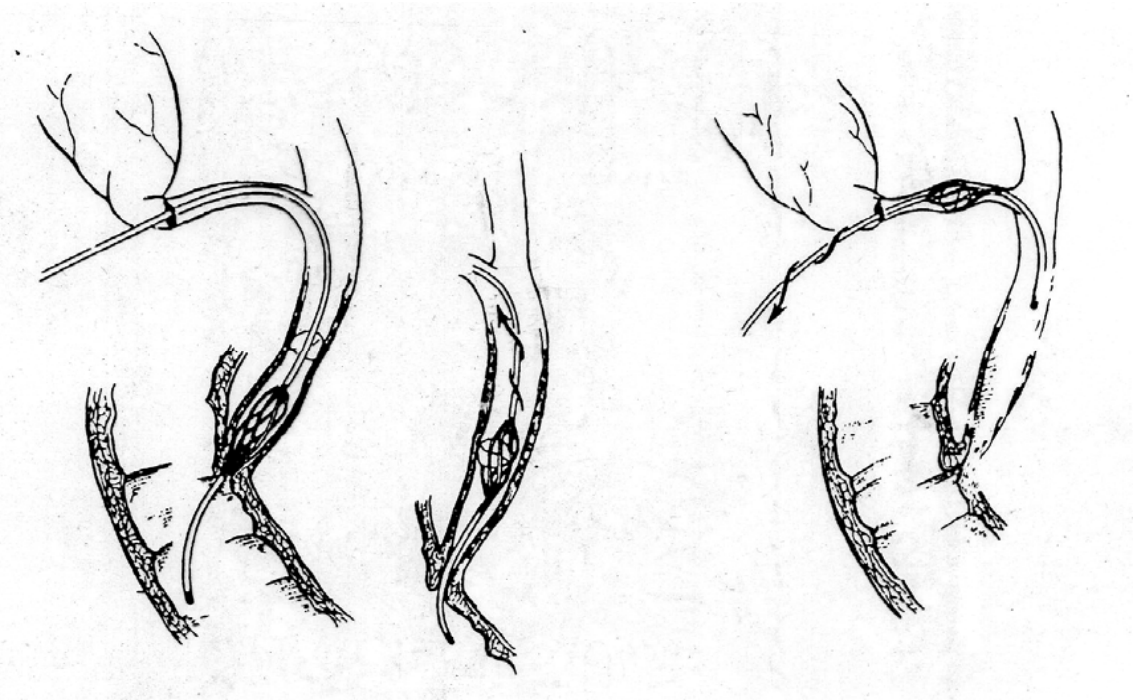

用于肾、膀胱、胆囊等部位的结石组织的收集取出。

镍钛合金圈套器 (snare)

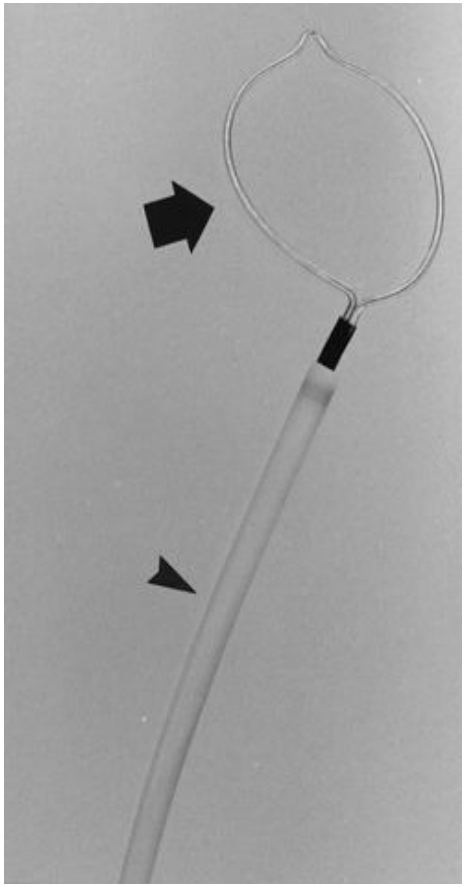

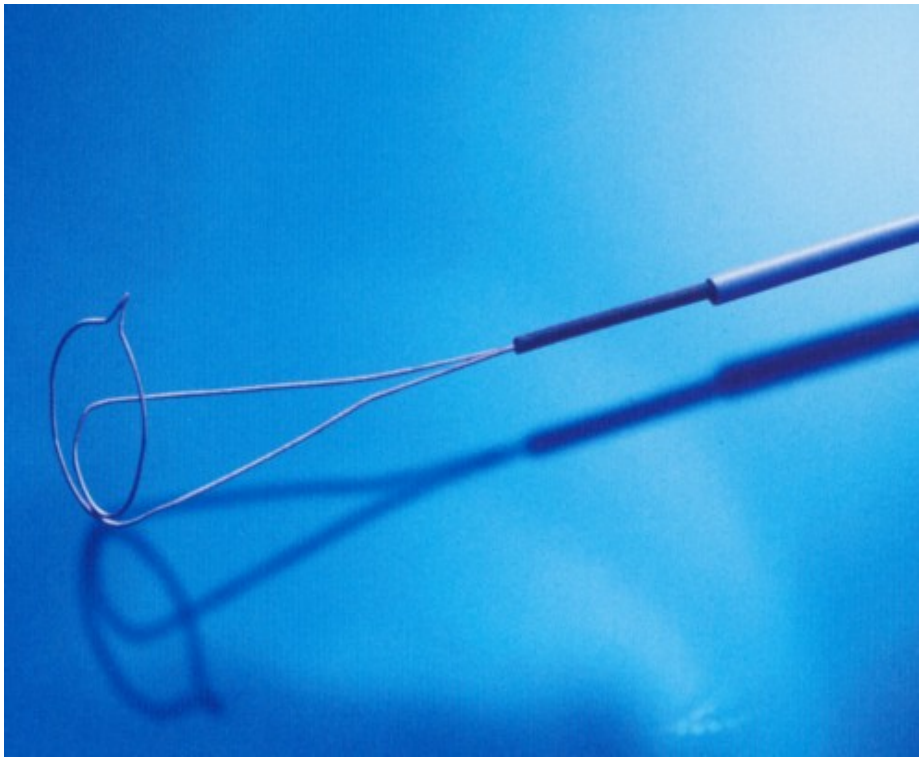

镍钛合金抓钳(Grasper)

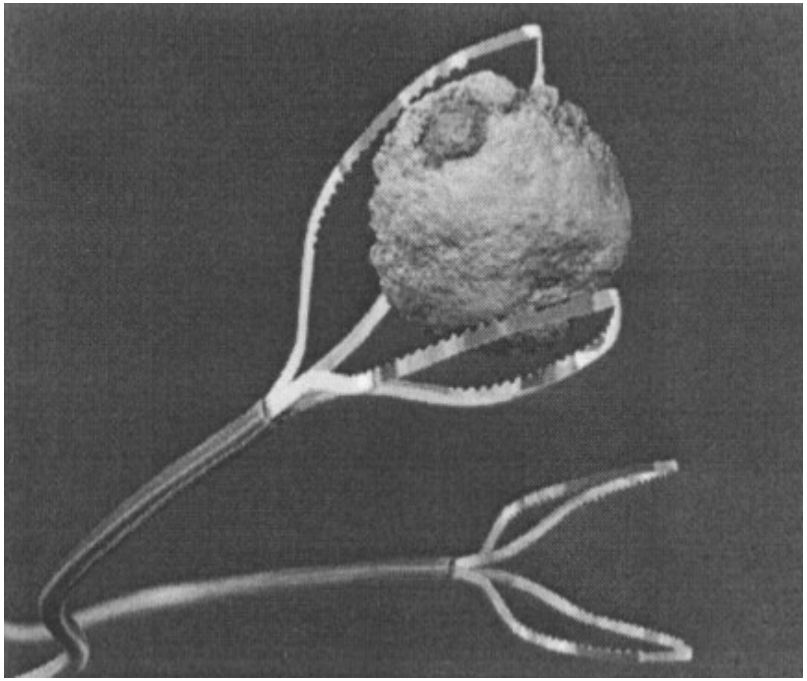

镍钛合金牵引器(retractor)

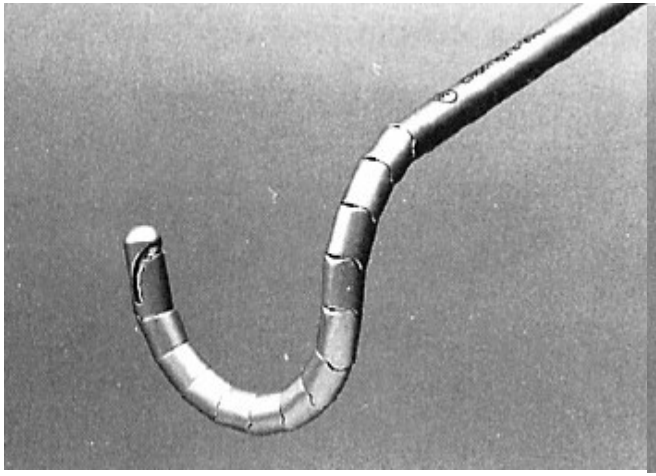

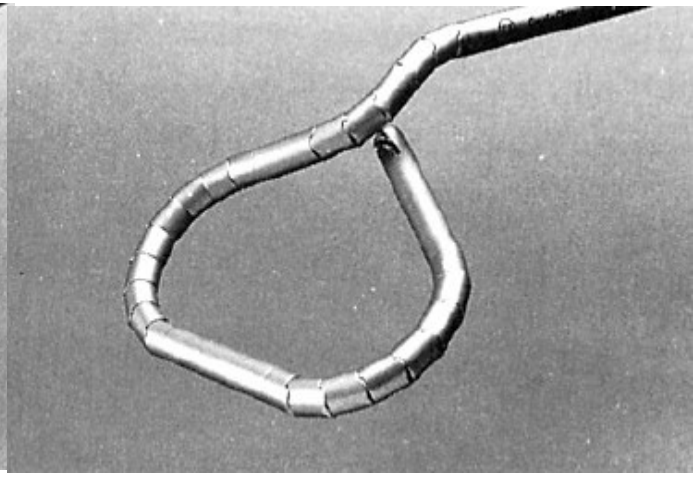

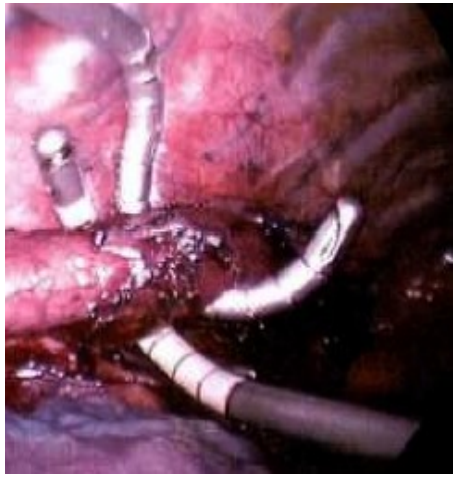

镍钛合金射频消融针

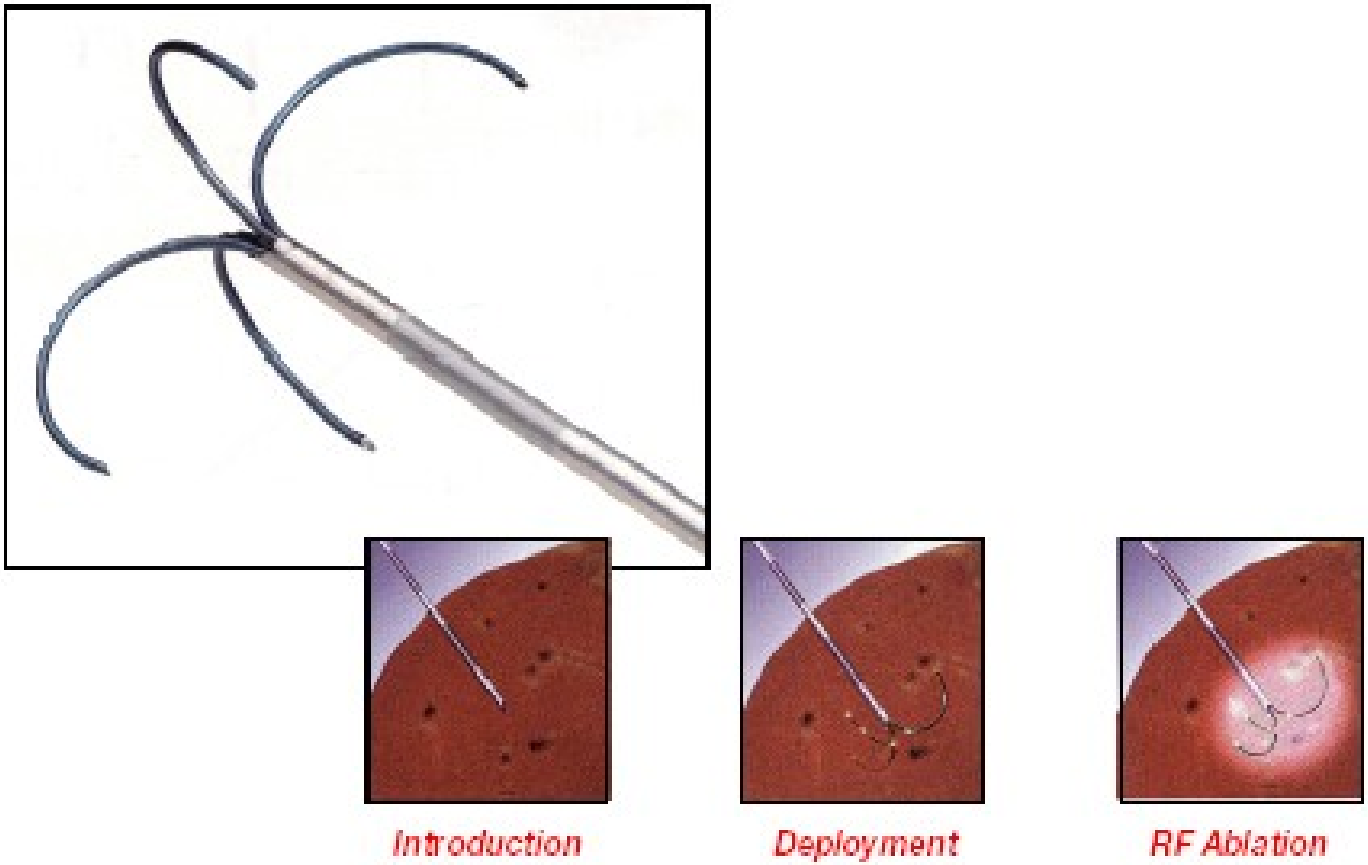

主要用于放射线工作者实现间质组织的射频消融。

镍钛合金药物注射管

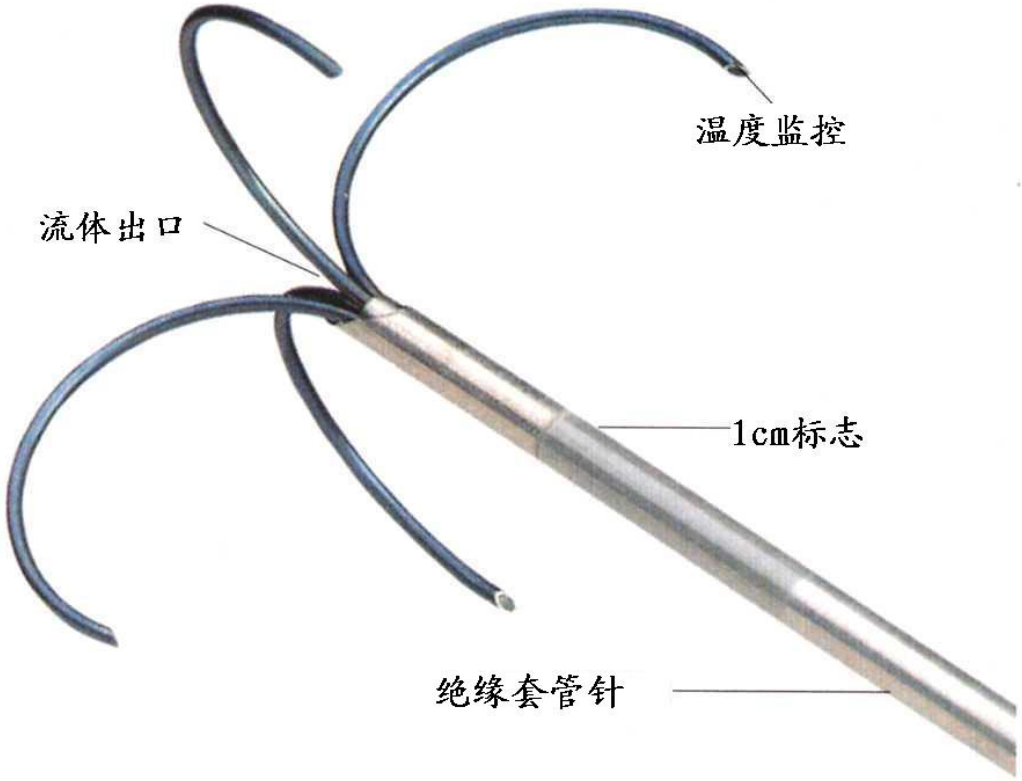

镍钛合金活剪钳

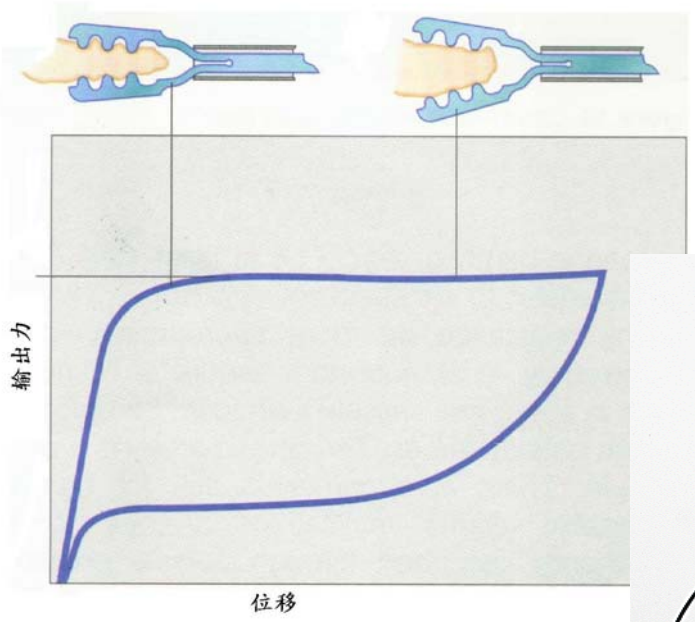

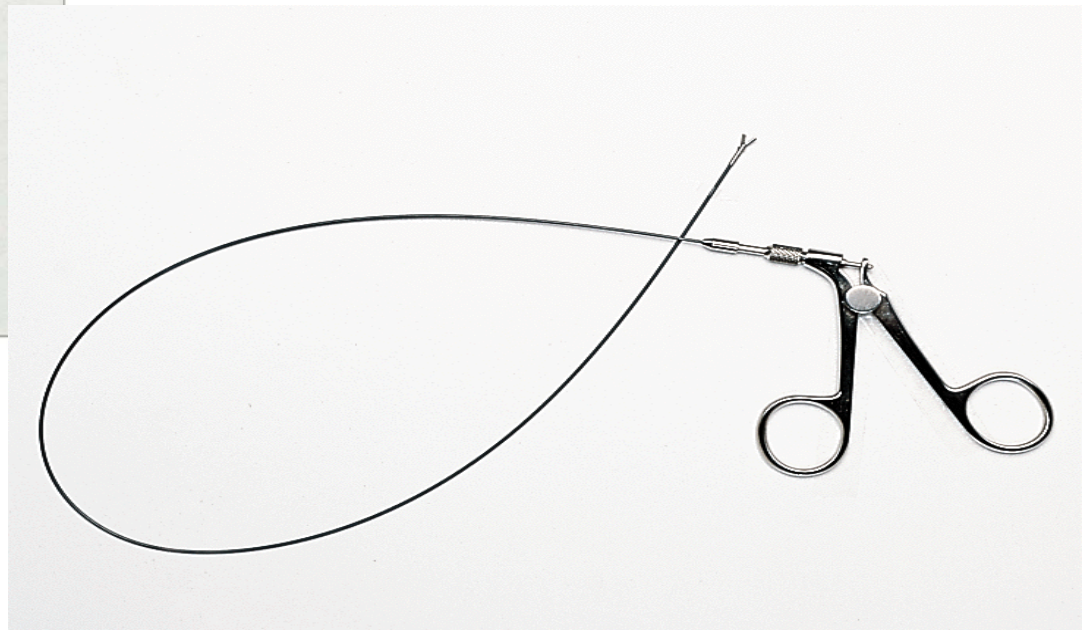

用于肿瘤等病变部位切片检查组织的夹取。

镍钛合金静脉瓣

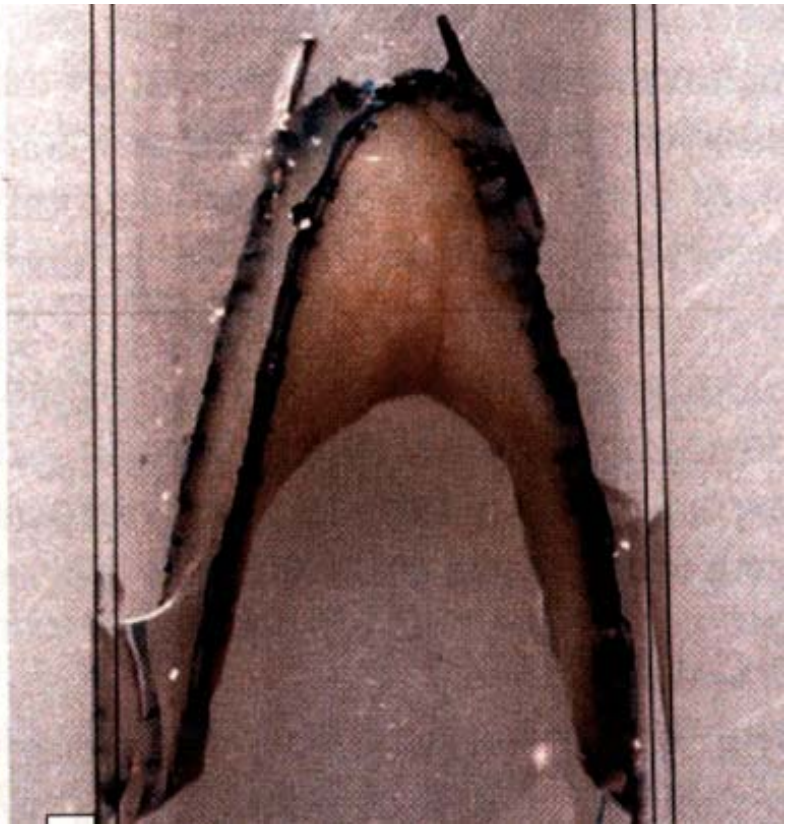

镍钛合金疝补丁夹

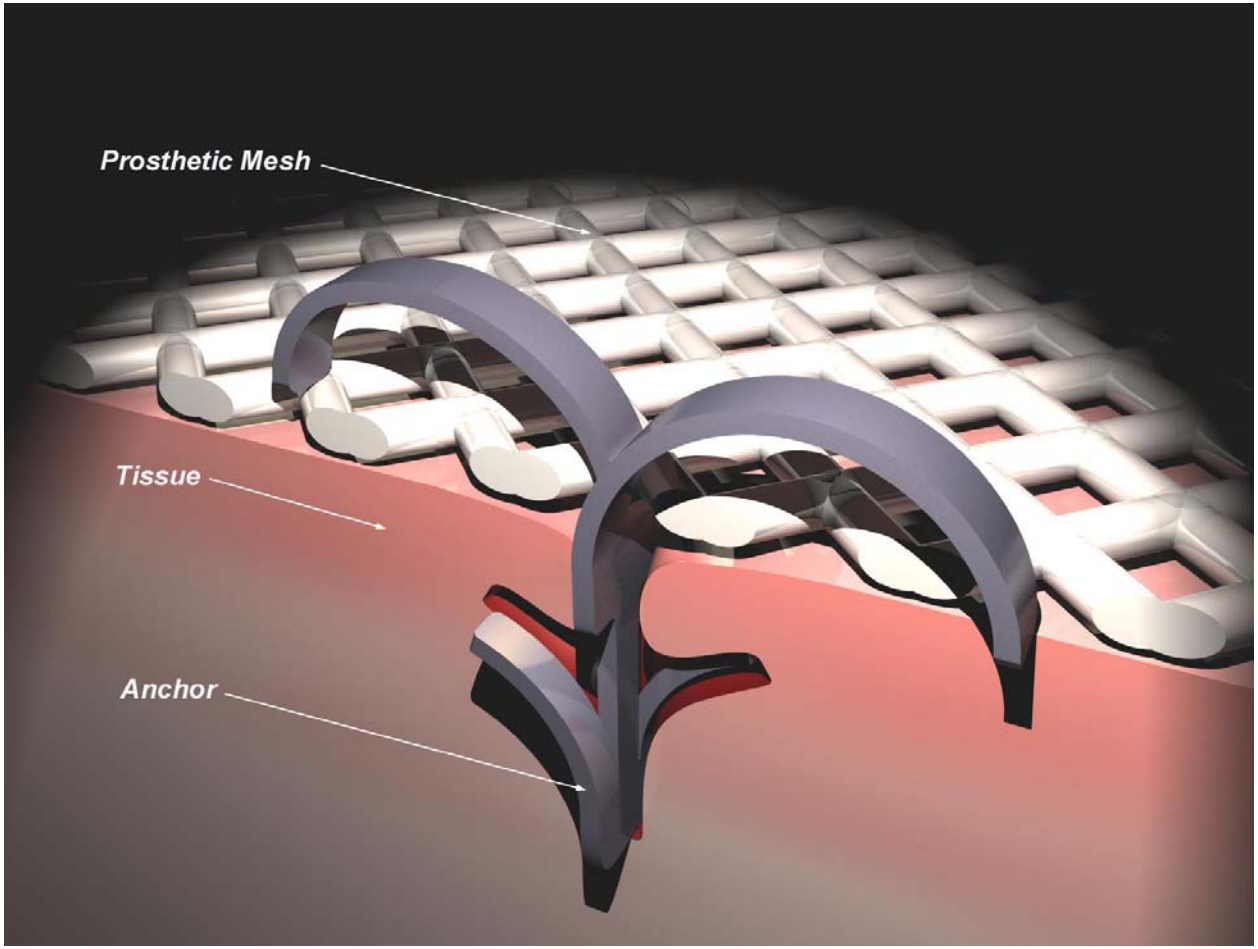

镍钛合金主动脉吻合夹

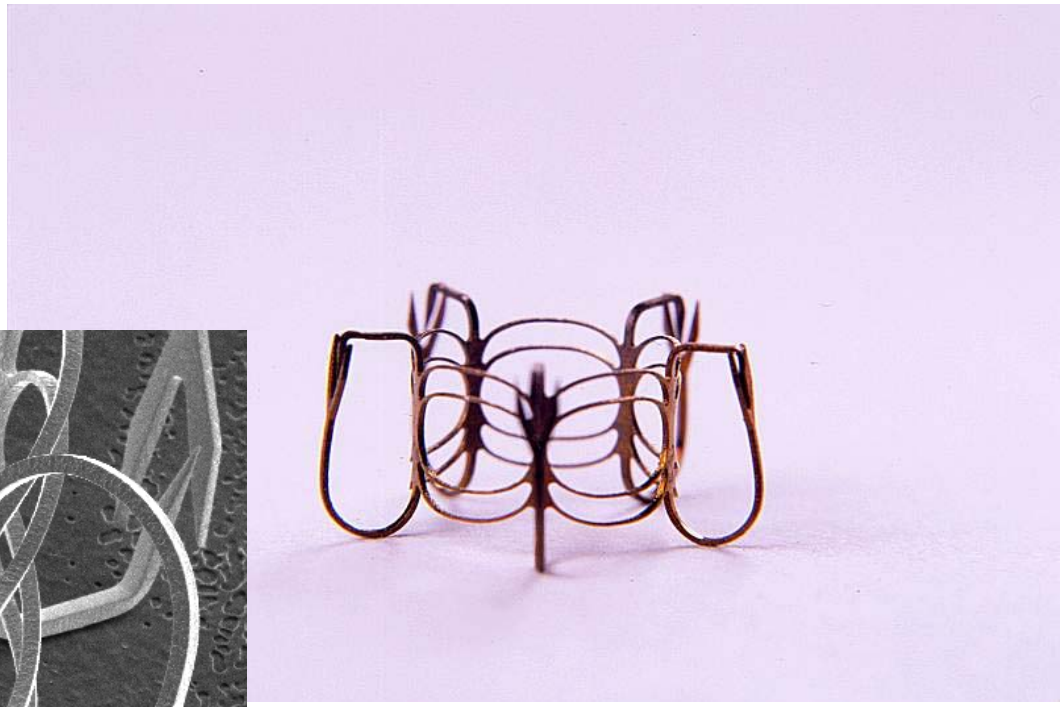

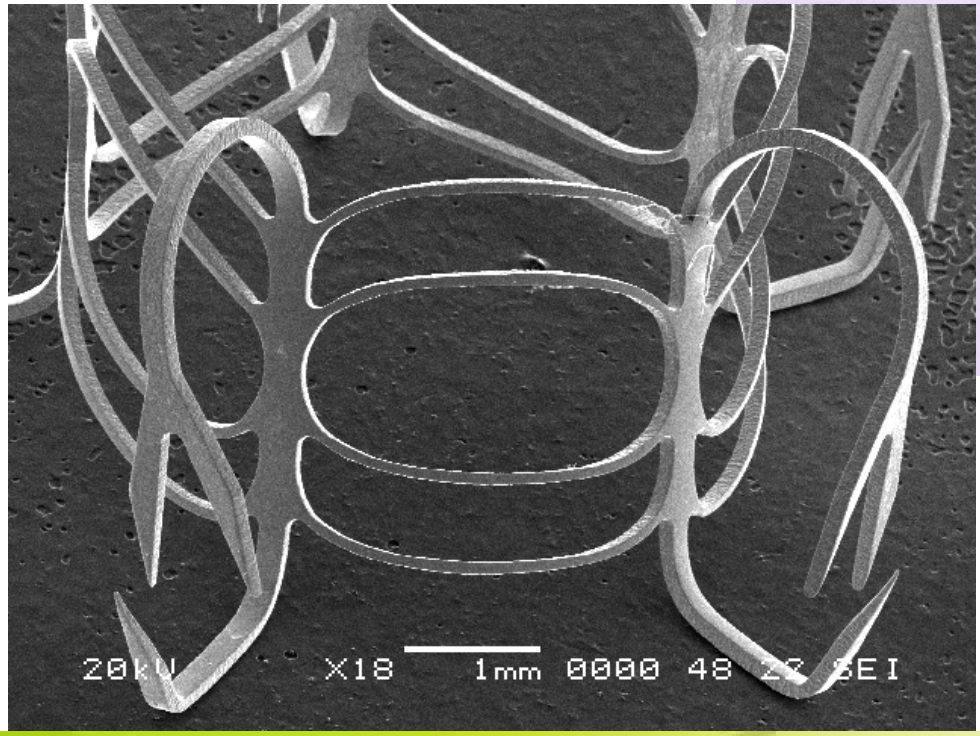

镍钛合金肠吻合夹

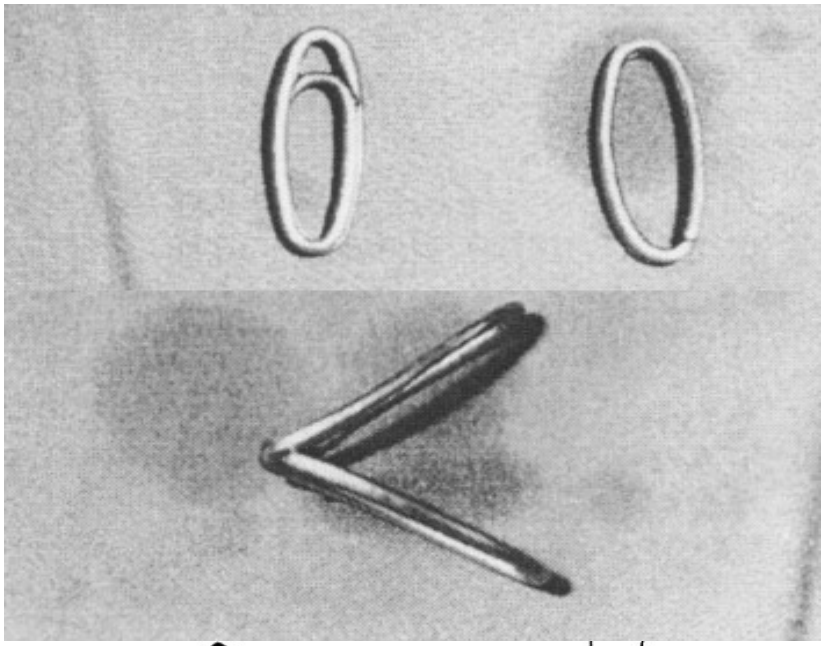

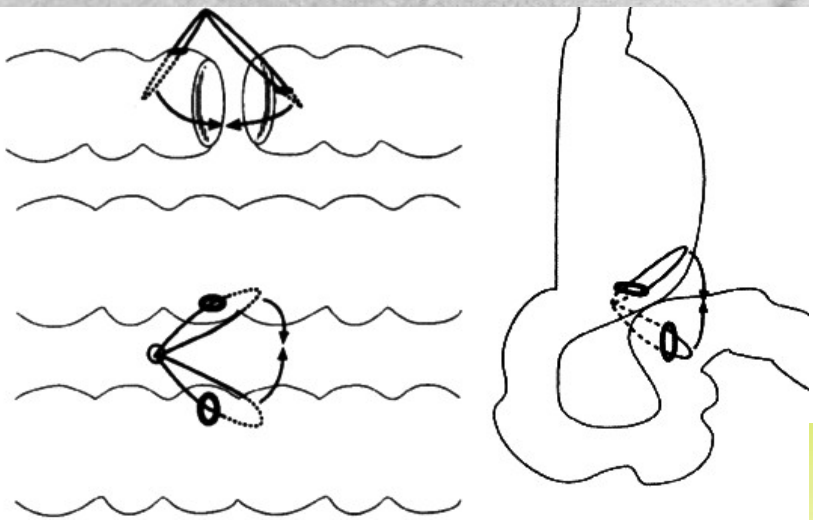

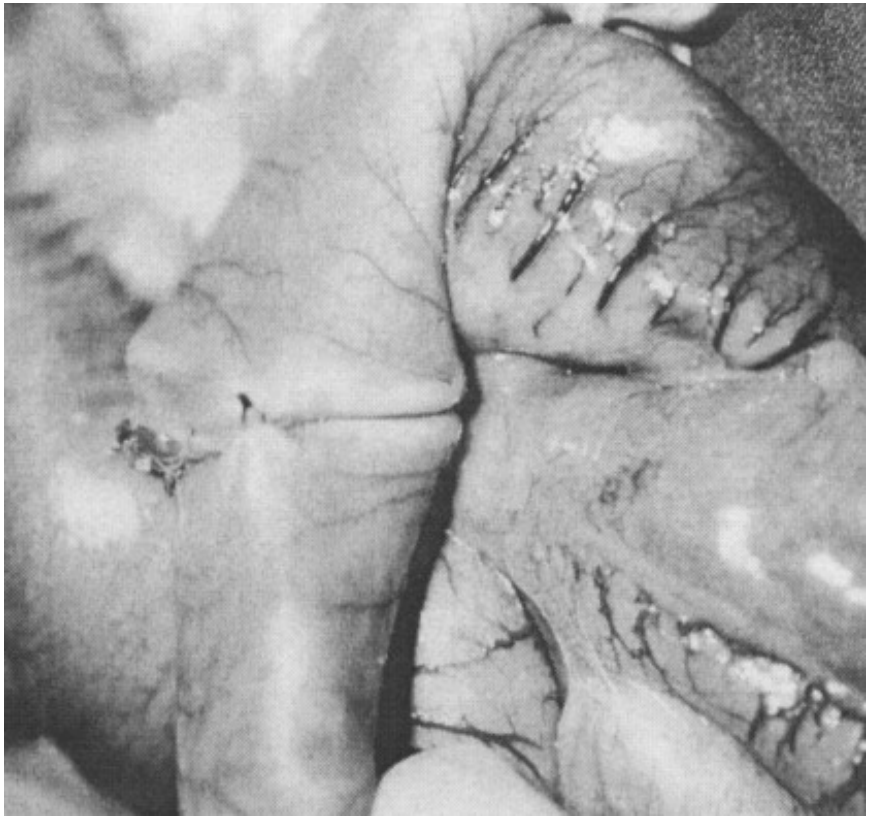

镍钛合金乳房肿块定位钩

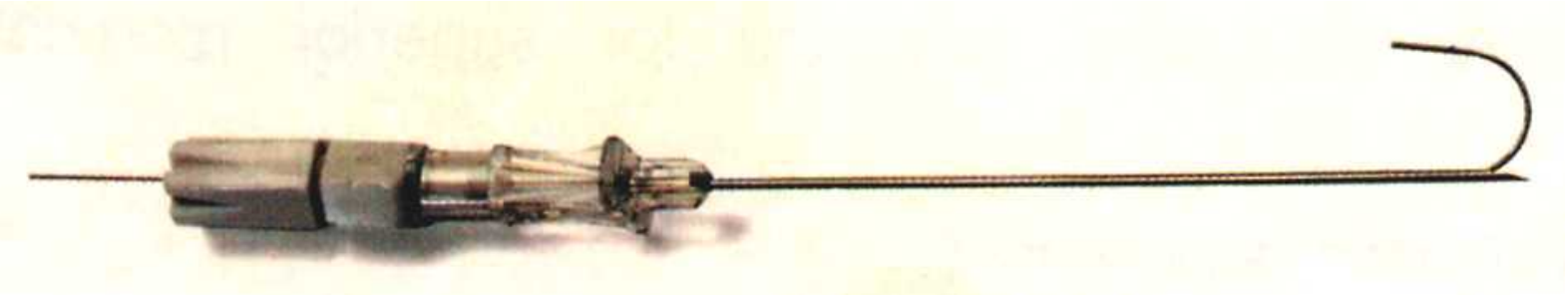

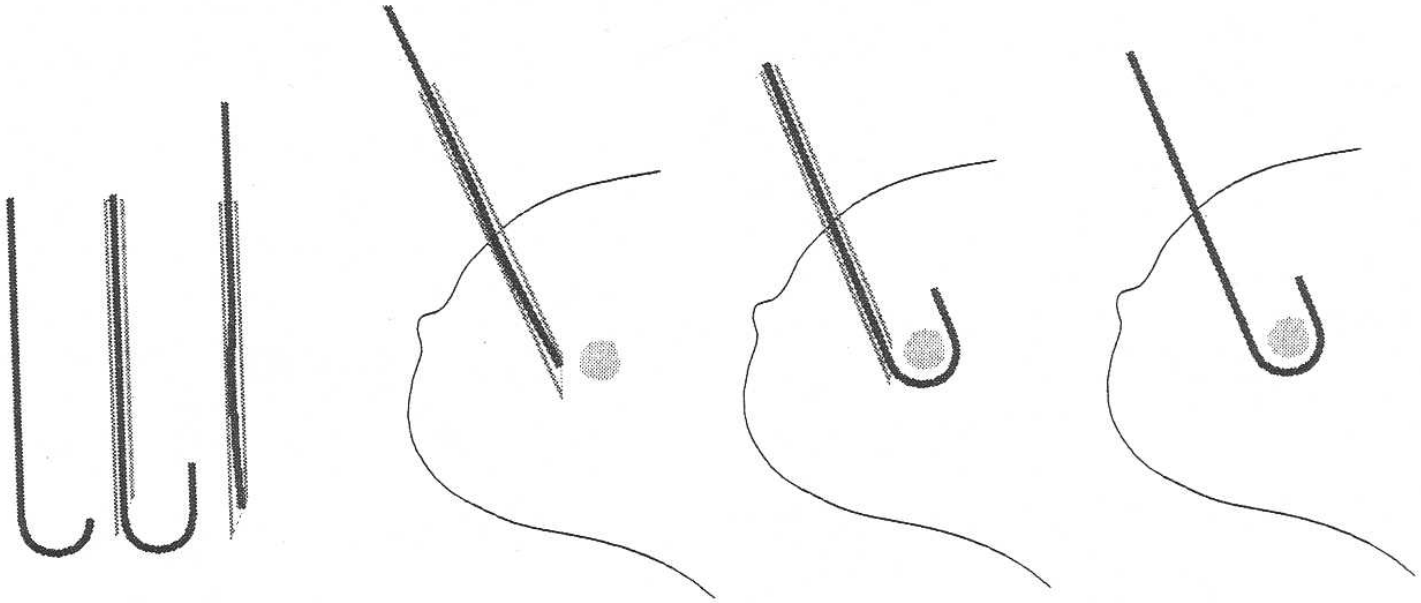

小　结

Perhaps the greatest challenge facing developers of SMA applications is not the discovery of new alloys, but rather the realization of how to take full advantage of an alloy already at hand.

http://www.devicelink.com/mddi/archive/98/03/005.html

举例2——

Developments of Biodegradable Fe-Based Alloys for Coronary Stents

- 铁是人体内必需的微量元素之一，成人含铁约4.0g左右，其中65%-70%的铁分布于血红蛋白中，约25%～30%的铁以铁蛋白和含铁血黄素的形式贮存于肝、脾、骨髓和肠粘膜中，称为储存铁，成人日摄铁量在10～15mg为宜。
- 在正常情况下，铁都处于蛋白质等复杂大分子包围之中，但当铁负荷过多时，便从“封闭”状态游离出来，催化自由基反应，生成大量的自由基,损伤脱氧核糖核酸(DNA)、蛋白质等生物大分子，造成基因突变，影响蛋白质的合成，甚至造成细胞死亡或癌变，体内铁超载与心血管疾病显著相关，是诱发动脉粥样硬化、冠心病、心肌缺血再灌注、心力衰竭等心血管疾病的一个重要因素。

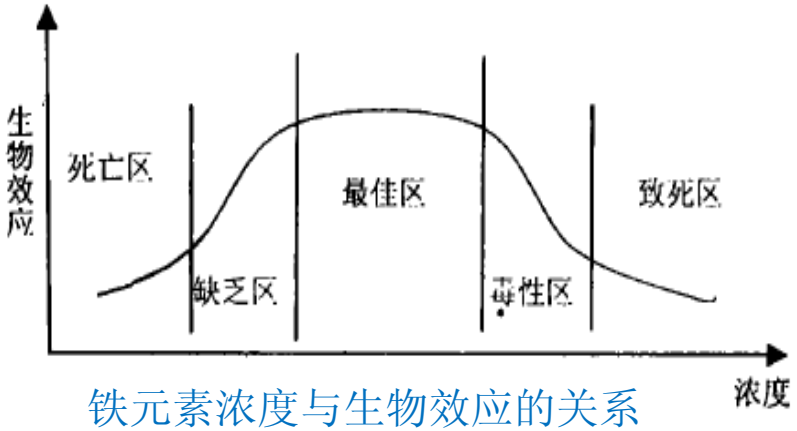

铁元素浓度与生物效应的关系

纯铁在体液中可形成微观电池而发生电化学腐蚀，其腐蚀反应为：

阳极(Fe)： $Fe \rightarrow Fe^{2+} + 2e^-$

阴极： $O_2 + 2H_2O + 4e^- = 4OH^-$

$$Fe^{2+} + 2OH^- \leftrightarrow Fe(OH)_2$$

在大多数生理体液的pH值以及有氧存在的情况下，二价铁可通过下列反应被自动氧化成三价铁：

$$Fe^{2+} \leftrightarrow Fe^{3+} + e^-$$

$$Fe^{3+} + 3OH^- \leftrightarrow Fe(OH)_3$$

或者： $Fe^{2+} + O_2 + 2OH^- \leftrightarrow Fe^{3+}(OH^-)_2 + O_2^-$

二价铁本身也可通过Fenton通路产生羟自由基

$$Fe^{2+} + H_2O_2 \rightarrow Fe^{3+} + OH^- + OH\cdot$$

Introduction

Coronary stent implantation is an invasive procedure performed to reduce blockages in coronary arteries.

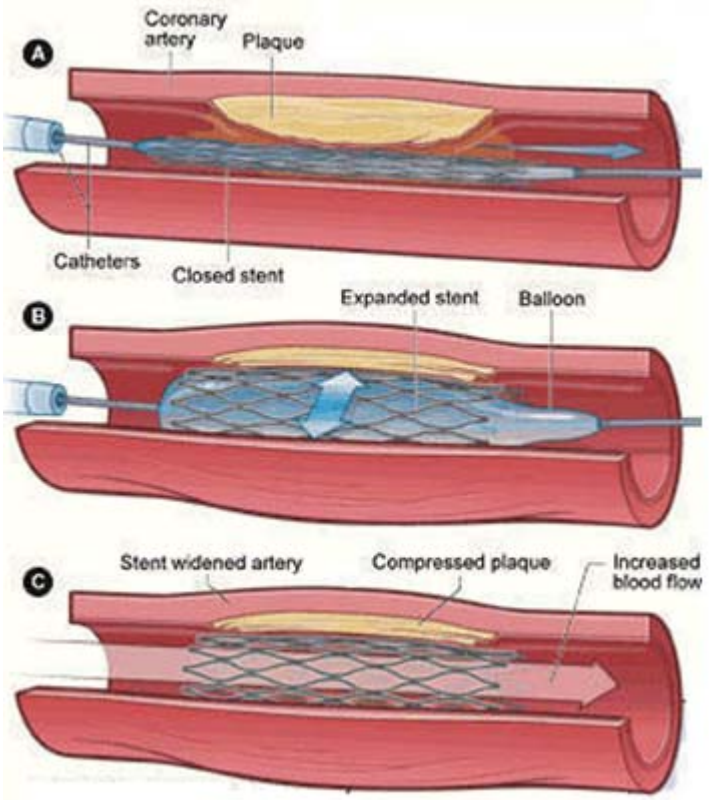

Introduction

The characteristics of an ideal stent

- **Low profile**
- **Good expandability ratio**
- **Sufficient radial hoop strength and negligible recoil**
- **Sufficient flexibility**
- **Adequate radiopacity/magnetic resonance imaging (MRI) compatibility**
- **Thromboresistivity**
- **Drug delivery capacity**

Introduction

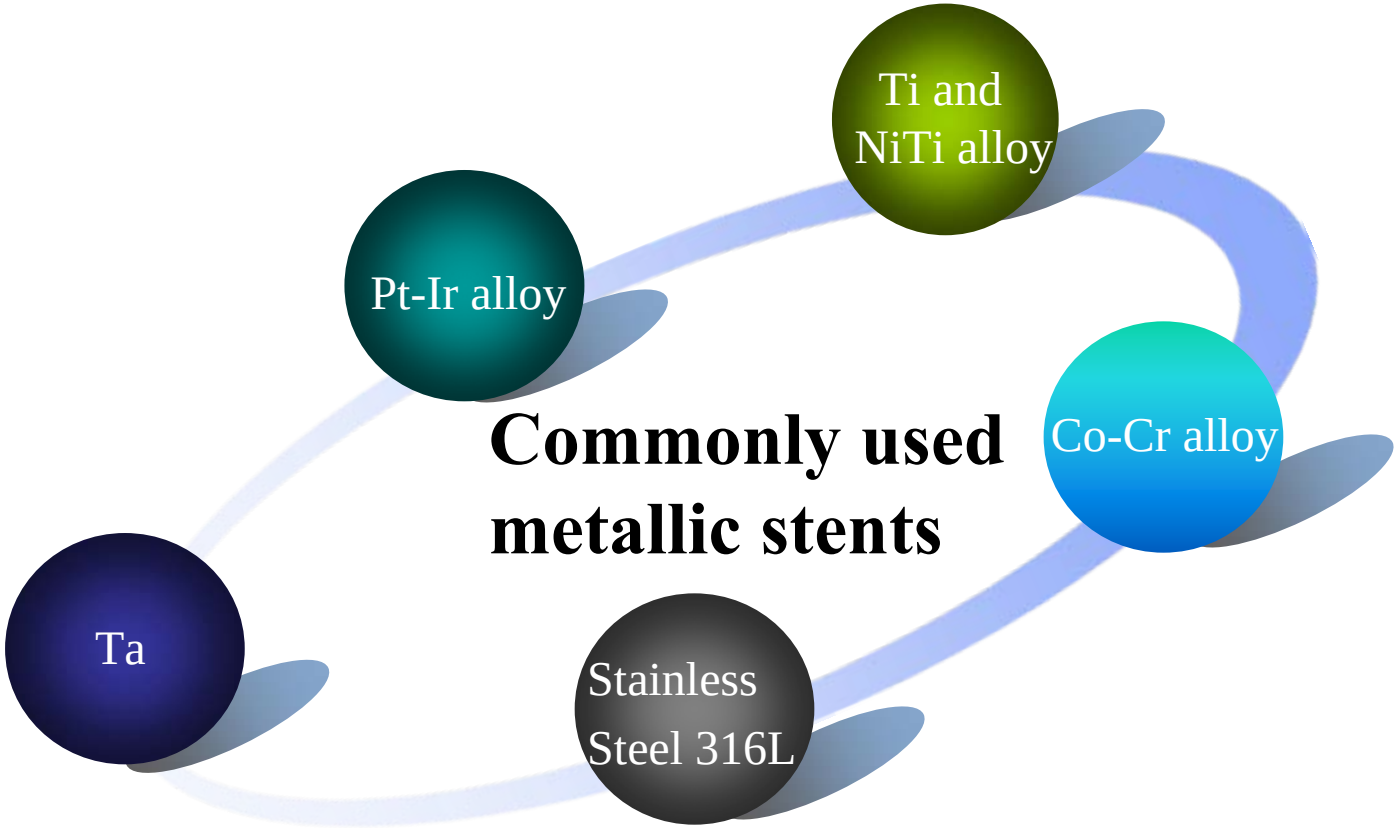

用来制备支架的金属材料的力学性能

金属	弹性模量（GPa）	屈服强度（MPa）	极限强度（MPa）	密度（g/cm³）
316L不锈钢	190	331	586	7.9
纯钽	185	138	207	16.6
纯钛	110	485	760	4.5
镍钛合金	83（奥氏体） 28-41(马氏体)	195-650(奥氏体) 70-140（马氏体）	895	6.7
钴铬合金	210	448-648	951-1220	9.2
纯铁	211.4	120-150	180-210	7.87
镁合金（WE43）	44	162	250	1.84

Introduction

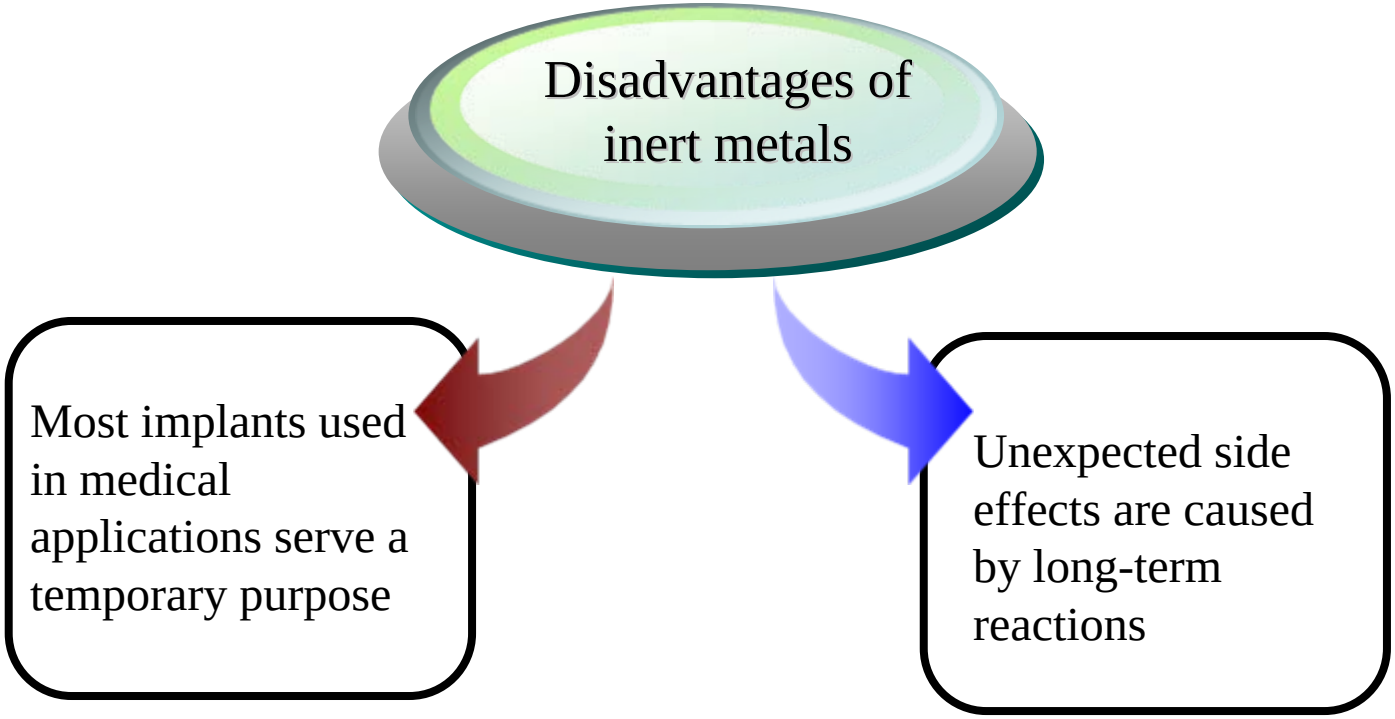

Recently metals used for making biodegradable coronary stents include：

- Magnesium alloys
- Pure iron

Introduction

Disadvantages of magnesium alloys:

- **poor mechanical properties: low elastic modulus and ductility**
- **low corrosion resistance: loosing mechanical integrity before the tissue has sufficiently healed**

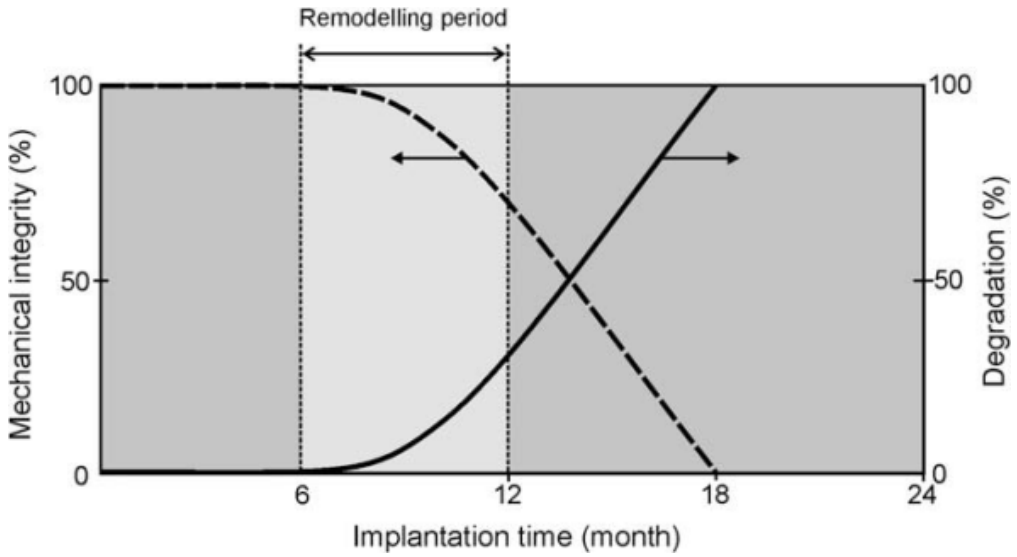

Illustration of an ideal compromise between mechanical integrity and degradation of a biodegradable stent

H. Hermawan et al. Acta Biomateialia. 2010.5, 5(6):1693-1697

Introduction

- **Iron is essential to human life. The slow degradation rate and the small amount of Fe in a coronary stent compared with the high Fe-load of blood results in a relatively unlike systemic toxicity.**

- **The mechanical properties of pure iron are closer to those of 316LSS and excellent for stent application.**

- **Preliminary in vivo studies have validated the good biocompatibility of iron and shown the potential of iron for degradable application.**

In vivo study of pure iron (animal testing)

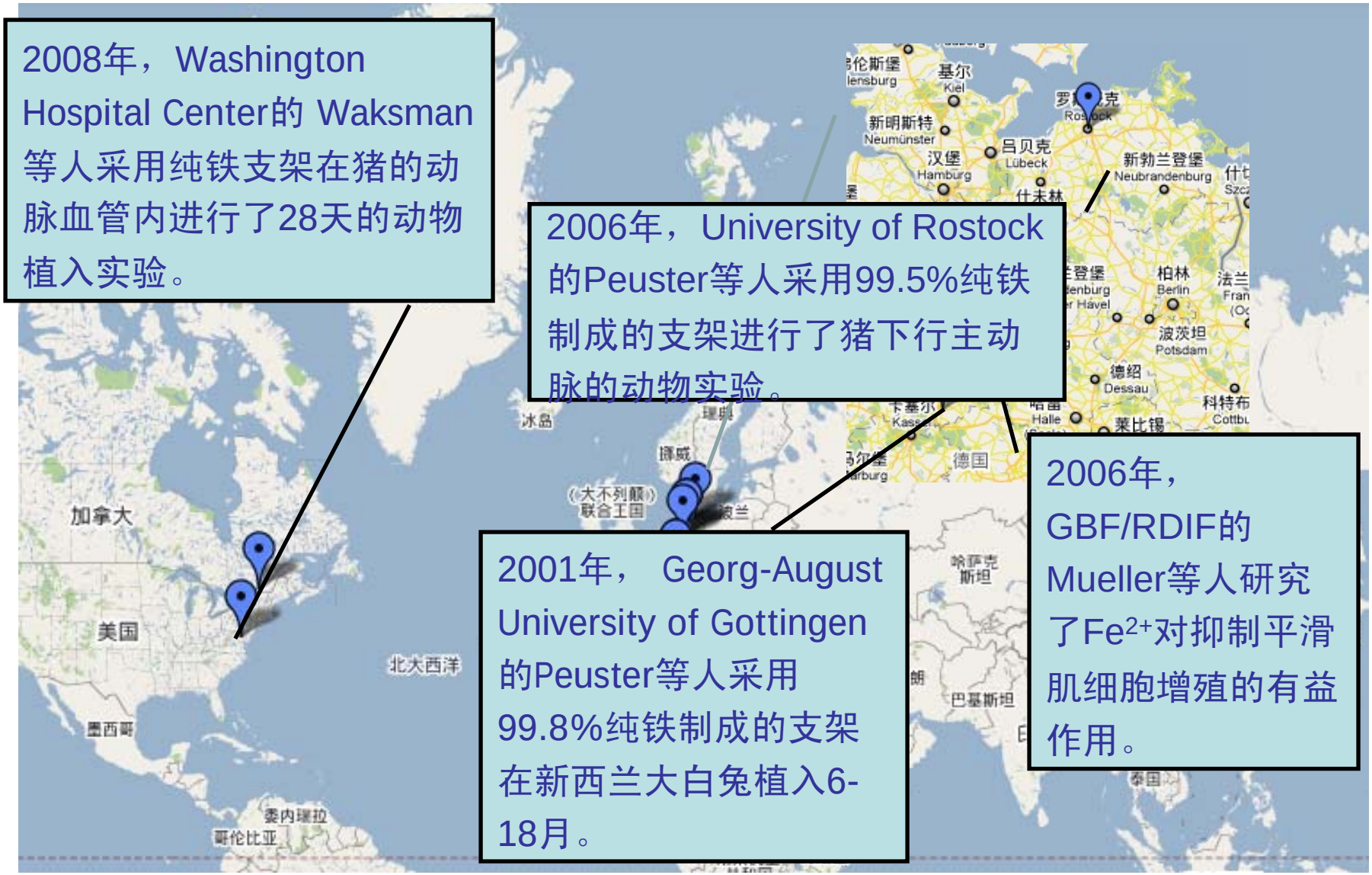
2008年，Washington Hospital Center的 Waksman等人采用纯铁支架在猪的动脉血管内进行了28天的动物植入实验。
2006年，University of Rostock的Peuster等人采用99.5%纯铁制成的支架进行了猪下行主动脉的动物实验。
2001年， Georg-August University of Gottingen的Peuster等人采用99.8%纯铁制成的支架在新西兰大白兔植入6-18月。
2006年，GBF/RDIF的Mueller等人研究了Fe^{2+}对抑制平滑肌细胞增殖的有益作用。
加拿大
美国
北大西洋
墨西哥
委内瑞拉
哥伦比亚
冰岛
挪威
（大不列颠）联合王国
德国
基尔
Kiel
新明斯特
Neumünster
汉堡
Hamburg
吕贝克
Lübeck
罗斯托克
新勃兰登堡
Neubrandenburg
柏林
Berlin
波茨坦
Potsdam
德绍
Dessau
莱比锡
哈萨克斯坦
巴基斯坦
泰国

Investigation of pure iron

- The study was performed to test whether corrodible iron stents (> 99.8% iron) may safely be used for endovascular stenting of the descending aorta with minimal inflammatory response and low thrombogenicity.
- Corrodible iron stents were produced from pure iron and laser cut with a stent design similar to a commercially available permanent stent. The stents were implanted into the native descending aorta of New Zealand white rabbits.

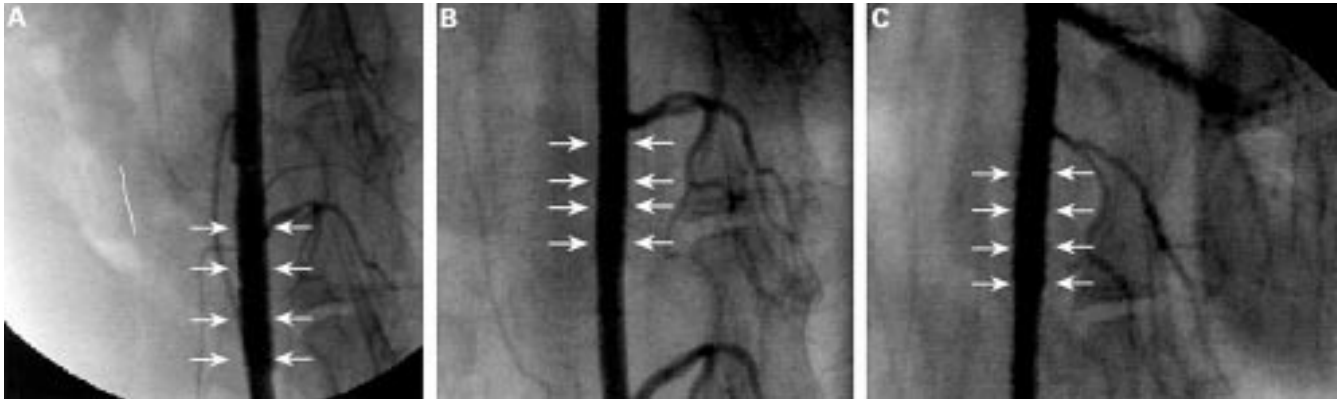

Lateral angiography of the stented descending aorta (A) six months, (B) 12 months, and (C) 18 months after implantation. There is complete patency of the vessel. (Arrows indicate stent implantation site.)

Peuster M, et al., Heart, 2001, 86:563-569

Investigation of pure iron

- Macroscopic evaluation of the stented vessel specimen found a continuously smooth and intact endothelial surface without evidence of thrombus formations or significant narrowing of the stented artery in any of the animals. The surface of the cut stent struts was brown to black. The vascular wall adjacent to the stent also had a brownish tinge.
- At the junctions of the stent struts, there was pronounced accumulation of degradation products, which led to a slight elevation of the vessel wall and a focal brownish discolouration of the intima.

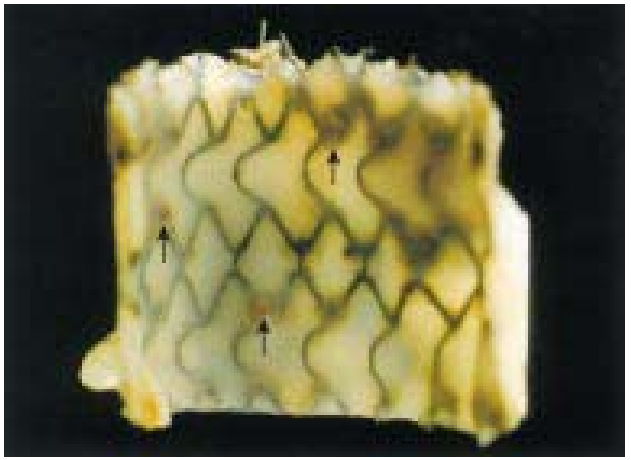

Rabbit aorta with degradable iron stent 12 months after implantation.

Peuster M, et al., Heart, 2001, 86:563-569

Investigation of pure iron

- Degradable iron stents can be safely implanted without significant obstruction of the stented vessel caused by inflammation, neointimal proliferation, or thrombotic events.

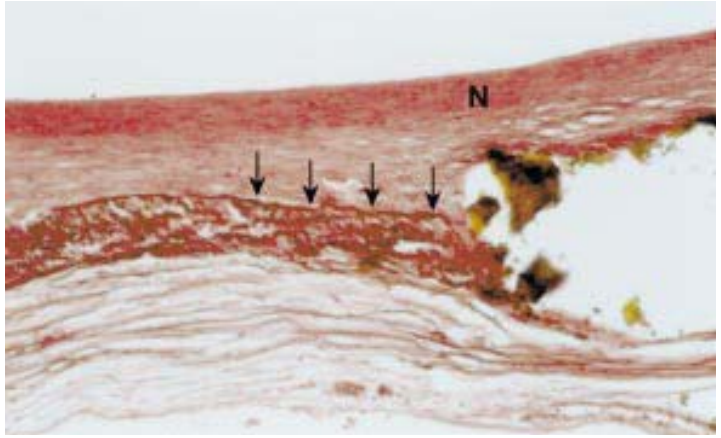

Rabbit aorta with degradable iron stent 18 months after implantation showing a stent strut covered by neointima (N); media and internal elastic membrane destroyed adjacent to the stent strut.

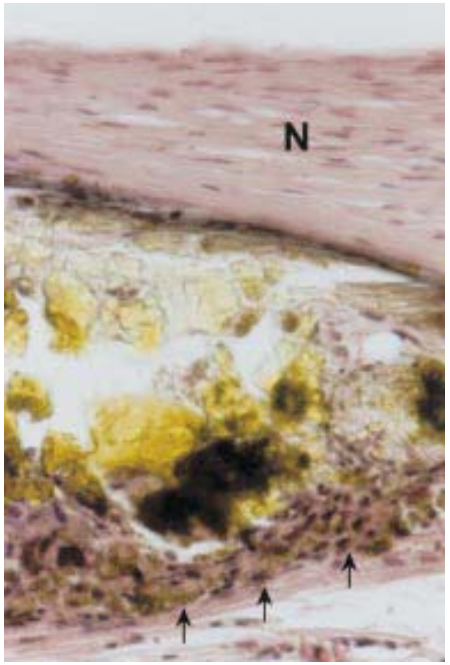

Rabbit aorta with degradable iron stent 18 months after implantation.A stent strut is covered by neointima (N); along the adventitial side there is moderate infiltration of macrophages (arrows)

Peuster M, et al., Heart, 2001, 86:563-569

Investigation of pure iron

- The amount of pure iron implanted with a single iron (99.8%) stent (41 mg) equals the monthly oral intake of iron: it is less than the recommended daily dose of intravenous iron dextran (右旋糖苷)and much less than the amount of iron transfused with one unit of blood (200–250 mg)
- Since **degradation rates in vivo were found to be slower than expected in vitro**, future research has to focus on the kinetics of in vivo corrosion and its modification either by using an iron based alloy or by modifying the surface and structure of the stent to achieve a faster degradation

Peuster M, et al., Heart, 2001, 86:563-569

Investigation of pure iron

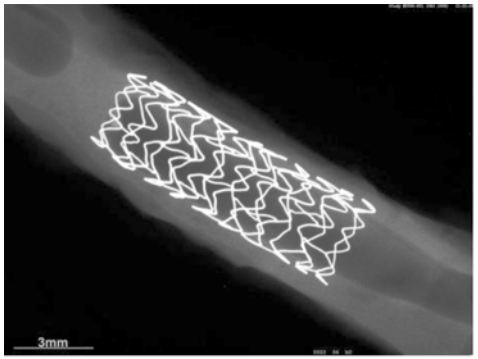

Iron

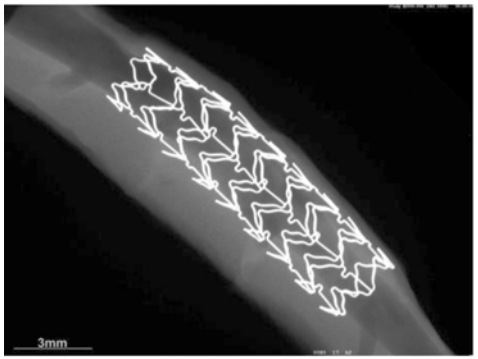

Cobalt-Chromium

Representative X-ray photograph of iron and cobalt chromium stents 28 days after implantation in porcine coronary arteries.

- Iron stents and cobalt chromium stents were randomly deployed in the coronary arteries of juvenile domestic pigs. Animals were sacrificed at 28 days, and the vessels were fixed and processed for histochemistry.
- Lower kilo-voltage radiographs taken at 28 days showed that continuity of the stent struts in the iron stent was distorted as compared to that of the Co-Cr stent.

Ron Waksman, M.D., et al., Journal of Interventional Cardiology, 2008, 21(1):15-20

Investigation of pure iron

- At 28 days, iron stents started to show signs of degradation without evidence of stent particle embolization or thrombosis without traces of excess inflammation, or fibrin deposition. The surface of the iron stent struts was black to brown and the vascular wall adjacent to the iron stent had a brownish tinge. There were no statistically significant differences in any of the measured parameters between segments implanted with iron and cobalt chromium stents. There were also no adverse effects in the persistent areas.

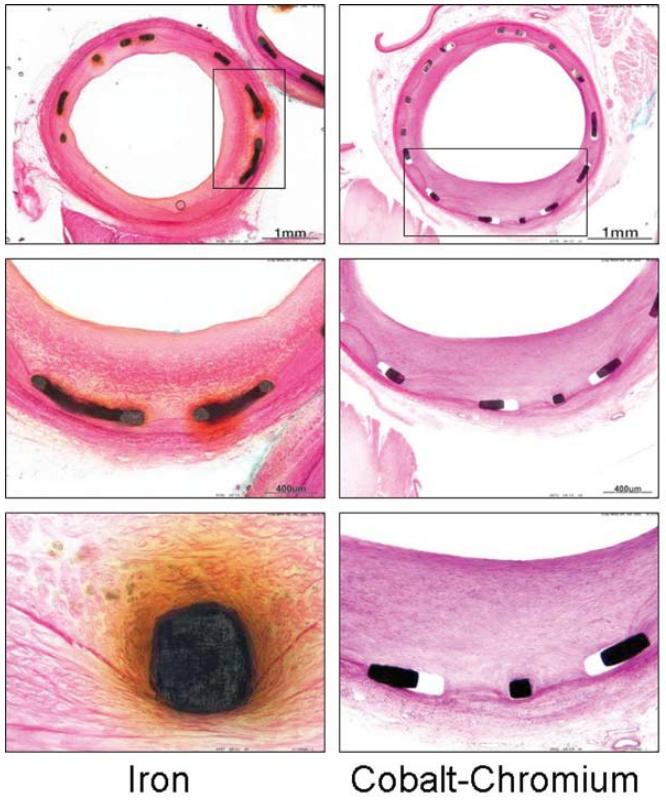

Representative photomicrographs of hematoxylin eosin–stained sections of porcine coronary arteries 28 days after iron stent and cobalt chromium stent implantation.

Ron Waksman, M.D., et al., Journal of Interventional Cardiology, 2008, 21(1):15-20

Investigation of pure iron

- The corrosive stents produced from pure (99.5 mass%) iron in a peripheral stent design (expanded stent diameter: 6–12 mm) were implanted into the native descending aorta of 29 minipigs with a follow-up of up to 12 months. Permanent stents produced from stainless steel served as anintra-individual control.

A peripheral corrodible iron stent produced in the stent design of a peripheral Saxx stent (CR Bard, Tempe, AZ, USA) after electropolishing prior to mounting on the balloon catheter

Peuster M, et al., Biomaterials, 2006, 27:4955-4962

Investigation of pure iron

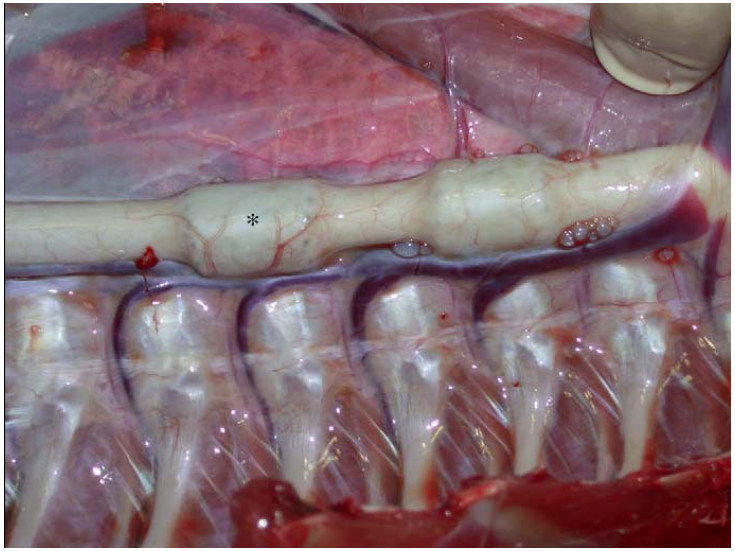

Macroscopical aspect of the stented descending aorta after expiration of the animal(Porcine). The iron stent is marked with an asterisk.

- In the animals sacrificed after 3 months, there was evidence of focal accumulation of pigment in the spleen staining positive for iron and further accumulation of ironcontaining macrophages within the lymphatic pathways along the aorta. This process of iron-clearance from the implantation site was still observed after 6 and 12 months, respectively. However, no signs of significant iron overload were encountered in any of the histopathologic specimens. There were no abnormalities on macroscopic inspection of the implantation site.

Peuster M, et al., Biomaterials, 2006, 27:4955-4962

Investigation of pure iron

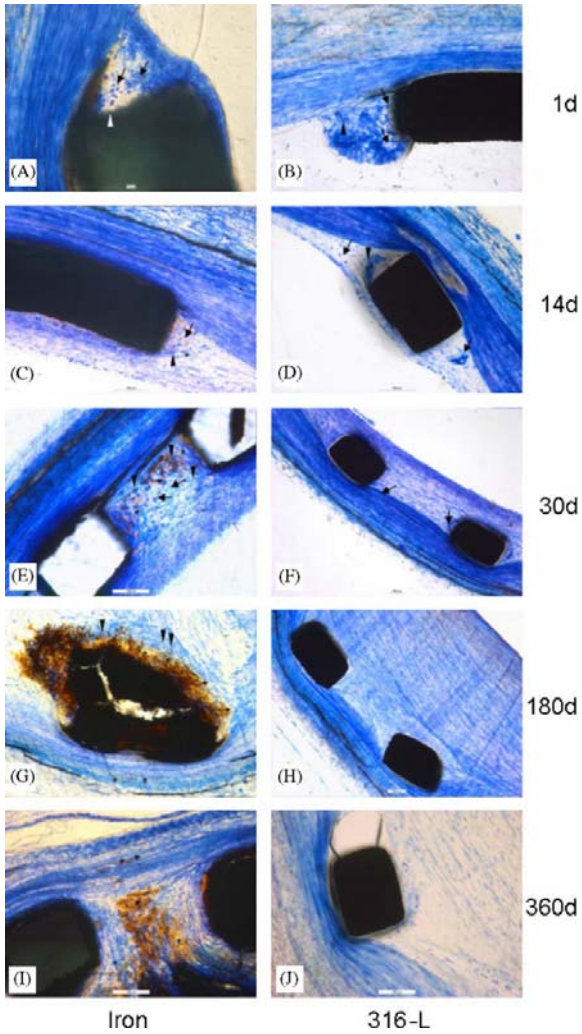

- Histological appearance of the iron and 316-L stent struts in relation to the duration of the follow-up. One day after implantation a membranous thrombus covers the stent strut of both the iron (A) and 316-L (B) stent. Within the thrombus, there is accumulation of granulocytes, macrophages (arrowheads) and lymphocytes (arrows). After 14 days, the stent struts are covered completely with a neointima (C, D). Adjacent to the iron stent struts, there is accumulation of degradation products (*) accompanied by macrophages. After 180 days, the iron stent strut is fragmented and mostly degraded. Degradation products can be observed within the adventitia (G).

Peuster M, et al., Biomaterials, 2006, 27:4955-4962

Investigation of pure iron

- Iron stents have mechanical properties allowing for the production of a stent with a broad range of stent diameters (6–12 mm).
- Biocompatibility of such an iron stent is excellent with little neointimal proliferation and no signs of local or systemic iron toxicity.
- Thrombogenicity of corrosive iron stents is low.
- Degradation of a stent produced from pure iron is slow thereby preventing fragment embolization.

Peuster M, et al., Biomaterials, 2006, 27:4955-4962

In vitro study of Fe-based alloys (New Fe-based Alloy Development)

2007年，University of Laval的Hermawa、Moravej分别报道了Fe-Mn合金和超细晶粒纯铁作为可降解铁基材料的体外实验研究结果。

2010年，北京大学的郑玉峰课题组报道了Fe-30Mn-6Si、Fe-X二元合金的体外实验研究结果。

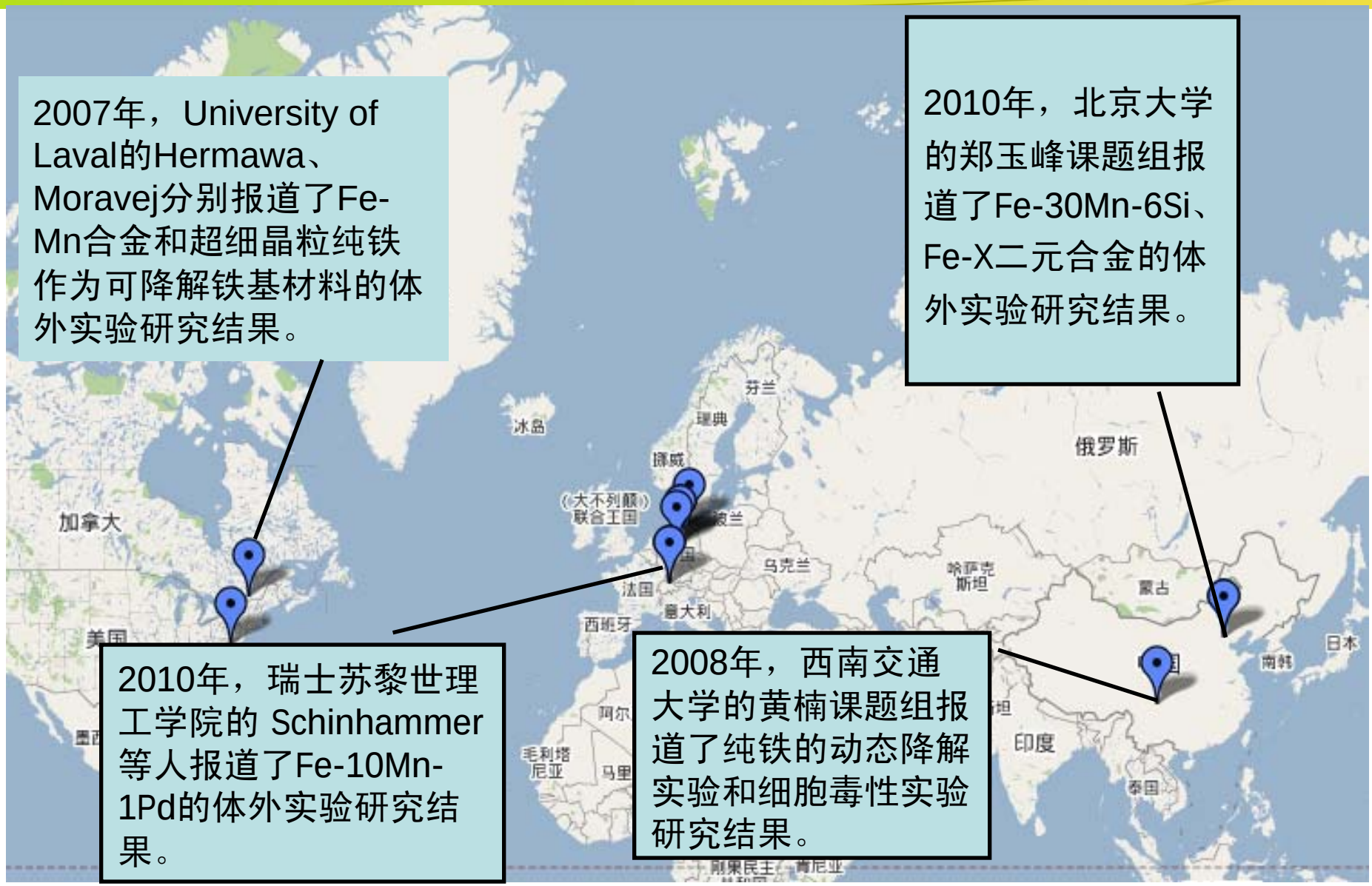

2010年，瑞士苏黎世理工学院的 Schinhammer等人报道了Fe-10Mn-1Pd的体外实验研究结果。

2008年，西南交通大学的黄楠课题组报道了纯铁的动态降解实验和细胞毒性实验研究结果。

Investigation of pure iron

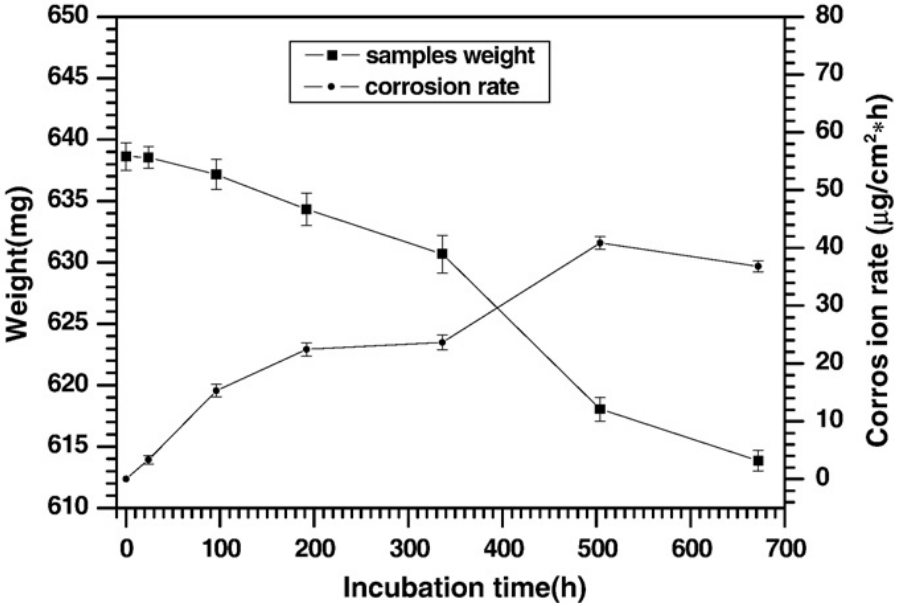

Degradation kinetics of iron incubated at 37 ° C in SBF solution.

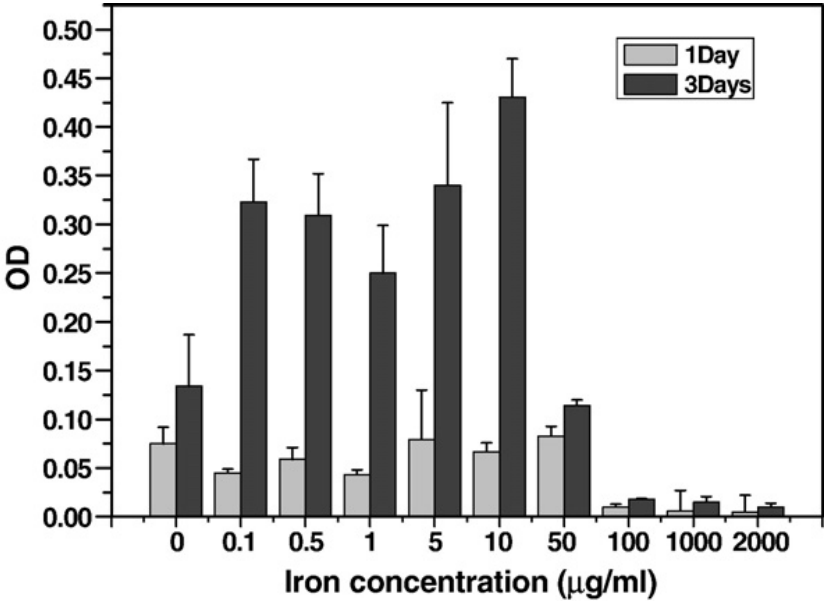

Metabolic activity of EC after cultured in different iron concentrations for 1 day and 3 days.

The degradation rate of pure iron in vitro is determined and the interaction of individual corrosion products from biocorrodible iron stents with endothelial cells was characterized.

SF Zhu, et al. Materials Science and Engineering C, 2009, 29:1589-1592

Investigation of Fe-based alloys

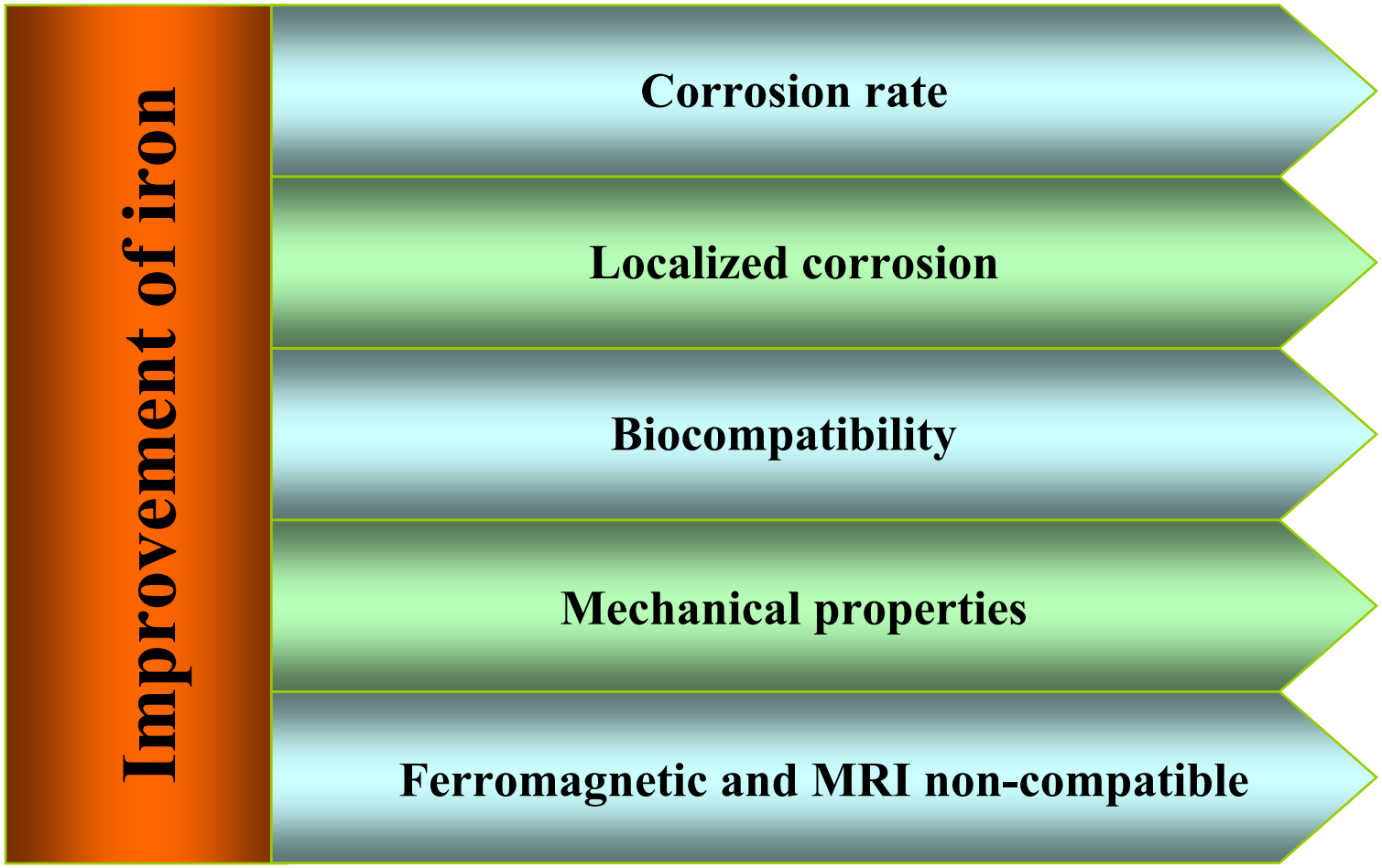

Investigation of Fe-based alloys

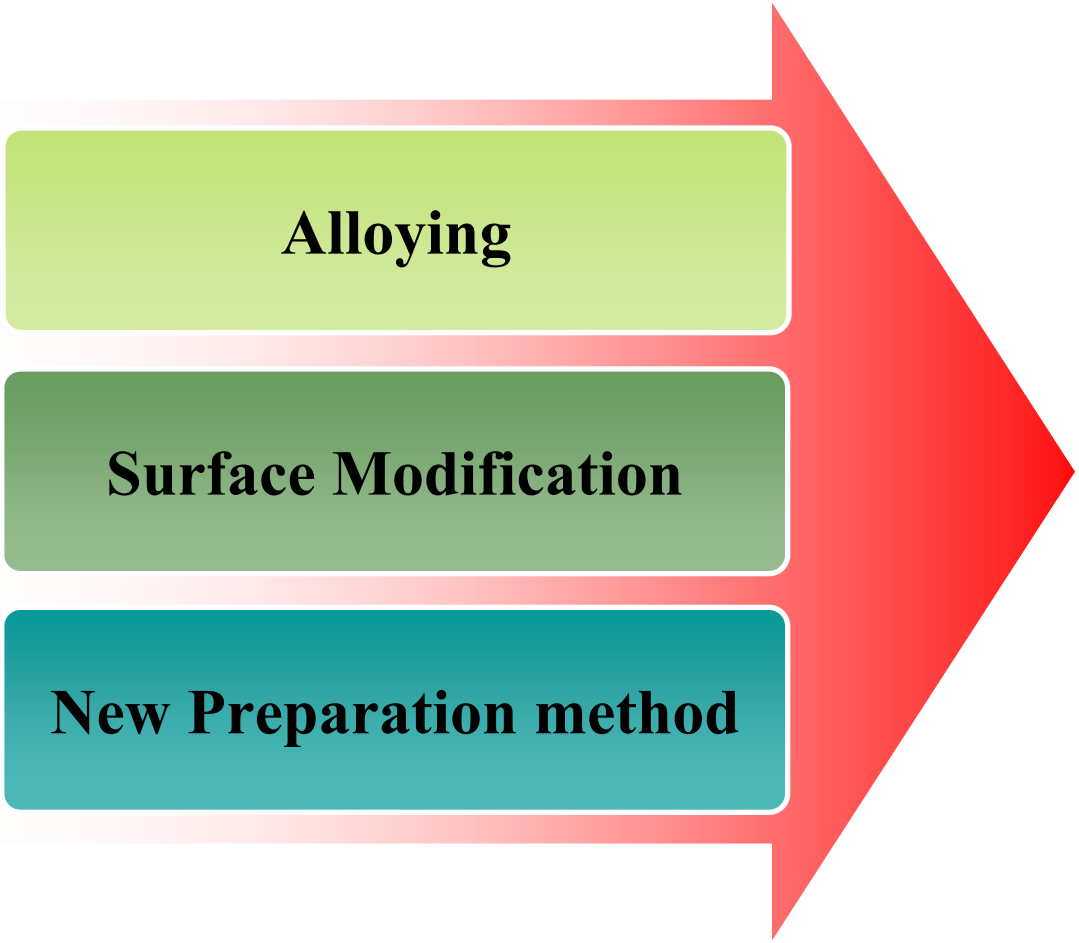

Improve the biocompatibility and degradation rate of pure iron

Investigation of Fe-based alloys

Alloying

Investigation of Fe-based alloys

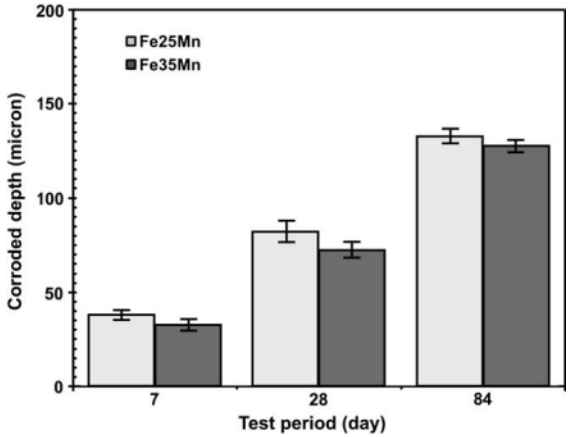

Corroded depth as a function of test period for Fe25Mn and Fe35Mn alloys

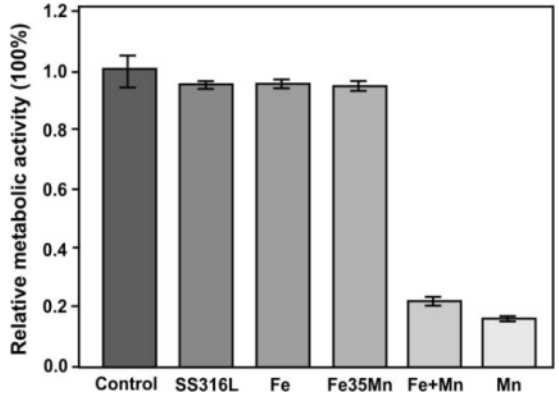

Relative metabolic activity of 3T3 fibroblast cells in presence of various metal powders at a fixed concentration of 0.5 mg ml^{-1}.

- Materials used in this study were iron-based alloys containing 20–35 wt.% manganese denoted as Fe20Mn, Fe25Mn, Fe30Mn and Fe35Mn.
- Fe-Mn alloys were corroded at an average rate up to 520 μm $year^{-1}$ which is about two times faster than that of pure iron. The degradation products constituted of iron hydroxides and calcium/phosphorus containing layers.
- The Fe–Mn alloys possess a low inhibition effect to 3T3 fibroblast cells metabolic activities compared to pure manganese. Its 50% inhibition effect reached at concentration of 6 mg ml^{-1} while its 100% inhibition effect was reached when the concentration exceeded 16 mg ml^{-1}.

Hermawan H. et al. Acta Biomateialia. 2010, 6(5): 1852-1860

Investigation of Fe-based alloys

- The alloying elements have the function of decreasing the degradation resistance of the iron, taking into account two aspects: (i) the formation of a solid solution such that the Fe matrix becomes more susceptible to corrosion; (ii) the formation of noble IMP particles that generate microgalvanic corrosion and promote active dissolution of the matrix.
- The newly developed Fe–Mn–Pd alloys reveal a degradation resistance that is one order of magnitude lower than observed for pure iron. Additionally, the mechanical performance is shown to be adjustable.

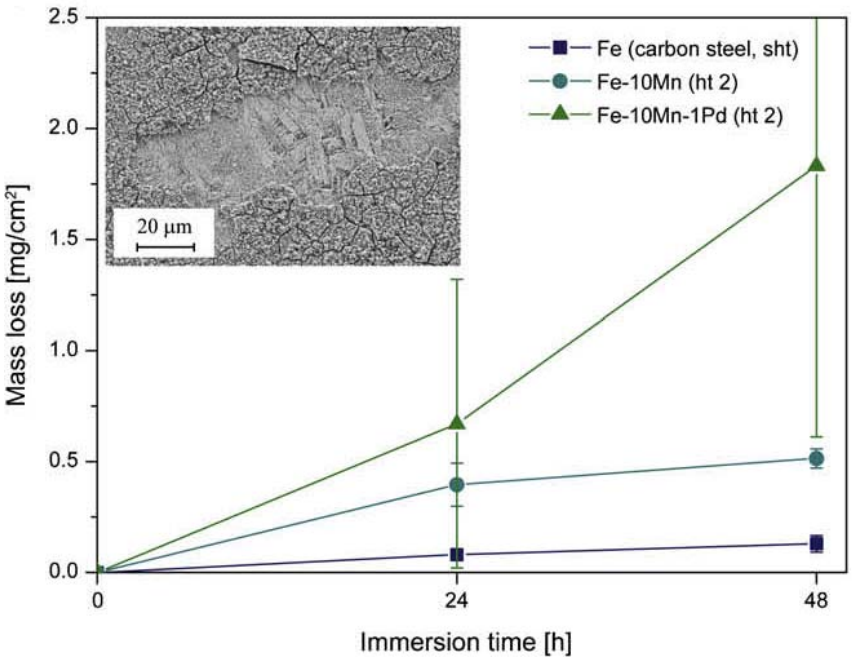

Mass loss over immersion time of Fe (carbon steel, sht), Fe–10Mn (ht 2) and Fe–10Mn–1Pd (ht 2) subjected to immersion testing. The insert shows a SEM image of the surface of a Fe–10Mn–1Pd (ht 2) sample immersed for 48 h in SBF

Schinhammer M, et al. Acta Biomateialia. 2010, 6(5): 1705-1713

Investigation of Fe-based alloys

- In vitro effects of alloying elements Mn, Co, Al, W, Sn, B, C, S on pure iron were investigated for future design of new biodegradable Fe-based alloys used for coronary stents.

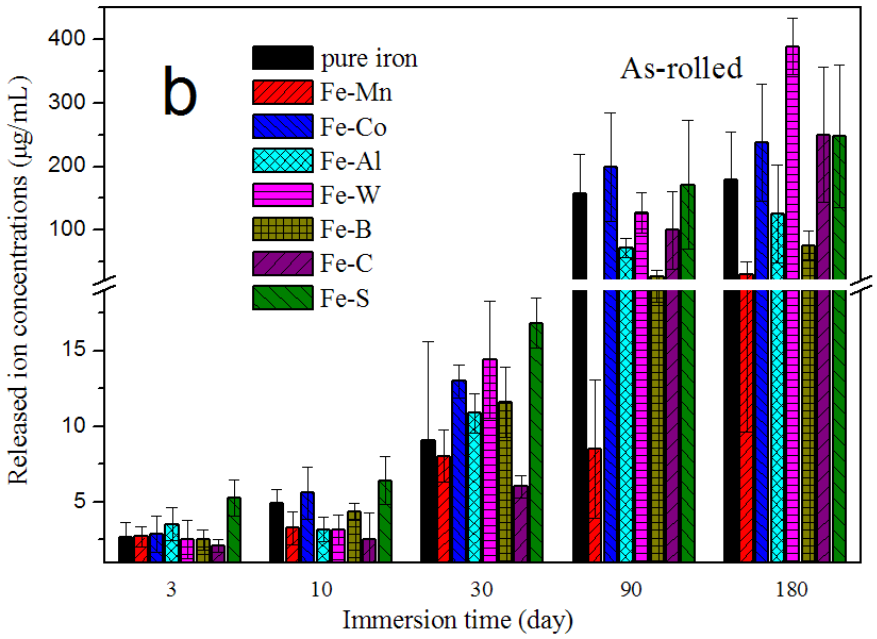

Released ion concentrations of as-rolled Fe-X binary alloys with pure iron as control in Hank's solution at 3, 10, 30, 90 and 180 days

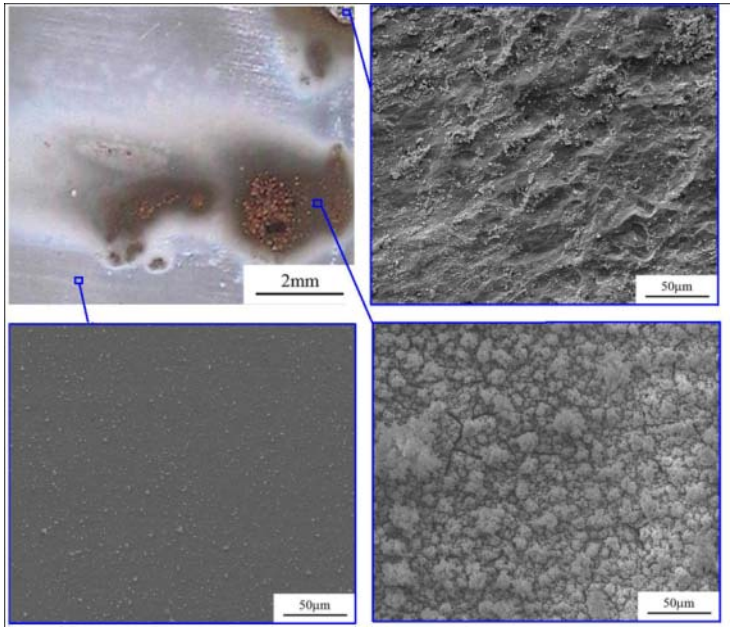

Surface morphologies of as-rolled Fe-3W alloy after 180 days immersion indicates the localized corrosion

Zheng Y.F., et al. Acta Biomateialia. 2011, 7(3): 1407-1420

Investigation of Fe-based alloys

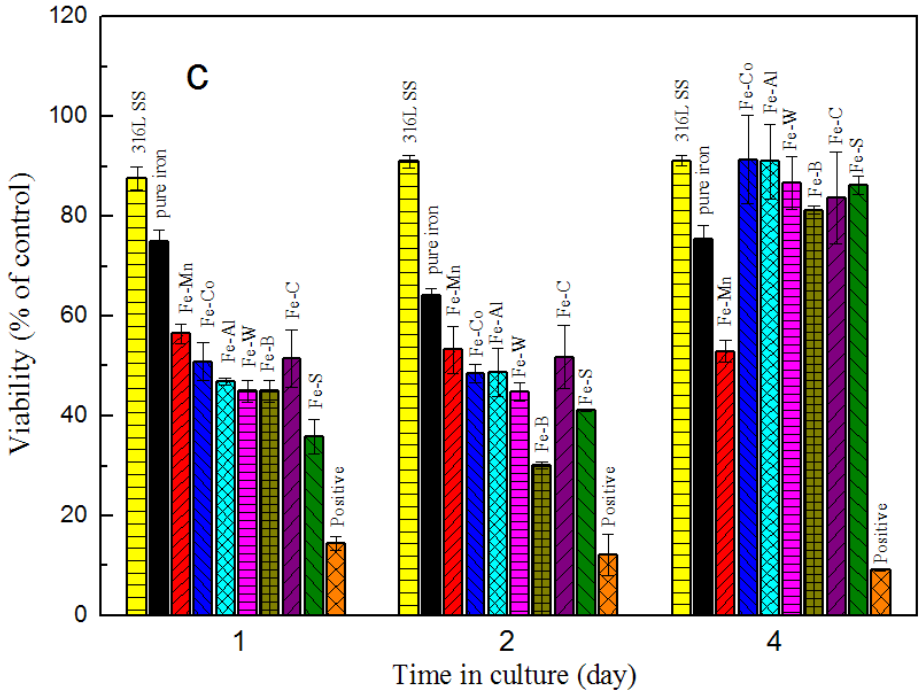

Cell viability of ECV304 after 1, 2 and 4 days incubation in as-rolled Fe-X binary alloys and pure iron extraction mediums, with 316L stainless steel as a reference.

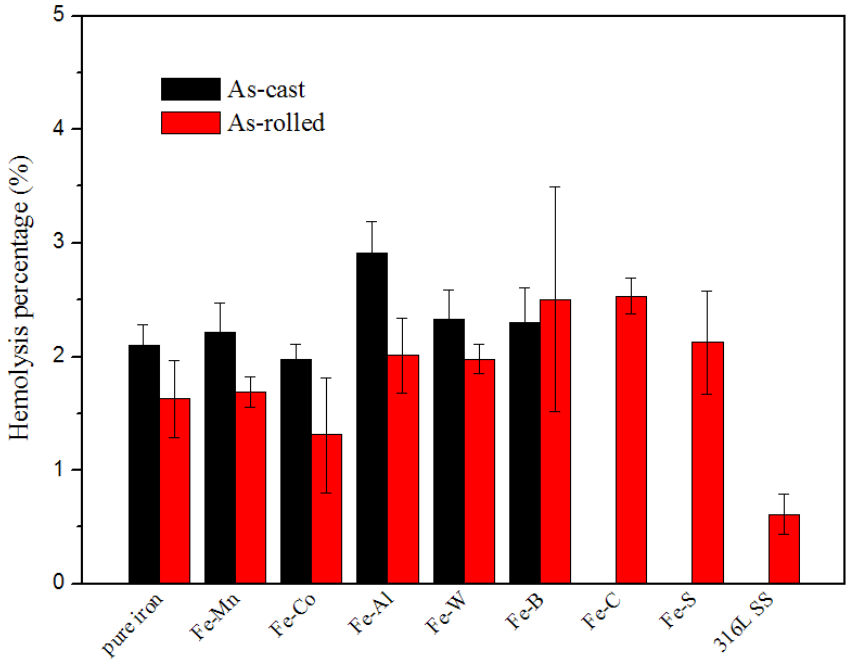

Hemolysis percentage of as-cast and as-rolled Fe-X binary alloys and pure iron, with 316L stainless steel as a reference.

Zheng Y.F., et al. Acta Biomateialia. 2011, 7(3): 1407-1420

Investigation of Fe-based alloys

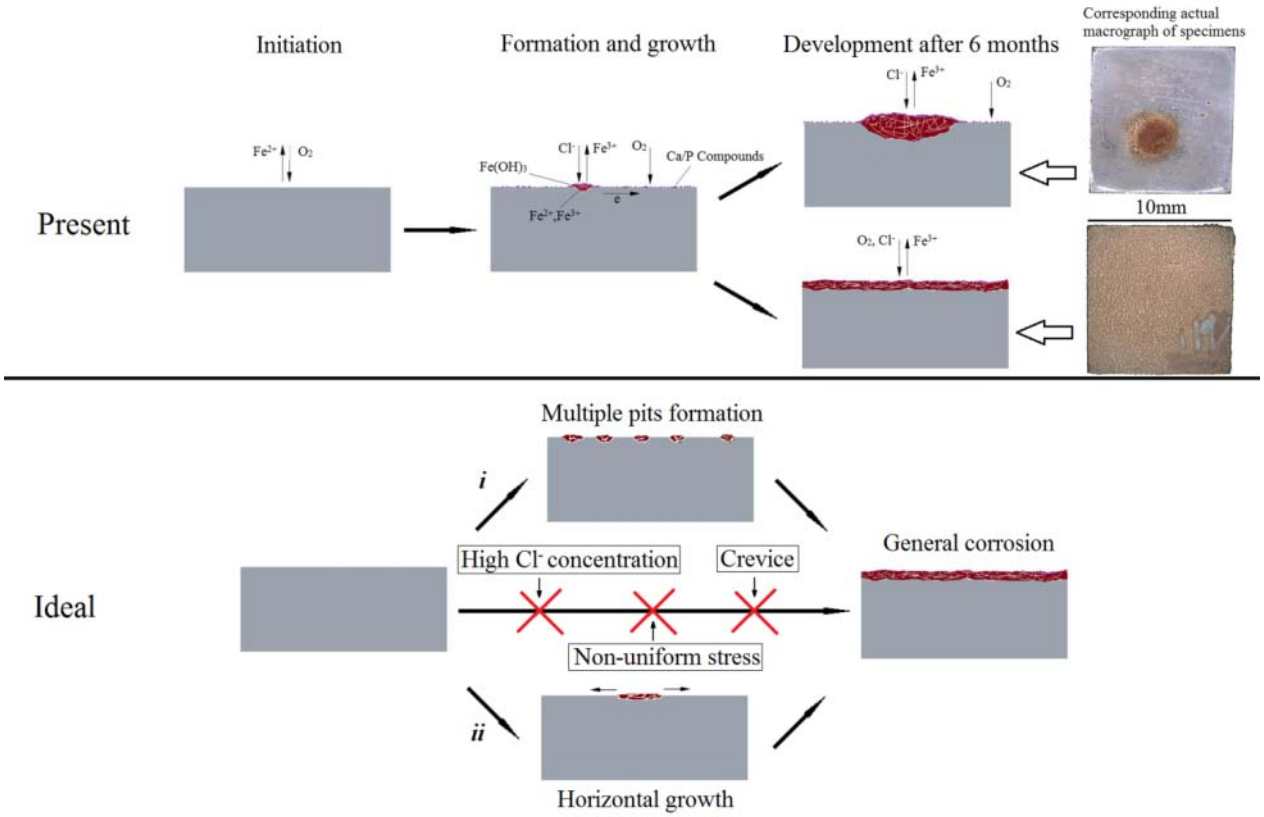

The schematic diagrams illustrating both the corrosion mechanism and ideal corrosion process of Fe-based biodegradable alloys in Hank's solution.

Zheng Y.F., et al. Acta Biomateialia. 2011, 7(3): 1407-1420

Investigation of Fe-based alloys

- Fe30Mn6Si alloy was investigated as a potential degradable biomaterial, with the recently well-developed biodegradable metals, pure iron and Fe30Mn alloy, as comparison.
- Fe30Mn6Si alloy consists of ε-martensite and γ-austenite at room temperature, the mechanical property of Fe30Mn6Si alloy is higher than that of the pure iron.
- The corrosion rate of Fe30Mn6Si alloy is higher than that of Fe30Mn alloy.
- Fe30Mn6Si alloy shows good performance for blood vessel related cellular application and the hemolysis percentage is less than 2%.

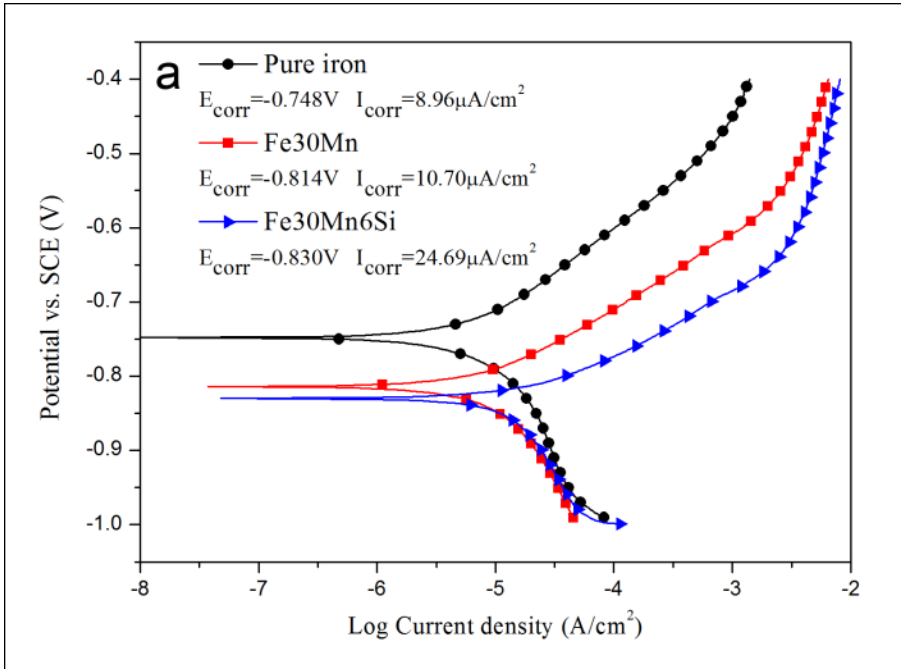

Potentiodynamic polarization curves of Fe30Mn6Si immersed in Hank's solution with pure iron and Fe30Mn as control

Zheng Y.F., et al. Materials Letters. 2011, 65: 540-543

Investigation of Fe-based alloys

Surface Modification

Investigation of Fe-based alloys

- Fe–O thin films were prepared on the pure iron by plasma immersion ion implantation and deposition (PIII&D) to improve its corrosion resistance and biocompatibility.
- The phase structure of the films transformed from FeO to Fe_3O_4 with the increase of the oxygen flux. The number of platelet adhesion, platelet activation on the surface of FeO film were remarkably decreased compared with pure iron.
- After synthesized Fe–O films by PIII&D at low oxygen flux, the blood compatibility and cell compatibility of pure iron were significantly improved.

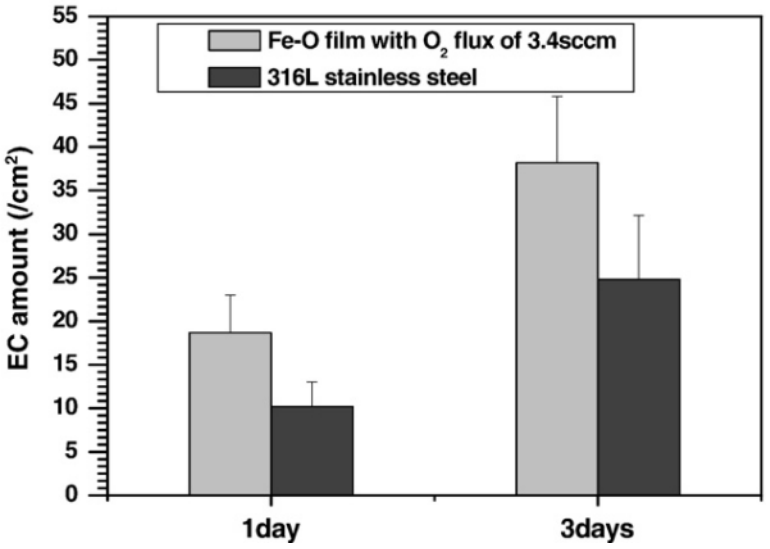

Statistical results of the number of adhered endothelial cells on Fe–O film with oxygen flux of 3.4 sccm and 316L stainless steel.

Schinhammer M, et al. Acta Biomateialia. 2010, 6(5): 1705-1713

铁支架材料表面La离子注入

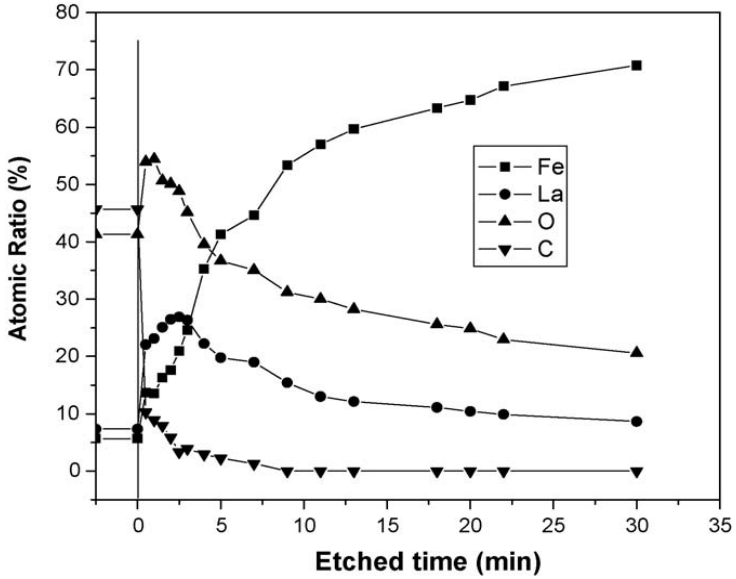

La元素在铁中的分布

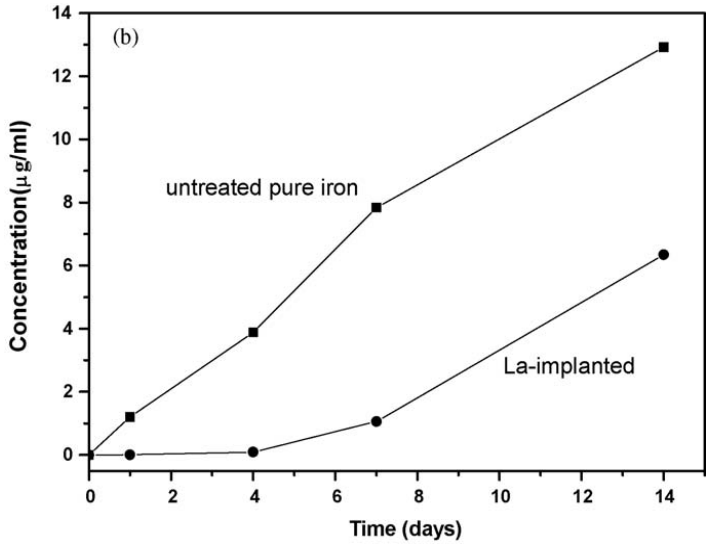

La离子注入前后的铁离子释放行为

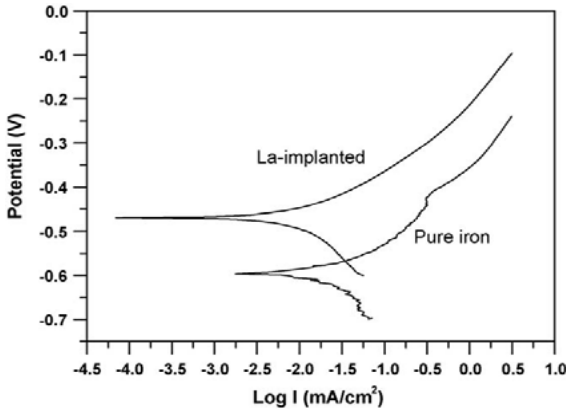

La 离子注入Fe的电化学行为

Investigation of Fe-based alloys

Novel Preparation Method

Investigation of Fe-based alloys

- An electroforming technique was developed for fabricating iron foils targeted for application as biodegradable cardiovascular stent material.
- E-Fe possesses fine-grain microstructure, suitable mechanical properties and moderate corrosion rate as a degradable stent material.

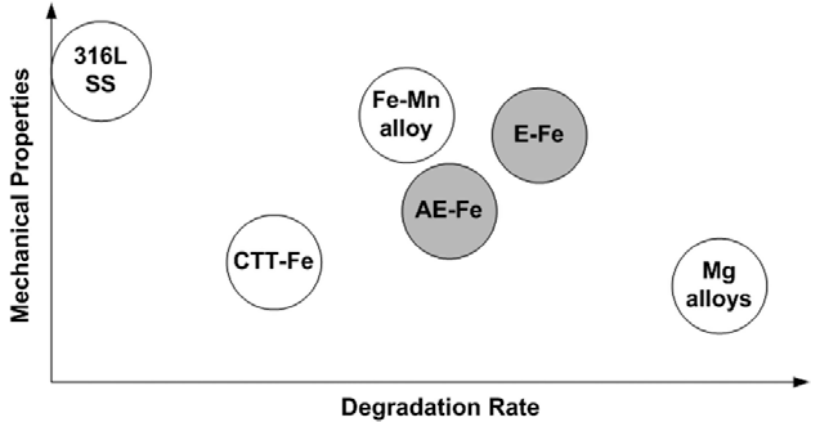

Comparison of different cardiovascular stent materials. 316L SS is not degradable and is presented in this figure as the reference stent material for Comparison.

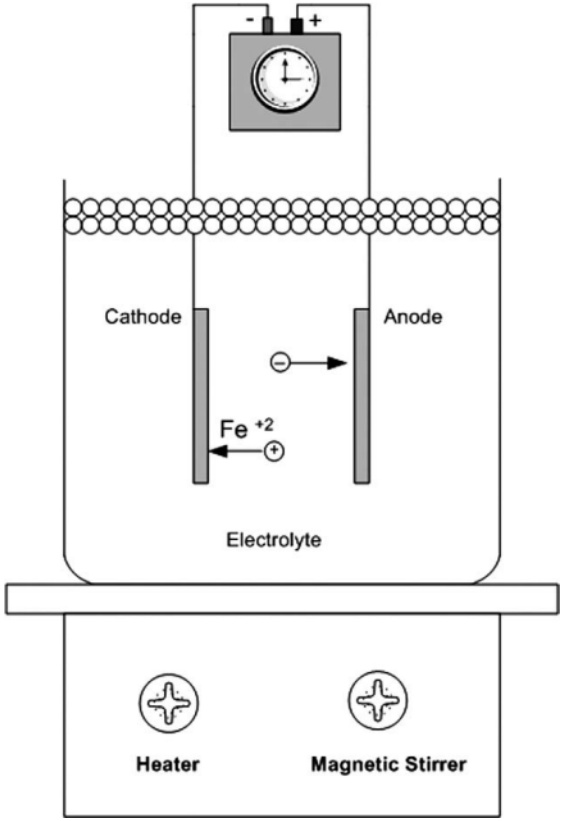

Schematic of electroforming apparatus

Moravej M., et al. Acta Biomateialia. 2010, 6(5): 1726-1735

Investigation of Fe-based alloys

- Cell viability results showed that E-Fe did not result in a decrease in metabolic activity when exposed to primary rat smooth muscle cells. However, it caused a decrease in cell proliferation activity which could be beneficial for the inhibition of in-stent restenosis.

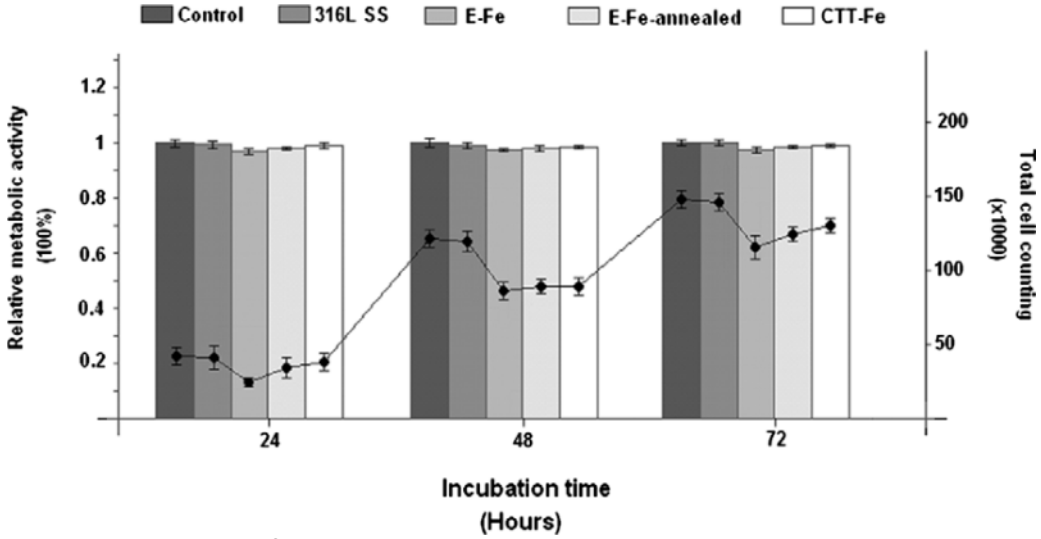

Cell viability of iron and 316L SS: the column charts are related to the relative cell metabolic activities as a function of incubation time at 24, 48 and 72 h (left axis), while the curve is the total cell count measured at 24, 48, and 72 h (right axis).

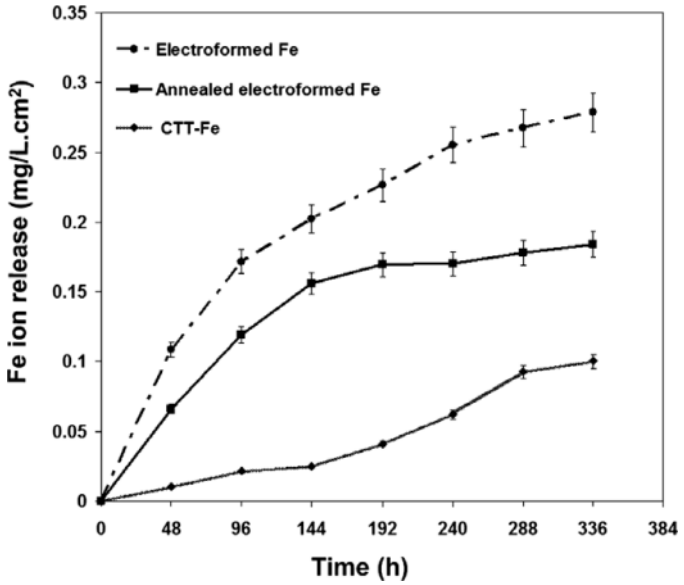

Fe ion release behaviour of electroformed and CTT iron: E-Fe released a higher quantity of Fe ion than CTT-Fe did during the testing period. After annealing, the ion release of E-Fe decreased. However, it was still higher than that of CTT-Fe.

Schinhammer M, et al. Acta Biomateialia. 2010, 6(5): 1843-1851

结 论

1.铁基材料与生物体的相互作用已经被初步证明在一定条件下铁基材料是可能作为血管支架材料的。

2. 加强对铁基材料与生物体的相互作用的深入研究，在机理认识上搞清楚可降解铁基材料的安全性的条件是非常重要的。 需要进行评价体系的标准研究。

3.需要在系统认识铁基材料与生物体的相互作用的生物学规律、力学性能演变规律的基础上进行植入器械的设计与临床应用。

北京大学
PEKING UNIVERSITY

Thank you!

LBMD
Laboratory of Biomedical Materials and Devices

http://lbmd.coe.pku.edu.cn